Analysis of the effects of metformin administered alone or in combined treatments in colorectal cancer

Thesis

Maria Valeria Maiorana

Degree in Biotechnology

Analysis of the effects of metformin administered alone or in combined treatments in colorectal cancer

Thesis presented to The Open University of Milton Keynes

for the Degree of Doctor of Philosophy

Discipline: Life and Biomolecular Sciences

Date of Submission: 31st January 2017

Affiliated Research Centre: Fondazione IRCCS “Istituto Nazionale dei Tumori”

TABLE OF CONTENTS

LIST OF FIGURES

LIST OF TABLES

ABBREVIATIONS

4-OHT	4-hydroxytamoxifen
4E-BP1	4E-Binding Protein 1
5-FU	5-Fluorouracil
ACC	Acetyl-CoA Aarboxylase
AMP	Adenosine Monophosphate
AMPK	5'-AMP-activated Protein Kinase
APC	Adenomatous Polyposis Coli
ATM	Ataxia Telangiectasia Mutated
ATP	Adenosine Triphosphate
BrdU	Bromodeoxyuridine
CapeOx	Capecitabine/oxaliplatin
CI	Combination Index
CIN	Chromosomal Instability
CPT	Camptothecin
CRC	Colorectal Cancer
CRC-pc	Colorectal Cancer-peritoneal carcinomatosis
CSC	Cancer Stem Cell
Ctrl	Control
DCC	Deleted in Colon Cancer
DDR	DNA Damage Repair
EGFR	Epidermal Growth Factor Receptor
ERK	Extracellular signal–Regulated Kinase
FACS	Fluorescence-Activated Cell Sorting
FAP	Familial Adenomatous Polyposis
FAS	Fatty Acid Synthase
FDA	Food and Drug Administration
FFPE	Formalin Fixed Paraffin Embedded
FGFR	Fibroblast growth factor receptor
FOLFIRI	5-FU/LV/irinotecan
FOLFOX	5-FU/LV/oxaliplatin
FOLFOXIRI	5-FU/LV/oxaliplatin/irinotecan
GLUT-4	Glucose Transporter 4
GSK3β	Glycogen Synthase Kinase 3 beta
HIF-1α	Hypoxia-Inducible Factor 1 α
HK2	Hexokinase 2
HNPCC	Hereditary Non-Polyposis Colorectal Cancer
IC_{50}	Inhibitory Concentration 50
IGF1R	Insulin-like Growth Factor 1 R
IL	Interleukin
IRI	Irinotecan
ISH	In Situ Hybridization
LC3	Light Chain 3
Lgr5	Leucine-Rich Repeat Containing G Protein-Coupled Receptor 5
LKB1	Liver Kinase B1

LV	Leucovirin
mAb	monoclonal Antibody
MAPK	Mitogen- Activated Protein Kinase
mCRC	metastatic Colorectal Cancer
Met or MET	Metformin
MLH1	MutL Homolog 1
MMP	Matrix Metalloproteinases
MMR	Mismatch Repair
MSH2	MutS Homolog 2
MSI	Microsatellite Instability
mTOR	mammalian Target Of Rapamycin
MTT	3-[4,5-Dimethylthiazol-2-yl]-2,5-diphenyltetrazolium bromide
NADH	Nicotinamide Adenine Dinucleotide Hydride
NCCN	National Comprehensive Cancer Network
NF-κB	Nuclear Factor kappa B
OCT1	Organic Cation Transporter 1
OS	Overall Survival
OXA	Oxaliplatin
PARP	Poly (ADP-Ribose) polymerase protein
PDGFR	Platelet Derived Growth Factors Receptor
PFS	Progression Free Survival
PI3KCA	Phosphatidylinositol-4,5-Bisphosphate 3-Kinase Catalytic subunit Alpha
PMS1	Postmeiotic Segregation increased 1
PTEN	Phosphatase and Tensin homolog
qRT-PCR	Quantitative Real-Time PCR
R	Rescued
REDD1	Regulated in Development and DNA Damage responses 1
ROS	Reactive Oxygen Species
RR	Response Rate
S6	40S ribosomal protein subunit S6 kinase
SD	Standard Deviation
SMAD	Small Mother Against Decapentaplegic
TGFβ	Transforming Growth Factor-β
TGFβIIR	TGF-β type II Receptor
TNF-α	Tumour Necrosis Factor α
TSC	Tuberous Sclerosis Complex
TUNEL	Terminal deoxynucleotidyl transferase dUTP Nick End Labeling
VEGF	Vascular Endothelial Growth Factor
WT	Wild Type

ABSTRACT

The aim of this project was to investigate the anticancer activity of the anti-diabetic drug metformin, individually or combined in various settings with chemotherapy, on *in vitro* models of colorectal cancer (CRC). I found that metformin reduced cell proliferation by inducing cell cycle arrest in the G0/G1 phase, but did not lead to cell death. The anti-proliferative action of metformin resulted mediated by the inactivation of the mTOR pathway and of IGF1R protein. However, the drug only transiently arrested cell growth, since its effects were reversed after drug removal.

When I combined the biguanide with the chemotherapy drugs commonly used to treat CRC I observed different responses in the cell lines analysed that reflected their genetic background and their different sensitivities to both the biguanide and chemotherapy. I found that metformin added before chemotherapy drugs antagonised their effects in the majority of the treatments. On the contrary, its administration after long chemotherapeutic treatments significantly reduced the cell viability. I noted that metformin better inhibits cell proliferation in cell lines with rapid growth.

I have also assessed the dual treatment combination of metformin with different drugs that target specific genes or proteins (targeted therapies), focusing on BRAF-mutant cell lines. For most of the tested treatments the simultaneous administration of metformin and target drugs gave no advantages over the single drugs, and often resulted in antagonism.

Overall, our results show that although further investigations are still needed to elucidate the results of the treaments including metformin, these data suggest that caution should be used in administering chemotherapy to indviduals taking metformin.

CHAPTER 1
INTRODUCTION

1.1 Colorectal cancer

Colorectal cancer (CRC) is the third most common worldwide cancer in men, after lung and prostate cancer, and the second in women, after breast cancer (Ferlay et al., 2015). CRC is the fourth leading cause of cancer-related deaths with an estimated incidence of 1.4 million new cases and a mortality of >690,000 deaths annually. The incidence of the disease is influenced by several factors, such as geographical location and ethnicity (for example, African Americans are the racial group with the highest incidence of CRC in the United States and Ashkenazi Jews are the ethnic group with the highest risks of CRC; American Cancer Society), gender (incidence rate in men is higher by 35-40%) and age (more common in those over 50 years). The highest rates are found in Europe, North America, Japan and Oceania. CRC is increasing rapidly in Latin America, Asia and Eastern Europe (Torre et al., 2016), reflecting the adoption in these countries of western lifestyles such as the intake of high-fat diets, physical inactivity and smoking. In the United States, Oceania and Europe the introduction of established screening tests that allow the early detection, and consequent removal, of precancerous lesions has decreased incidence of CRC. On the contrary, in Central America, South America and Eastern Europe, where screening procedures have not yet been adopted, CRC continues to increase.

1.1.1 Risk factors for colorectal cancer

Risk factors for CRC can be divided into modifiable, which are part of the diet and lifestyle (smoking, obesity, alcohol, physical inactivity and diabetes), and non-modifiable, that include age, gender and genetic or hereditary factors.

Smokers and ex-smokers have an increased risk of incidence and mortality for CRC with respect to non-smoker individuals. Alcohol abuse appears to be related to alterations of mechanisms of DNA methylation, leading to changes in intestinal absorption, metabolism, and renal excretion of folates.

As for obesity, in obese individuals the excess of adipose tissue can produce hormones such as insulin or oestrogens, which may promote carcinogenic mechanisms. The high consumption of fat and proteins (especially from animals), in particular the excessive consumption of red or processed meat, increases the risk of CRC. In contrast, a diet rich in fibers, mainly derived from fruits and vegetables, seems protective against CRC. Fibers can absorb faecal carcinogens, reduce faecal transit time and increase the production of short chain fatty acids (which increase the absorption of sodium and water in the colon), all processes associated with a lower risk of neoplastic transformation. Finally, a physically active lifestyle that improves immune functions, reduces inflammation and insulin levels diminishes CRC risk. Taken together, changes in diet and lifestyle integrated with preventive screenings represent potential prevention tools for CRC.

As regards the non-modifiable risk factors, CRC incidence and death rates increase with age, and they are higher in men than in women (American Cancer Society).

1.1.2 Histopathological characteristics of colorectal cancer

The intestinal epithelium is formed by a one cell depth layer in many sites, and this population of cells is in constant flux to maintain homeostasis of cell renewal process, in which cell proliferation, differentiation and apoptosis of enterocytes is highly regulated both spatially and temporally (Senda et al., 2007). Epithelial cells are anchored on a basement membrane (basal lamina) that forms part of the extracellular matrix and is assembled from proteins secreted by both epithelial and stromal cells, mostly fibroblast, lying beneath the membrane. Other cell types including endothelial cells, which form the walls of capillaries, lymphatic vessels and immune cells are also present. Beneath this

layer of stromal cells there is a thick layer of smooth muscles responsible for intestinal peristalsis through periodic contractions (Weinberg 2007).

Most of the pathological changes associated with the development of colon cancer occur in the epithelial layer, which undergoes transformation through a series of intermediate steps from carcinoma, where it is possible to observe a variety of tissue states with different degrees of abnormality, to mildly deviant tissues and high malignancy state, and later into multiple metastatic growths (Figure 1).

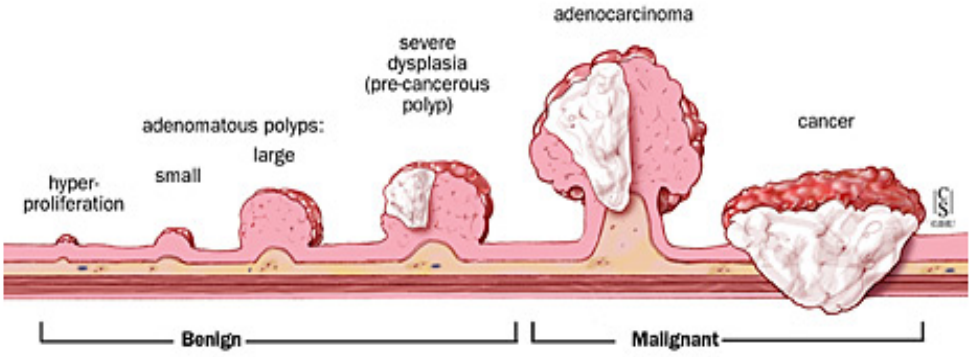

Figure 1. Progression from polyp to cancer (modified from John Hopkins Medicine Colorectal Cancer http://www.hopkinscoloncancercenter.org).

Focusing on the histopathological alterations of the colonic epithelium, there are some hyperplastic areas where epithelial cell proliferation is unusually high although the individual cells have normal phenotype. Other areas are characterized by growth with abnormal histologies and it is not possible to identify the well-ordered cell layer typical of the normal colonic epithelium and where the morphology of the individual cells is deviating from that of normal cells.

During further stages of progression deviant growth that forms adenoma is observed (Weinberg 2007). All these forms are considered benign until they pass through the basal membrane and invade the underlying tissues and cells switch into a malignant direction and the deeper they penetrate into the stromal layers, the higher is the risk that they can migrate to anatomically distant sites in the body, and metastasize.

1.1.3 Genetics of colorectal cancer

About 70-75% of CRCs are sporadic (i.e. occurs following the acquisition of somatic mutations), and the remaining 20-25% can be familial (if the affected individuals are in close degree) or hereditary (if germline mutations are present and can be transmitted between generations). Hereditary factors that increase CRC risk include a personal or family history of CRC and/or polyps, a personal history of inflammatory bowel disease, and different inherited genetic conditions. About 5% of all CRCs present a hereditary origin, the most common types are Hereditary Non-Polyposis Colorectal Cancer (HNPCC, also named Lynch syndrome) and familial adenomatous polyposis (FAP). HNPCC, the most common form of hereditary colorectal cancer (3-4% of all cases), is an autosomal dominant disease caused by germline mutations in the DNA mismatch repair (MMR) genes, mainly *MSH2* and *6*, *MLH1* and *3* and *PMS1* and *2,* leading to microsatellite instability (MSI; Fearon 2011). HNPCC patients may also develop endometrial, ovarian, stomach, small intestine, pancreas, brain and upper urinary tract tumours. FAP is an autosomal dominant disease characterized by the development of hundreds to thousands of colonic adenomas (polyps) of different sizes that can evolve to CRC when not treated. FAP is caused by germline mutations in the tumour suppressor gene Adenomatous Polyposis Coli (*APC*) that regulates the degradation of β-catenin in the Wnt pathway. Loss of *APC* function increases the transcription of β-catenin target genes, including *c-MYC*, resulting in cell proliferation, which increases the probability of transformation of polyps into cancerous polyps.

Familial CRC is probably related to inheritance, but the genetic loci responsible for the risk genotype are mainly unknown. It is likely to be caused by alterations in genes that are less penetrant, but more common that those associated with the familiar syndromes. Polymorphisms in genes that regulate metabolism or in genes regulated by environmental factors could be related to familiar predisposition to CRC. Sibling studies and studies with

parent/child pairs have estimated that up to 35% of all CRC cases can be attributed to genetic susceptibility (Lichtenstein et al., 2000).

1.1.3.1 Vogelgram – a progression model for colorectal cancer

The adenoma-carcinoma transition is a model of CRC development in which specific somatic mutations promoting tumorigenesis were acquired. Sporadic tumours can be caused by chromosomal instability (CIN, an unbalance in chromosome number provoked by amplifications or losses of chromosomal regions) present in 80-85% of cases of CRC, follow the model proposed by Fearon and Vogelstein (Vogelgram) according to which any transition from normal mucosa to carcinoma involves specific and well-defined alterations in oncogenes or tumour suppressor genes (Fearon et Vogelstein, 1990; Figure 2).

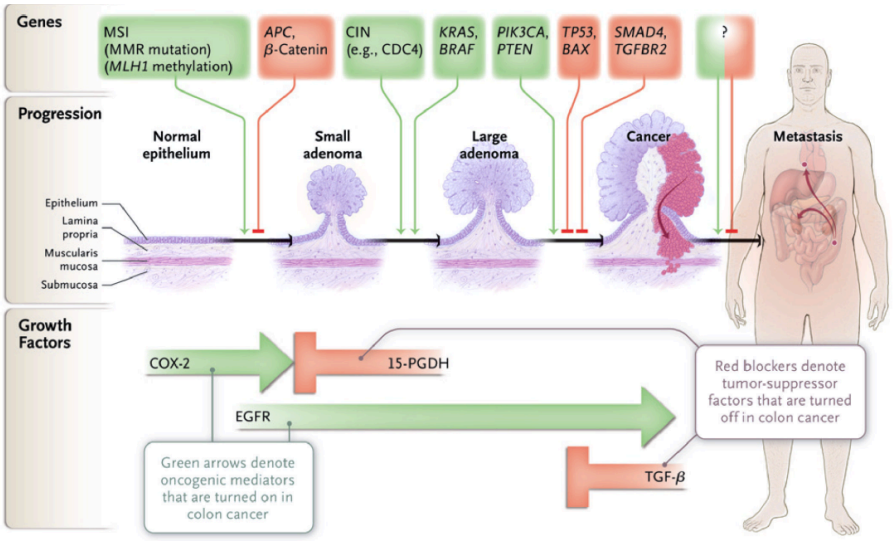

Figure 2. Vogelgram. Transformation of normal colon epithelium into malignant carcinoma by step-wise accumulation of genetic aberrations. Adapted from Markowitz and Bertagnolli 2009.

The Vogelgram suggests that the adenoma to carcinoma sequence is initiated by alterations in the *APC* gene, followed by mutations in *KRAS* or *BRAF* genes, *PI3KCA* or *PTEN*, mutations or loss of *TTP53* gene and of SMAD family member 4 (*SMAD4*).

Two mutations in *APC* are required for the initiation of colorectal carcinogenesis, in agreement with the hypothesis of the "two-hits" of Knudson (Knudson, 1993). Loss of

APC gene, which also controls cell growth, leads to the formation of the typical small benign polyps. The best-known role of the APC protein is to regulate the levels of β-catenin in the Wnt pathway, where APC is part of multi protein complex APC-axin-GSK3β that interacts with β-catenin causing its phosphorylation, ubiquitination and consequent degradation in the proteasome (Barker, 2008; Figure 3 left panel). Mutations in *APC* gene prevent the formation of the APC-axin-GSK3β complex, allowing β-catenin to accumulate in the cytoplasm and then translocate to the nucleus. In the nucleus β-catenin can interact with several transcription factors of the T-Cell Factor Family, promoting the transcription of genes that regulate cell cycle and proliferation such as *cyclin D* and *c-MYC*, and genes related to tumour progression as metalloproteinases *MMP7* and *MMP26* (Figure 3 right panel).

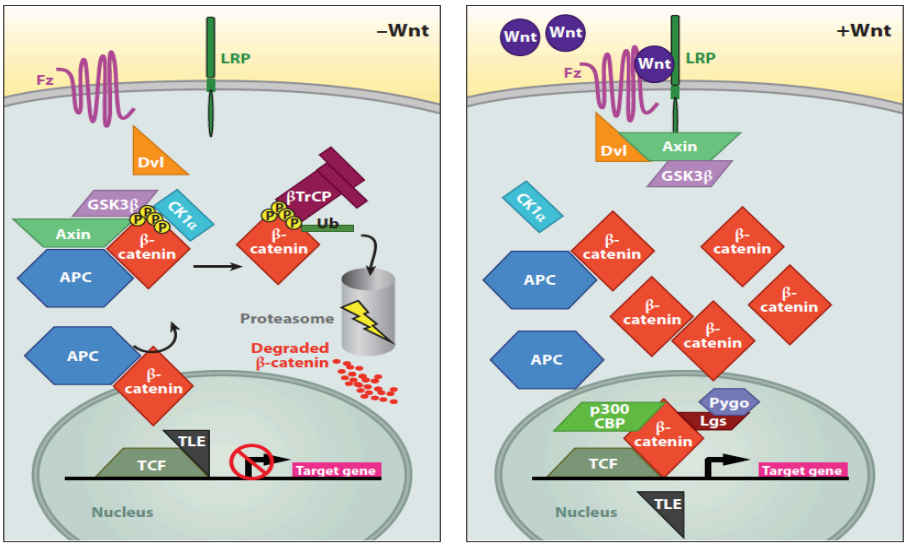

Figure 3. Wnt signalling pathway. In absence of Wnt ligand β-catenin can be phosphorylated for proteasome degradation (left panel). In the presence of Wnt ligand or of inactivating mutations on APC protein, Wnt signalling is activated and the oncoprotein β-catenin regulates genes involved in cancer progression (Fearon, 2011).

Other mutations that lead to cancer progression are found in the *KRAS* and *BRAF* genes. In normal cells RAS and BRAF proteins are activated in response to extracellular signals and act as molecular switch in the cell proliferation, specifically by activating the MAPK

pathway. *KRAS* mutations, that constitutively activate the gene and cause adenomas progression, were detected in about 50% of CRCs, BRAF mutations in 5-10 % of CRCs.

Other somatic mutations can occur in PI3KCA gene and lead to activation of PI3K signalling. The deregulation of this pathway can also occur after loss of the tumour suppressor gene *PTEN* that acts as inhibitor of PI3K signalling (Markowitz and Bertagnolli 2009).

The progression to carcinoma continues as a result of inactivation or loss of tumour suppressor gene *TP53*, which suppresses cell division or induces apoptosis in response to stress damage, driving progression to carcinoma (Kinzler and Vogelstein, 2002).

Finally the loss of some genes mapping on chromosome 18q has an oncogenic effect in the gastrointestinal system (Taketo et al., 2000). Among the lost genes, *DCC* encodes for a transmembrane protein acting as receptor for netrins (factors involved in axonal guidance in the nervous system) involved in the regulation of apoptosis (Arakawa, 2004). Other tumour suppressor genes on chromosome 18q are S*MAD2* and *SMAD4*, which act as signal transducers in the Transforming Growth Factor β (TGF-β) signalling pathway (Montgomery et al., 2001). Moreover, inactivating mutations in the TGF-β type II receptor (TGFβIIR) are found in one third of CRCs (Markowitz et al., 1995).

1.1.4 Colorectal cancer stem cells

Stem cells, present in adult tissues, are characterised by self-renewal and multipotency. Lineage tracing experiments have shown that in the intestinal epithelium the stem cells reside at the bottom of the crypts (the base of glands) and symmetrically divide from a single clone (Winton et al., 1988); they are constantly renewed and migrate from the crypt base, towards the crypt-villus axis and (Snippert al al., 2010). Stem cells can be traced using endogenous molecular markers such as leucine-rich repeat (LRR)-containing G-protein-coupled receptor 5 (Lgr5) gene they express (Barker et al., 2007; Figure 4).

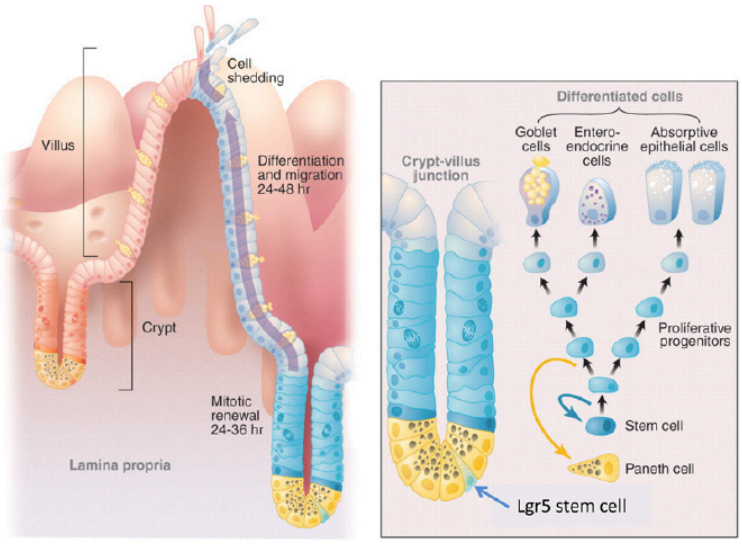

Figure 4. Organization of the intestinal epithelium. The intestinal epithelium consists of repetitions of villus-crypt units (left panel). At the crypt base Lgr5 positive cells represent the stem component and are intercalated with Paneth cells. Lgr5-expressing stem cells lead to the production of highly proliferative progenitors of differentiated cells that migrate along the crypt-villus axis (right panel). Adapted from de Lau et al., 2014.

The identification of Lgr5 positive cells as intestinal stem cells was provided by *in vivo* Lgr5-based lineage tracing experiments (Barker et al., 2007). Through this technique candidate stem cells are marked and the cells descendants, inheriting the same marker, can be visualised. Because the marker was present in all epithelial cells, Lgr5-positive cells have been established as self-renewing and multipotent population of adult intestinal stem cells. Moreover it was demonstrated that single Lgr5-positive cells can generate and maintain the stem-cell hierarchy in *in vitro* matrigel culture systems (Sato et al., 2009).

Lgr5 is encoded by a Wnt target gene and constitutes a facultative component of the Wnt receptor complex (de Wetering et al., 2002, de Fllier et al., 2007, de Lau et al., 2011). The Wnt signalling plays indeed a pivotal role in stem cells maintenance and its deregulation in the stem compartment can lead to adenoma formation (Barker et al., 2009).

Other well established CRC stemness markers are CD133 and CD44, both related to Wnt pathway: CD133 positive cells express high levels of β-catenin (Kawamoto et al., 2010) and CD44 is a gene targeted by β-catenin (Wielenga et al., 1999).

CD133 is a transmembrane glycoprotein with yet unclear function. In CRC it can promote tumour growth with self-renewal capability (O'Brien et al., 2007, Ricci et al., 2007). CD44 is a transmembrane glycoprotein involved in cell-cell and cell-matrix interaction (Sahlberg et al., 2014). Dalerba et al. demonstrated that in human CRC xenografts, tumours derived from CD44 positive cells maintained a differentiated phenotype and reproduced the morphology and phenotype of their parental lesions (Dalerba et al., 2007).

1.1.5 Colorectal cancer stages

The classification of cancer lesions is the most important prognostic predictor of the clinical outcome in patients with CRC. The staging system used for CRC is the American Joint Committee on Cancer (AJCC) TNM system. The TNM system is based on tumour infiltration degree and discriminates to which of the intestinal wall layer tumour has arrived (T), if it has spread to regional lymph nodes (N) and/or it has invaded other organs resulting in metastases (M; American Cancer Society).

The transition from carcinoma in situ (Tis), in which the tumour does not exceed the *lamina propria*, to stage T1 invasive carcinoma occurs when the tumour comes to the *submucosa*. Following the sequential invasion of *muscularis* and *subserosal mucosa,* the progression to the next stages T2 and T3 happens. Finally, the T4 stage occurs when the cancer invades other organs and / or perforates visceral peritoneum (Figure 5).

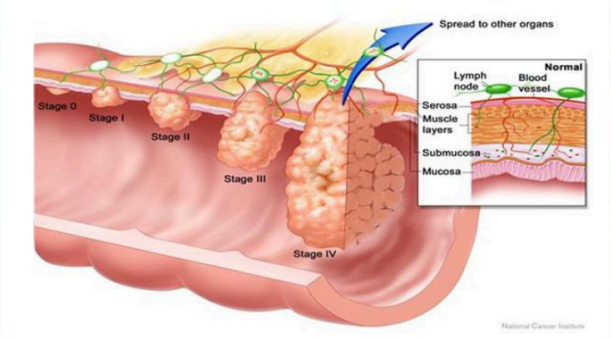

Figure 5. Stages of colorectal cancer. Image from National Institute of Health (NIH) and National Cancer Institute (NCI).

The detection of any positive lymph node is critical to predict the outcome of patients. It is therefore necessary to examine an adequate number of regional lymph nodes (at least 7-14). The TNM staging system for lymph nodes start from N0, classification for which the lymph nodes are metastases free. In N1 stage metastases are detected in 1-3 lymph nodes, in N2 metastases are found in 4 or more regional lymph nodes. Although CRC can metastasize in almost all organs, the liver and the lungs are the most common sites but it is usual to detect metastases in other segments of the colon, small intestine and peritoneum. The TNM staging for metastases has M0 and M1 values, indicating the presence or absence of metastases respectively. The TNM categories are combined in stage groups, ranging from 0 (in situ tumour) to IV (distant metastasis; Table 1).

Table 1. TNM staging of colorectal cancer

TNM stage	T	N	M
0	Tis	N0	M0
I	T1- T2	N0	M0
IIA	T3	N0	M0
IIB	T4	N0	M0
IIIA	T1-T2	N1	M0
IIIB	T3-T4	N1	M0
IIIC	any T	N2	M0
IV	any T	any N	M1

The staging degree is inversely proportional to the probability of survival. In fact, the survival rate at 5 years passes from 75-80% in individuals with stage I diagnosis to 15% in individuals with stage IIIC diagnosis (Gunderson et al., 2010). In stage IV the 5-year survival after diagnosis is less than 5%.

1.1.6 Treatments for Colorectal Cancer

Four key approaches are currently used for the treatment of CRC: surgery, chemotherapy, radiotherapy and targeted therapies. Treatment for colon cancer is based largely on the stage (extent) of the cancer, and people with early stage disease (stage I and II) usually have surgery as the main or first treatment, in some cases followed by adjuvant chemo or radiation therapies. Adjuvant therapy is the standard of care for patients with stage III disease, which have a high survival benefit. Patients with metastatic disease (stage IV) require chemotherapy or targeted therapies combined with surgery, where appropriate.

1.1.6.1 Chemotherapy

Chemotherapeutic agents include fluoropyrimidines (5-Fluorouracil (5-FU) and capecitabine), oxaliplatin and irinotecan (Meyerhardt et Mayer, 2005, Koopman et al., 2007, Seymour et al., 2007, Kelly and Cassidy 2007).

5-FU remains the most widely used chemotherapeutic agent for the treatment of CRC. Following metabolic activation to 5-fluoro-2′-deoxyuridylate, this fluorinated pyrimidine combines with methylenetetrahydrofolate to form a ternary complex with thymidylate synthase, an enzyme involved in pyrimidines synthesis, thus interfering with DNA synthesis by inhibiting the conversion of deoxyuridylate to thymidylate. 5-FU is often given with Leucovirin (LV, also called folinic acid) to improve the effect of the chemotherapy drug. Capecitabine is a precursor of 5-FU that is converted to 5-FU through three sequential enzymatic reactions. The final enzyme in the pathway, thymidine phosphorylase (TP), is believed to be present at very high levels in tumour tissue, thus increasing both the efficacy and tolerability of the agent through targeted delivery.

Oxaliplatin, a platinum analogue, forms intra- and inter-strand DNA adducts, leading to inhibition of DNA replication and transcription.

Irinotecan is a semi-synthetic derivative of the natural alkaloid camptothecin, which inhibits the activity of Topoisomerase I, a nuclear enzyme involved in DNA synthesis.

During DNA replication, Topoisomerase I relaxes the supercoiled DNA helix with reversible and transient single-stranded DNA breaks. The active metabolite of irinotecan (SN-38) stabilizes the DNA–topoisomerase complex, resulting in replication arrest and apoptosis.

Current international guidelines (National Comprehensive Cancer Network, NCCN) suggest the use of these chemotherapy agents alone or in combinations (NCCN guidelines 2015). According to NCCN guidelines the drugs, to increase their effectiveness, can be combined in the following regimens: FOLFOX (5-FU/LV/oxaliplatin), FOLFIRI (5-FU/LV/irinotecan), CapeOx (Capecitabine/oxaliplatin) and FOLFOXIRI (5-FU/LV/oxaliplatin/irinotecan). In fact, patients treated with regimens seem to have an increase in overall survival (OS) and in progression free survival (PFS), compared with patients treated with single chemotherapeutic agents (Rodrigues et al., 2016, Doullard et al., 2000, Grothey et al., 2004).

1.1.6.2 Targeted therapies for colorectal cancer

Targeted cancer therapies include drugs or other substances that block the growth and spread of cancer by interfering with specific molecules ("molecular targets") that are involved in the growth, progression and spread of cancer. Targeted therapies are often cytostatic. Used alone or in combination with chemotherapy, these therapies have been proven to increase the OS in patients with metastatic CRC (mCRC). Many targeted cancer therapies have been approved by the Food and Drug Administration (FDA) to treat specific types of cancer. As for mCRC, the current FDA-approved targeted therapies can be divided into three groups: inhibitors of angiogenesis targeting Vascular Endothelial Growth Factor (VEGF) or its receptors, monoclonal antibodies (mAbs) against Epidermal Growth Factor Receptor (EGFR) and inhibitors of kinases involved in various signalling cascades [VEGF receptors, RET, KIT, Platelet Derived Growth Factors Receptor (PDGFR), and Raf kinases]. Others are being studied in clinical trials, and many more are

in preclinical testing.

VEGF is the most important factor regulating tumour angiogenesis (Ferrara et al., 2003). The drug developed to inhibit the VEGF signalling processes is Bevacizumab, a recombinant humanised mAb that specifically targets circulating VEGF-A, which is synthesised during tumour growth. Bevacizumab prevents VEGF from interacting with appropriate receptors in vascular endothelial cells, resulting in diminished cell signalling pathways that enhance angiogenesis (Ferrara et al., 2004). The mAb, when administered in combination with chemotherapy increases the activity of any active cytotoxic regimen and improves OS, response rate (RR) and PFS in patients with mCRC (Saltz et al., 2008, Bennouna et al., 2013).

Cetuximab and panitumumab are two EGFR antagonists, chimeric and fully humanized mAbs respectively. Both antibodies prevent EGFR auto-phosphorylation by binding to the extracellular domain and thus inhibiting activation of the downstream cell signalling pathways of MAPK and PI3K/Akt involved in proliferation and cell survival respectively (Ciardiello and Tortora 2008). Cetuximab and panitumumab are active in different lines of treatment and in various combinations and patients treated with anti-EGFR mAbs administered with FOLFOX or FOLFIRI regimens show a significantly improved RR, OS and PFS (Venook et al., 2006, Douillard et al., 2010, Bokemeyer et al., 2014). However their benefit, either as a single agent or in combination with any chemotherapy regimen, is limited to patients in whom a *RAS* mutation is excluded. *KRAS* oncogenic mutations, seen in 35-45% of CRCs, occurring prevalently in the codons 12 and 13 of exon 2, exclude patients from cetuximab/panitumumab therapies. In fact, the anti-EGFR drugs are currently indicated only in patients with wild type *RAS* (Lievre et al., 2006, De Roock et al., 2010, Van Cutsem et al., 2015). An 'expanded RAS' analysis that also includes additional mutations in exons 3 and 4 of the KRAS gene and in exons 2–4 of *NRAS* gene that reduce the efficacy of anti-EGFR treatments has improved the efficacy of the treatment (Bokemeyer et al., 2014).

Regorafenib is a multikinase inhibitor that blocks the activity of multiple protein kinases involved in the regulation of angiogenesis (VEGFR-1, -2, -3, angiopoietin-1 receptor), oncogenesis (KIT, RET, BRAF, including BRAF V600E) and of tumour microenvironment (PDGFR-β, Fibroblast growth factor receptor (FGFR; Wilhelm et al., 2011). In patients with mCRC refractory to standard chemotherapy, treatment with regorafenib increased median RR, OS and PFS (Grothey et al., 2013).

1.1.6.2.1 New targeted therapies for colorectal cancer

Although patients are eligible for the therapies described, not all respond to them. To fill up this gap, increasing new targeted therapies for CRC are emerging, concurrently to the identification of biological markers that can predict the response to therapy.

BRAF, involved in EGFR signalling, is mutated in 5-10% of CRC (Tol et al., 2009). The most common mutation V600E leads to constitutively activation of the kinase protein, conferring a very poor prognosis. Clinical results with the selective BRAF V600E inhibitor vemurafenib as single agent in CRC have been disappointing, although the inhibitor is very effective for melanoma treatment (Flaherty et al., 2010, Chapman et al., 2011, Sosman et al., 2012, Kopets et al., 2015). It has been observed that in CRC the inhibition of BRAF V600E caused a rapid feedback activation of the EGFR signalling pathway, through ERK activation, which is inhibited in melanoma. Therefore, combinatorial treatments with BRAF V600E and EGFR inhibitors appear a rational strategy and already seem to provide clinical benefits (Corcoran et al., 2012, Prahallad et al., 2012, Yaeger et al., 2015, Elez et al., 2015, Van Cutsen et al., 2015).

Recently, other *BRAF* mutations have been found at codons 594 or 596, which occur in <1% of CRCs. These mutations identify a molecular subtype unexplored with clinical and pathological features different from *BRAF* V600E mutated cases and characterised by a longer OS. *BRAF* 594 and 596 mutations cause only modest and indirect activation of the

MAPK pathway and preclinical and clinical data are suggestive of their potential sensitivity to anti-EGFR treatment (Cremolini et al., 2015).

Much attention has recently been directed to the inhibition of downstream components of the RAS/RAF/MAPK/MEK/ERK pathway. Different MEK 1/2 inhibitors, such as trametinib, and selumetinib, have already been approved for the treatment of mCRC. MEK inhibitors alone do not seem to be effective, but their combination with BRAF inhibitors can produce clinical benefits in metastatic patients with mutations in *BRAF* (Corcoran et al., 2015).

Other novel therapies in clinical development, targeting different pathways involved in cancer progression such as MET, mammalian target of rapamycin (mTOR), Wnt etc. are being developed and are summarised in Table 2 (Seow et al., 2016).

Table 2. Targeted therapies in clinical development for colorectal cancer.

Target gene	Type of drug
IGF1R	Dalotuzumab, Cixutumumab
MET	Tivantinib
PI3K	BKM120
mTOR	PF-05212384
Wnt pathway	OMP-18R5, OMP-24F28, PRI-724, WNT974
NOTCH	R04929097, PF-03084014
Sonic HedgeHog	Vismodegib

1.1.6.3 New frontiers: immunobased therapies

Immunotherapy approaches based on the exploitation of the immune system to treat cancer, have recently yielded various degrees of success to treat certain tumor types, including melanoma, lung and kidney. These approaches exploit the fact that cancer cells often have molecules on their surface (including PD-1/PD-L1 and CTLA-4/B7-1/B7-2)

that can be detected by the immune system and prevent immune T cells from killing cancer. When these proteins are blocked, T cells are able to kill cancer cells better. As shown by Le et al. in CRC immunotherapy seems to be effective only in the subset of MSI-high tumours that present an increased mutational load due to DNA mismatch-repair deficiencies that stimulates the immune system. Indeed, patients with mismatch repair-deficient CRC had better clinical response to PD-1 blockade by pembrolizumab than those whose CRC did not have mismatch-repair deficiencies (Le et al., 2015).

1.2 Metformin

The biguanide metformin (1,1-dimethylbiguanide hydrochloride) is a widely prescribed oral anti-hyperglycaemic agent used as first line treatment for patients with type 2 diabetes mellitus. In diabetic patients metformin can reduce the hepatic gluconeogenesis and increases glucose uptake and use in skeletal muscle. Compared to other anti-diabetic drugs metformin is well tolerated, it does not induce hypoglycaemia and has a low risk of causing lactic acidosis. Metformin is also used to treat polycystic ovarian syndrome, metabolic syndrome and for diabetes prevention (Pierotti et al., 2013).

1.2.1 Metformin as anticancer drug

Different retrospective studies showed that patients with type 2 diabetes treated with metformin have lower cancer incidence and/or reduced cancer mortality (Evans et al., 2005, Libby et al., 2009, Noto et al., 2012, Zhang et al., 2013), focusing the interest in metformin as anticancer agent. The mechanisms through which metformin seems to promote anticancer effects can be either indirect or systemic, that modulate metabolic whole body physiology, or direct, which acts directly on cancer cells inhibiting cancer progression.

1.2.1.1 Indirect or systemic effects of metformin on cancer cells

The liver, exposed to high levels of the drug after oral administration, is considered the main target organ of metformin. In fact, hepatocytes express high levels of the cell surface organic cation transporter 1 (OCT1), necessary for the active transport of metformin (which is positively charged) into the cells (Gong et al., 2012). Inside the cell, mitochondria seem to be the primary target of metformin (El-Mir et al., 2000), in which the drug inhibits the respiratory complex I causing reduction of the synthesis of ATP and oxidation of NADH. The depletion of ATP production and the concomitant increase in the levels of AMP induces the activation of the cell energy sensor 5'-AMP-activated protein kinase (AMPK; Zhou et al., 2000). When activated, AMPK down-regulates the processes that require ATP, such as protein synthesis, and promotes catabolic pathways that generate ATP. This energy stress leads to a decrease of hepatic gluconeogenesis (Minassian et al., 1998) with a consequent reduction of the circulating glucose and insulin levels. The reduction of haematic levels of glucose is also a consequence of increase of sugar uptake in skeletal muscle caused by the metformin-induced membrane translocation of the glucose transporter GLUT-4 specifically expressed in this tissue (Fischer et al., 1995). Because elevated serum levels of insulin and insulin-like growth factor-1 (IGF-1) are often necessary to sustain the growth and survival of cells in different cancer types, the systemic reduction of these hormones can impair malignant growth (Pollak, 2012; Figure 6).

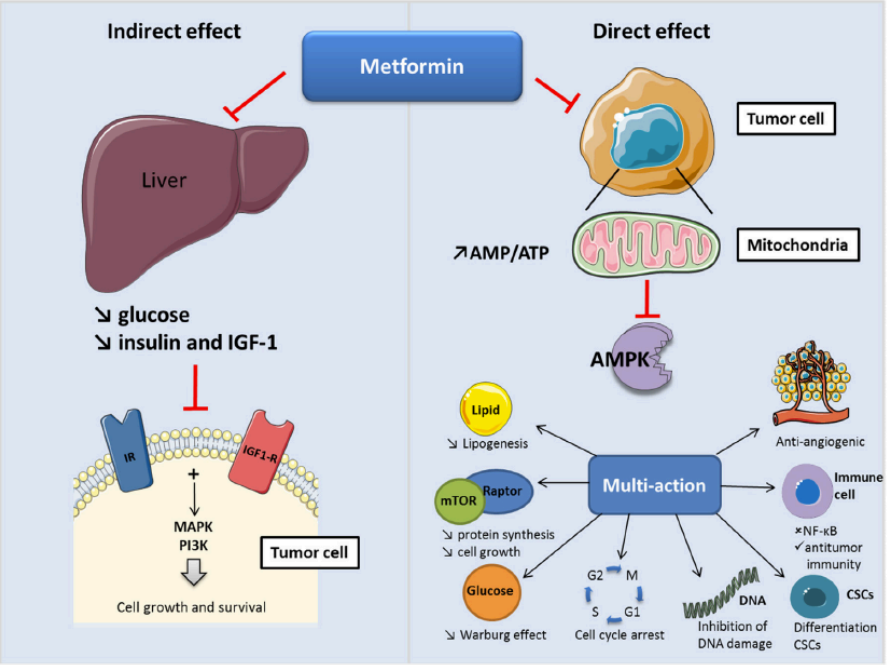

Figure 6. Antineoplastic mechanisms of action of metformin. Metformin indirect (left) and direct (right) effects are shown. Adapted from Daugan et al., 2016.

1.2.1.2 Direct effects of metformin on cancer cells

The direct anticancer effects of metformin can be differentiated in AMPK-dependent and AMPK-independent. AMPK can be directly activated by the previously described increase of AMP/ATP ratio, or indirectly, through its upstream regulator serine/threonine liver kinase B1 (LKB1; Woods et al., 2003). The activated form of AMPK suppresses the mammalian target of rapamycin (mTOR) pathway either through the phosphorylation and activation of tuberous sclerosis complex 2 (TSC2) that in turn inhibits the mTOR activator Rheb (Inoki et al., 2003) or by phosphorylation of Raptor, a positive regulator of mTOR (Gwinn et al., 2008). The block of mTOR inhibits the activation of its downstream target 40S ribosomal protein subunit S6 kinase (S6K or S6) and of the translational repressor 4E-binding protein 1 (4E-BP1), inactivated by mTOR mediated phosphorylation (Pierotti et al., 2013; Figure 7).

Metformin can also inhibit mTOR signalling independently from AMPK activation by suppressing the Ragulatory complex, consisting of the RAG family of GTPases (Kalender

et al., 2010), or by activating the negative regulator of mTOR regulated in development and DNA damage responses 1 (REDD1; Ben Sahra et al., 2011; Figure 7).

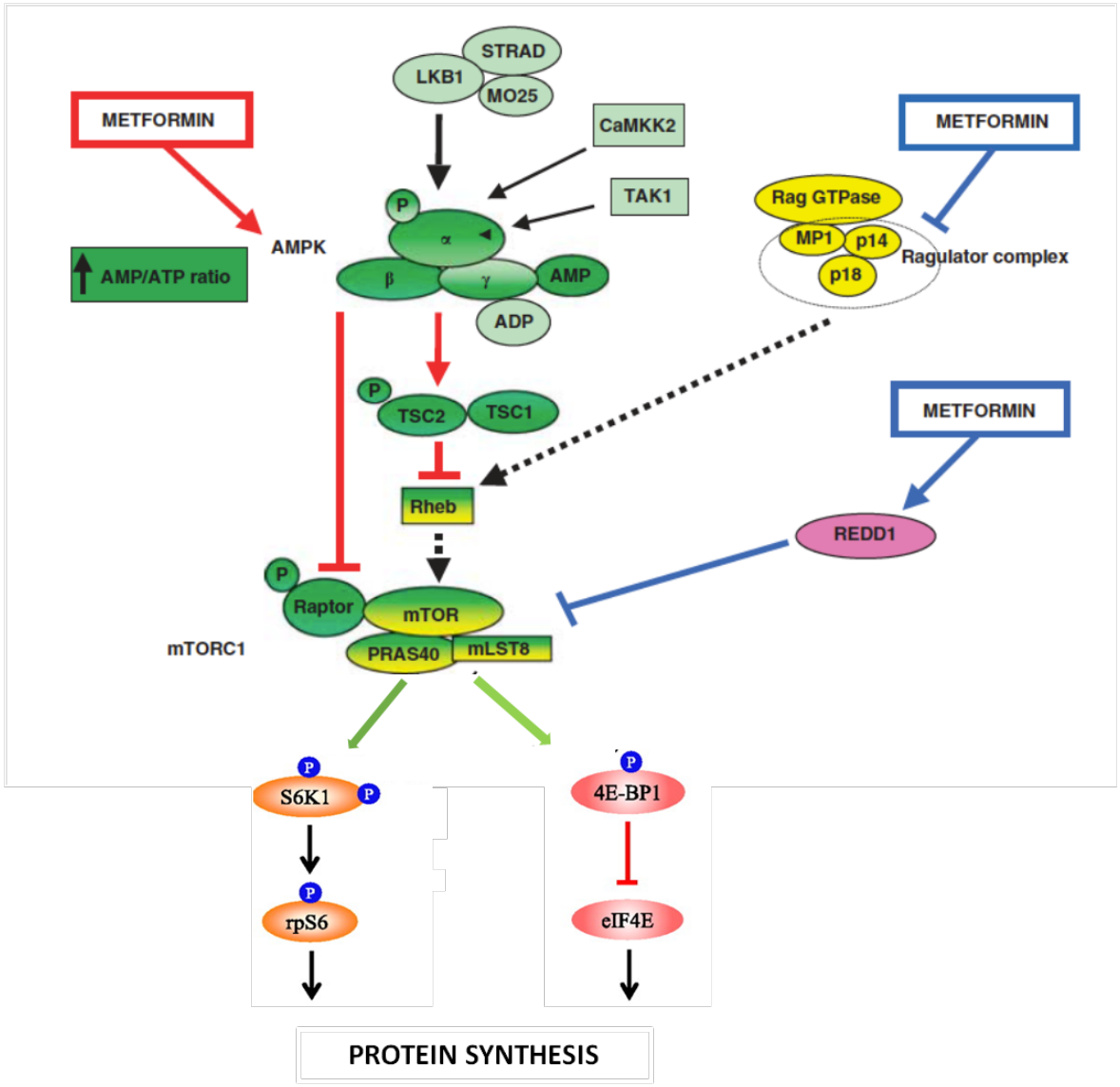

Figure 7. Metformin mechanisms of actions. AMPK dependent mechanisms are marked as red lines, AMPK-independent mechanisms as blue lines. Adapted from Pierotti et al., 2013.

The inhibition of protein synthesis via mTOR is only one of the mechanisms by which metformin can reduce cancer growth (Figure 6). Metformin exerts an inhibitory effect on glucose metabolism; in fact it can revert the Warburg effect, present in most cancer cells, either through the decrease of the glycolytic enzyme hexokinase 2 (HK2; Salani et al., 2014) or through the suppression of oncogenes such as c-Myc, Akt and hypoxia-inducible factor 1 α (HIF-1α that support the glycolytic phenotype (Daugan et al., 2016). The

metformin-induced AMPK activation can reduce enzymes involved in fatty acids biosynthesis as acetyl-CoA carboxylase (ACC) and fatty acid synthase (FAS), reducing energy supply and counteracting tumour progression (Algire et al., 2010, Lettieri et al., 2014). The biguanide can also promote cell cycle arrest through AMPK-mediated activation of TP53 and reduction of cyclin D1 expression (Ben Sahra et al., 2008, Zhuang et al., 2008, Alimova et al., 2009, Fujihara et al., 2015). It has also been reported that metformin can reduce the risk of mutagenesis in cancer cells, that can be escaped either by the inhibition of reactive oxygen species (ROS) in the mitochondria production or through the activation of ataxia telangiectasia mutated (ATM) protein, a tumour suppressor involved in DNA repair (Algire et al., 2012, Vazquez-Martin et al., 2011). Metformin can also inhibit the inflammatory signalling that promotes carcinogenesis by suppressing different pro-inflammatory cytokines such as tumour necrosis factor αTNF-α, nuclear factor kappa B (NF-κB) and interleukin 6 (IL-6; Takemura et al., 2007, Hirsch et al., 2013). The anti-angiogenetic effect of metformin is linked to reduction of the main factors involved in vascular remodelling such as VEGF and HIF-1α (Joe et al., 2015, Tadakawa et al., 2015). Finally it was also observed that metformin treatment can selectively target cancer stem cells (CSCs), a tumour sub-population characterised by self-renewal capacity, resistance to chemotherapy and increase in cancer recurrence (Hirsch et al., 2009, Vazquez-Martin et al., 2010, Song et al., 2012, Bao et al., 2012, Shank et al., 2012, Hirsch et al., 2013, Kim et al., 2014).

1.2.2 Metformin in CRC

Several studies have shown that metformin can be used for the treatment of CRC. Epidemiological evidences showed that patients with type 2 diabetes taking metformin had a lower risk of cancer incidence when compared with patients treated with other anti-diabetic drugs (Libby et al., 2009, Zhang et al., 2011, Garrett et al., 2012, Lee et al., 2012, Spillane et al., 2013). *In vitro* studies demonstrated that metformin can inhibit the

proliferation of CRC cells through AMPK activation (Zakikhani et al., 2008). *In vivo* models showed that metformin suppressed the development of intestinal polyps in in APC $^{Min/+}$ mice, a model of FAP (Tomimoto et al., 2008) and also inhibited the formation of intestinal aberrant crypt foci in a chemical carcinogen-induced mouse model (Hosono et al., 2010). Buzzai et al. demonstrated that metformin can selectively inhibit tumour growth and increase apoptosis in a mouse model of *TTP53* deficient CRC (Buzzai et al., 2007). Finally, Algire et al. showed that in mice fed with a high-energy diet metformin inhibited the growth of colon carcinomas and reduced insulin levels (Algire et al., 2010).

As regards the risk to develop CRC in non-diabetic patients, Hosono et al. demonstrated that the short term treatment with metformin administered at low doses (250 mg/day) suppressed the formation of rectal aberrant crypt foci (a surrogate marker for CRC) and decreased the proliferation of the colonic epithelium (Hosono et al., 2010).

Different studies combined metformin with other drugs in CRC. Nangia-Makker et al. demonstrated that metformin in combination with 5-FU and oxaliplatin promotes cell death in chemotherapy resistant CRC cell lines and inhibits their growth in an *in vivo* model (Nangia-Makker et al., 2014). Another study reported that combined treatment with metformin and 5-FU can reduce cell proliferation in chemo resistant CRC cell lines (Corti et al., 2015). Li et al. reported that combined use of metformin and vitamin D3 exerts a chemo-preventive effect reducing the number of rectal aberrant crypt foci in mice and rats (Li et al., 2015). Metformin in combination with 5-aminosalicylic acid increased apoptosis and inhibited inflammatory and metastatic pathways in CRC cell lines (Saber et al., 2015). Finally several clinical trials combining metformin with chemotherapy drugs are ongoing, for example: metformin plus irinotecan for refractory CRC (NCT01930864), metformin and 5-FU for refractory CRC (NCT01941953) and metformin in association with chemoradiotherapy for locally advanced rectal cancer (NCT02473094; Zhang et al., 2016).

CHAPTER 2
AIM OF THE STUDY

The aim of this thesis was to investigate the possible anticancer activity of metformin in *in vitro* models of CRC. In fact, although previous studies have shown that the drug inhibits the proliferation of CRC cells, its underlying mechanisms of action on CRC are still unclear.

I initially investigated the effects of metformin on four CRC cell lines characterized by different mutations at *LKB1, BRAF, KRAS* and *TP53* genes, and on 3D-organoids derived from a patient's peritoneal carcinomatosis. I evaluated: the proliferative potential of cells undergoing metformin treatment, changes in the expression of CRC stemness markers, cell cycle modifications, activation of modes of cellular death that could be induced by the drug, clonogenic capacity of the cells after metformin treatment and changes in the main biochemical pathways that could be targeted by the drug.

Then I studied the effects of metformin in combined settings with the standard chemotherapeutics drugs used in CRC: 5-FU, oxaliplatin and irinotecan. In particular I assessed if any combination of the biguanide with chemotherapeutic drugs could overcome the transient effect of metformin on cell proliferation I observed in the first part of the project.

Finally, I analyzed the biochemical effects of metformin and changes in the cell cycle in combination with different targeted drugs on BRAF-mutant CRC cell lines. BRAF-mutant tumours are characterised by a high proliferation rate, poor sensitivity to standard treatments, early development of resistance to targeted therapies and worse prognosis. Among the new therapeutic approaches, the combination of novel therapies for CRC with regulators of metabolism seems to be a promising strategy, to overcome resistance to the targeted therapies in BRAF-mutant CRC. For this reason, I studied the effects of the combination of metformin with targeted drugs on BRAF-mutant cell lines.

CHAPTER 3
MATERIALS AND METHODS

3.1 Genetics characteristics and culture conditions of the colorectal cancer cell lines

The cellular models used for the analysis of the effects of metformin in CRC were four cell lines characterised by different mutations frequently identified in CRC at *BRAF*, *KRAS* and *TP53* genes (all involved in CRC progression) and at *LKB1* gene (the main AMPK activator). HCT116*P53*-/- cells derived from the HCT116 cell line and carry a deletion of the region of chromosome 17 where *TP53* gene maps. The specific genetic features of the cell lines are summarised in Table 3.

Table 3. Genetic characteristics of the cell lines

	LKB1	***BRAF***	***KRAS***	***TP53***
HT29	WT	V600E	WT	R273H
HCT116	partially methylated	WT	G13D	WT
HCT116*P53*-/-	partially methylated	WT	G13D	null
DLD-1	methylated	WT	G13D	S241F

The analysis of the effects of metformin combined with the standard regimens was conducted on HT29 cells and on the two HCT116 cell lines.

Finally, three BRAF-mutant cell lines, differing for the type o BRAF mutation or for their mismatch repair activity, were used for the studing metformin in combination with the targeted therapies (Table 4). BRAF tumours carrying the common V600E mutation display a more aggressive phenotype than tumours with the rare G596R mutation. Indeed differences in MSI status seem to be associated with a different response to the therapies.

Table 4. BRAF and MSI status of the cell lines

	BRAF	MSI
HT29	V600E	MSS
RKO	V600E	MSI
NCI-H508	G596R	MSS

The cell lines HT29, HCT116, DLD-1, RKO and NCI-H508 were obtained from the collection available at IFOM (Istituto FIRC di Oncologia Molecolare, Milano). The HCT116*P53*-/- isogenic cell line, in which the *TP53* gene was inactivated by homologous recombination, was kindly provided by Professor Bert Vogelstein (Johns Hopkins University, Baltimore, USA). Each cell line was grown in a specific medium: HT29, HCT116 and HCT116*P53*-/- cell lines in McCoy's 5A medium (Modified) GlutaMAX^{TM} Supplement (Gibco) + 10% fetal bovine serum + 1% Penicillin-Streptamycin (Gibco); DLD-1 cells in RPMI (Gibco) + 10% fetal bovine serum + 1% Glutamine + 1% Penicillin-Streptamycin; RKO cells in MEM (Gibco) + 10% fetal bovine serum + 1% NEAA (MEM Non Essential Amino acids) + 1% Sodium Pyruvate + 1% Penicillin-Streptamycin; NCI-H508 cells in RPMI + 10% fetal bovine serum + 1% Glutamine + 1% Penicillin-Streptamycin. All cells were maintained as a monolayer in a humidified incubator at 37°C with a supply of 5% CO_2.

3.2 MTT viability assay

To test the cell viability, CRC cell lines were seeded into a 96 well plate (1500 - 3000 cells per well) in six replicates. After 24 hours cells were exposed to different concentrations of drugs: 0.16 - 20 mM for metformin (Sigma Aldrich); 0.3 - 64 μM for 5-FU (TEVA); 0.064 - 8 μM for oxaliplatin (Fresenius Kabi); 0.004 - 4 μM for irinotecan/SN-38 (Sigma Aldrich); 30 nM – 100 μM for dasatinib and regorafenib (Selleckchem); 0.007 nM – 0.12 μM for trametinib (Selleckchem); 7.75 nM - 20 μM for

vemurafenib (Selleckchem); 0.003 nM – 10 μM for panitumumab (Amgen). After the time points set for each experiment (72 hours for detection of the Inhibitory Concentration 50 (IC_{50}) and of the best concentrations combination of drugs; 96 – 144 hours for the sequential treatments with chemotherapy drugs) the cell proliferation rate was measured using an MTT (3-[4,5-Dimethylthiazol-2-yl]-2,5-diphenyltetrazolium bromide) assay, a colorimetric test for measuring the activity of enzymes produced by viable metabolically active cells that reduce MTT substrate to formazan, giving a purple colour. MTT powder (Sigma) was dissolved in the growth medium at the concentration of 1 mg/2 ml. After removal of the original medium, 100 μl of MTT solution were added to each well and incubated at 37°C. After two-three hours 100 μl of lysis buffer (10% SDS, HCl 0.01 M) was added to the MTT solution to dissolve the formazan crystals. Plates were then re-incubated at 37°C overnight under light protected conditions and the following day were read on a micro-plate reader (Infinite M200 TECAN) at a wavelength of 570 nm.

3.3 Colorectal cancer organoids derived from a peritoneal carcinomatosis

Organoids were derived from a peritoneal carcinomatosis (pc) obtained from a metastasis of a patient with stage IV, grade 3 CRC (a written informed consent to donate the tissues left over after the diagnostic procedures at Istituto Nazionale dei Tumori was provided).

The fresh aseptic surgical sample was minced into fragments and incubated with collagenase (Sigma) for three hours, after which the cell suspension was filtered through a 70 μM nylon mesh, treated with ACK (Ammonium-Chloride-Potassium) Lysing Buffer (Thermo Fisher), washed with RPMI medium supplemented with 0.5% BSA and seeded in a 100 x 200 mm tissue culture dish in DMEM/F-12 GlutaMAX^{TM} media (Gibco) + 1% Penicillin-Streptamycin. Approximately 15 days after seeding, spheroid cellular aggregates could be isolated and propagated. Organoids were maintained as suspension culture in a humidified incubator at 37°C with a supply of 5% CO_2.

Organoids culture was mainly composed of round-shaped cellular aggregates in which the cells exhibited adhesion loss and were organized in ring and/or ribbon-like structures. The corresponding tumour sample from which they were derived showed solid nests of poorly differentiated cells. Organoids showed a high expression of Ki-67 and the in situ hybridization (ISH) of Lgr5 marker showed that it was very focally expressed by some apical and peripheral cells.

Moreover, the mutation pattern of organoids in formalin fixed paraffin embedded (FFPE) sections reflected that in the original tumour sample (Table 5).

Table 5. Genetics characterization of the origin tumour and of the derived CRC-pc organoids

	LKB1	***BRAF***	***KRAS***	***TP53***
Surgical sample	N.D.	V600E	WT	R273H
CRC-pc organoids	WT	V600E	WT	R273H

N.D. not detected

3.4 Trypan blue viability assay

Organoids were disaggregated and seeded in triplicates into a 6 well plate (3-4 × 10^5 cells per well). After 24 hours they were treated with 5 mM metformin for 120 hours or left untreated. Fresh medium added with metformin was replaced every 24 hours. Cells were pelleted and disaggregated by vigorous pipetting in trypsin for 5-10 minutes. Disaggregated cells were put on ice and 50 ul in triplicate were added with an equal volume of trypan blue and loaded on a burker chamber for counting.

3.5 Bromodeoxyuridine (BrdU) proliferation assay

CRC cells were seeded at a concentration of 1 × 10^4 directly on 13 mm diameter coverslips (ThermoFisher Scientific). After 24 hours HT29, HCT116 and HCT116*P53*-/- cell lines were treated with 5 mM metformin and DLD-1 cells with 10 mM metformin,

dissolved in medium or left untreated for 24, 48 or 72 hours. Cells were incubated with 33 μM BrdU (Sigma Aldrich) dissolved in medium. After 2 hours coverslips were washed twice in 1X PBS and stored at 4°C. Cells were incubated 45 minutes with anti-BrdU primary antibody (BD Bioscience) diluted 1:5, and then they were treated 45 minutes with secondary antibody FITC-conjugated (Jackson Immuno Research) at 1:50 dilution. To visualize the nuclei, cells were treated with DAPI (4',6-diamidino-2-phenylindole; Sigma Aldrich) diluted 1:3000 in 1 X PBS. Images were acquired with an Olympus BX-61 automated upright microscope (Shinjuku).

3.6 Fluorescence-activated cell sorting (FACS)

Cells were plated in 10 mm Petri dishes (2 x 10^5 cells/well) and after 24 hours treated with metformin or left untreated for 72 or 120 hours. Cells were harvested, and washed with 0.5% BSA and 2 mM EDTA and dissolved in PBS. Then, 5 x 10^5 cells were suspended in 50 μl of buffer containing 1 X PBS, 0.5% BSA and 2 mM EDTA followed by the addition of 1μl of fluorescent dye-conjugated monoclonal antibody CD133-PE or CD44-PE (Myltenyi Biotec). Cells were incubated for two hours in the dark at 4°C, washed and suspended in 200 μl of the buffer described above and analyzed using a FACSCanto II (Becton Dickinson).

3.7 RNA extraction from cells

Total RNA was extracted from cells using the Trizol reagent (Invitrogen). After adding 500 μl of this reagent and 100 μl of chloroform, the samples were left at RT for 5 min. Subsequently, samples were centrifuged at 12000 rpm for 15 min at 4°C and the supernatant was transferred into a new tube where the same amount of isopropanol was added. After adding 5 μl of glycogen (5mg/mL, Ambion), the samples were left at RT for 15 min and then centrifuged again at 12000 rpm for 15 min at 4°C. The supernatant was removed, 400 μl of ice cold 75% ethanol was added to the aqueous phase and the mixture

was centrifuged at 13200 rpm for 10 min at 4°C. After removing the supernatant, the pellet was dried and resuspended with RNAse-free water.

3.8 Quantitative real-time PCR (qRT-PCR)

TaqMan gene expression assays were used for qRT-PCR. Briefly, 500 ng of total RNA in a final volume of 20 μl were reverse transcribed to cDNA using High-Capacity cDNA Reverse Transcription Kit according to the manufacturer's instructions (ThermoFisher). qRT-PCR was performed using the FAST chemistry (ThermoFisher) with the manufacturer provided gene-specific assay (CD44 Hs00153304_m1 and LGR5 Hs00173664_m1) in ABI PRISM 7900 HT Real-Time PCR system (ThermoFisher). The expression levels of each assay were normalized to that of *GAPDH* (Hs99999905_m1). Data analysis was done using the Sequence Detector version, SDS 2.1.

3.9 Cell Cycle analysis

Cells were plated in 10 mm Petri dishes (5×10^5 cells/well) and after 24 hours treated with metformin, targeted drugs (alone or in combination with metformin) or left untreated for 72 or 120 hours. Cells were scraped, rinsed twice with 1 X PBS and fixed in ice-cold 70% ethanol. For total DNA content 10^6 cells were stained with a solution containing 50 μg/ml propidium iodide and 250 μg/ml RNase I (Roche Diagnostics) and left overnight at 4°C. Cell cycle distribution was evaluated by flow-cytometric analysis of cellular DNA content via FACS instrument (Beckton & Dickinson).

3.10 Western Blotting analysis

Logarithmically growing cells were treated with metformin or targeted drugs (alone or in combination with metformin) or left untreated for 72 or 120 hours. Then cells were washed twice with ice-cold PBS, collected by trypsinisation and resuspended in 300

µl of 1X SDS sample buffer (50 mM Tris, pH 8.0, 50 mM NaCl, 0.5% Triton X-100, 0.1% sodium deoxycholate, 0.25% sodium dodecyl sulphate (SDS)) supplemented with protease inhibitors (Calbiochem), and phosphatase inhibitor cocktail (PhosSTOP Roche). The suspensions were then sonicated for 5 seconds (two cycles) to shear DNA and reduce viscosity. For each sample 40 µg of protein lysate were precipitated using 100% cold acetone for 20 minutes at -20°C, then centrifuged at 8000 rpm for 7 minutes and dried in a speed vacuum for 10 minutes. Protein quantification was performed using the BCA protein assay (Thermo Scientific). The pellets were resuspended in 20 µl of 1X loading buffer (200 mM Tris HCl pH 6.8, 8% SDS, 0.4% Bromophenol blue, 40% Glycerol) and then boiled at 98°C for 5 minutes. Samples were loaded onto to 8-12% polyacrylamide gels. Proteins were then transferred on Nitrocellulose membranes (Whatman PROTRAN) with porosity of 0.2 µm or 0.45 µm depending on the size of the protein being detected. Membranes were blocked with 5% non-fat dry milk in Tris-buffered saline with 0.1% Tween-20 and incubated with primary antibodies. The primary antibodies used for Western blotting are showed in Table 6. Immmunoreactive proteins were visualized using chemiluminescence (SuperSignal West Dura Chemiluminescent Substrate, Thermo Scientific) and protein level quantification was performed using the software Imagelab©.

Table 6. Antibodies used for immunoblotting analysis.

Antigen	Antibody	Type	Species	Dilution	Supplier
phospho-Rb (Ser780) (C84F6)	#3590	Monoclonal	Rabbit	1:1000	Cell Signaling
Cyclin D1 (H-295)	sc-753	Polyclonal	Rabbit	1:500	Santa Cruz Biotechnology
Cyclin E1 (HE12)	#4129	Monoclonal	Mouse	1:1000	Cell Signaling
c-Myc (D84C12)	#5605	Monoclonal	Rabbit	1:1000	Cell Signaling
cleaved-PARP (Asp214) (Human Specific)	#9541	Polyclonal	Rabbit	1:1000	Cell Signaling
LC3B	#2775	Polyclonal	Rabbit	1:1000	Cell Signaling
AMPKα	#2793	Monoclonal	Mouse	1:1000	Cell Signaling

phospho-AMPKα (Thr172) (40H9)	#2535	Monoclonal	Rabbit	1:1000	Cell Signaling
S6 Ribosomal Protein (54D2)	#2317	Monoclonal	Mouse	1:1000	Cell Signaling
Phospho-S6 Ribosomal Protein (Ser240/244)	#2215	Polyclonal	Rabbit	1:1000	Cell Signaling
4E-BP1(53H11)	#9644	Monoclonal	Rabbit	1:1000	Cell Signaling
phospho-4E-BP1 (Thr37/46)	#9455	Polyclonal	Rabbit	1:1000	Cell Signaling
mTOR	#2972	Polyclonal	Rabbit	1:1000	Cell Signaling
phospho-mTOR (Ser2448) (D9C2) XP	#5536	Monoclonal	Rabbit	1:1000	Cell Signaling
IGF-1 Receptor β	#3027	Polyclonal	Rabbit	1:1000	Cell Signaling
phospho –IGF-1 Receptor β (Tyr1135/1136)/Insulin Receptor	#3024	Monoclonal	Rabbit	1:1000	Cell Signaling
p44/42 MAPK (Erk1/2)	#9102	Polyclonal	Rabbit	1:1000	Cell Signaling
Phospho-p44/42 MAPK (Erk1/2) Thr202/Tyr204) (20G11)	#4376	Monoclonal	Rabbit	1:1000	Cell Signaling
Akt (pan) (40D4)	#2920	Monoclonal	Mouse	1:2000	Cell Signaling
phospho-Akt (Ser473) (D9E) XP	#4060	Monoclonal	Rabbit	1:2000	Cell Signaling
Src (36D10)	#2109	Monoclonal	Rabbit	1:1000	Cell Signaling
phospho-Src Family (Tyr416)	#2101	Polyclonal	Rabbit	1:1000	Cell Signaling
EGFR (1005)	sc-03	Polyclonal	Rabbit	1:1000	Santa Cruz Biotechnology
phospho-EGFR (Tyr1068) (D7A5) XP	#3777	Monoclonal	Rabbit	1:1000	Cell Signaling
Vinculin	V9131	Monoclonal	Mouse	1:5000	Sigma-Aldrich
β-actin	A2066	Polyclonal	Rabbit	1:5000	Sigma-Aldrich

3.11 Senescence-associated (SA)-β-galactosidase activity

CRC cell lines were seeded in a 35 mm multi-well plate ($3.75 - 30 \times 10^4$ cells/well) and treated with 5 mM metformin dissolved in medium or left untreated. After 72 hours the SA-β-galactosidase activity was detected using the Senescence β-galactosidase staining kit (Cell Signaling Technology) in accordance with the manufacturer's instructions. Cell images were acquired under reflected light using an Olympus IX81 motorized inverted microscope (Shinjuku). Positive control for β-galactosidase assay was obtained as described in Vizioli et al., 2014.

3.12 Apoptosis assays

For all the apoptosis assays the adherent cells were collected by trypsinization and then pooled together with the detached cells from the same sample.

3.12.1 TUNEL (TdT-FITC)

TUNEL assay was performed using the *In Situ* Cell Death Detection Kit Fluorescein (Roche) for detection of single and double stranded DNA breaks that occur at the late stages of apoptosis. Cells were seeded at concentration of 5×10^5 and, after 24 hours, treated with metformin or left untreated for 72 hours. Cells were harvested, washed with 1X PBS, fixed in 1% formaldehyde for 20 minutes on ice. Subsequently, the cells were washed with buffer (1 X PBS, 1% BSA) and fixed in ice-cold 70% ethanol. Cells were washed with buffer and incubated with the TdT (Terminal deoxynucleotidyl Transferase) enzyme and label solution (fluorescein-dUTP) for 1 hour at 37^{o}C. After washing with PBS containing 1% BSA, the label incorporated was visualized on a FACSCanto II (Becton Dickinson).

3.12.2 Caspase-3 assay

Cells were seeded at the density of 5×10^5 cells and after 24 hours treated with metformin or left untreated for 72 hours. Cells were harvested, washed with 1 X PBS, fixed in 1% formaldehyde dissolved in 1 X PBS for 20 minutes on ice. Cells were washed with buffer and fixed in ice-cold 70% ethanol. After another washing cells were resuspended in 1 X PBS, 0.1% Triton X-100 and incubated for 10 minutes at RT. Cells were washed in buffer and resuspended in 1 X PBS, 10% normal goat serum for 30 minutes. Cells were resuspended in 100 µl buffer containing antibody anti caspase-3 (Cell Signaling Technology) diluted 1:50 and incubated for 1 hour at RT. This was followed by a second staining with a rabbit anti FITC (fluorescein) polyclonal antibody (Cell Signaling Technology) diluted 1:50 and incubated for 1 hour at RT in the dark. Cells were analyzed on a FACSCanto II (Becton Dickinson).

3.13 Western blot for apoptotic control

Logarithmically growing HL-60 cells were treated with camptothecin (CPT) 0.1 µM or left untreated for 8 hours. Protein extraction and immunoblot protocol were performed as preliminary reported.

3.14 Immunofluorescent staining and image analysis for autophagy

CRC cell lines were seeded at the density range of $2.5 – 10 \times 10^4$ cells directly on 13 mm diameter coverslip. After 24 hours cells were treated with 5 mM metformin dissolved in medium or left untreated. After 72 hours cells were fixed in 4% paraformaldehyde, permeabilized with ice-cold 100% methanol and blocked with 1 X PBS, 5% normal goat serum and 0.3% Triton X-100. After blocking, the coverslips with cells were incubated with anti-LC3B antibody, used 1:400 in dilution buffer (1 X PBS, 1% BSA, 0.3% Triton X-100), overnight at 4°C in the dark. Coverslips were incubated with

secondary antibody for 2 hours in the dark at RT. To visualize the nuclei, cells were treated for 2 min with DAPI (4',6-diamidino-2-phenylindole) and diluted 1:3000 in 1 X PBS. Finally the coverslips were placed on a support in presence of mowiol mounting solution overnight at RT in the dark. Images were acquired with Olympus BX-61 automated upright microscope (Shinjuku).

Hela cells were used as positive control for the autophagy assay. Cells were seeded at the density of 12.5×10^4 cells directly on 13 mm diameter coverslip (Fisher Scientific). After 24 hours cells were treated for 24 hours with 50 μM chloroquine dissolved in medium or left untreated.

3.15 Clonogenic Assay

CRC cells were seeded in 35 mm multi-well plates (10^2 cells/well) and treated with 5 mM metformin dissolved in medium or left untreated for 6, 12 and 18 days. Every 3 days medium was refreshed. To verify their ability to restart their growth after prolonged treatments with metformin, cells were treated with metformin for 6, 12 and 18 days and allowed to grow for 6, 12 and 18 days respectively in fresh medium in absence of the drug. At the end of treatments, the wells were rinsed with PBS and stained with Crystal Violet (Sigma Aldrich) for 2 min. Only the clearly visible colonies were counted under the microscope.

3.16 Viability assays in combinatorial treatments: chemotherapy drugs and metformin

To assess the effects of chemotherapy drugs in combination with metformin, MTT viability assays were performed as previously described. The drugs were tested alone or combined in different settings. For each drug the concentration administered was its IC_{50}; metformin was used at the concentration of 5 mM. The cells were exposed to

individual drugs alone or to their combined treatment for 96 hours or in different sequences, metformin at first or *vice versa* (where metformin and the chemotherapy drugs were given for 72 and 24 hours, respectively). Cells were also exposed to longer treatments where chemotherapy drugs were administered for 3 days and then the medium was replaced with metformin for 3 more days and *vice versa* (at first metformin and then chemotherapy drugs). For each treatment the medium was refreshed every 48 hours.

The experimental design showing the different sequences of the treatments administered is summarised in Figure 8.

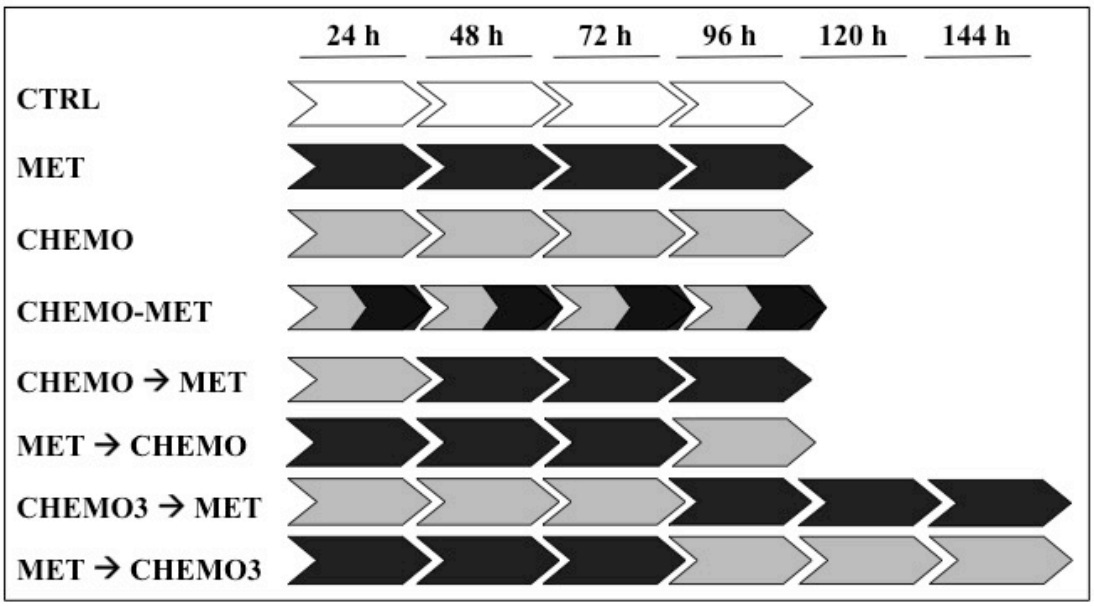

Figure 8. Experimental design of the treatments with metformin and chemotherapy drugs. The cells were left untreated (CTRL, white arrows) or treated with metformin (MET, black arrows) and chemotherapy drugs, 5-FU, Oxaliplatin and irinotecan - (CHEMO, grey arrows), given alone or administered simultaneously (CHEMO-MET, grey/black arrows) for 96 hours. The cells were also exposed to drugs in different sequences: metformin at first or *vice versa*; where metformin was always administered for 72 hours (replaced in fresh medium after 48 hours) and the chemotherapy drugs were given for 24 (MET→CHEMO or CHEMO→MET) or 72 hours (MET→CHEMO3 or CHEMO3→MET). In CTRL, MET, CHEMO and CHEMO-MET treatments fresh medium (with or without drugs) was replaced every 48 hours. In CHEMO→MET treatment the medium with chemotherapeutics drugs was added for 24 hours and then replaced for 72 hours with medium containing metformin (fresh medium with metformin was added after 48 hours); in MET→CHEMO treatment the cells were treated with metformin for 72 hours (fresh medium with metformin was added after 48 hours) and then for 24 hours with new medium containig chemotherapeutic drugs. In CHEMO3→MET treatment the cells were treated with chemotherapeutic drugs for three days (chemotherapeutics drugs were added at the beginning of treatment and after 48 hours) then for 72 hours with metformin (replaced after 48 hours); in MET→CHEMO3 treatment the cells were treated with

metformin for 72 hours (metformin was added at the beginning of treatment and replaced after 48 hours), then for 72 hours with chemotherapeutic drugs (replaced after 48 hours). Because in CHEMO→MET and MET→CHEMO treatments the chemotherapeutic drugs were administered once, while in the other treatments they were administered twice, a treatment with chemotherapeutic drugs administered for 24 hours would be added as control.

3.17 Drug synergy testing

Analyses for the detection of drug interactions among chemotherapy drugs (5-FU and oxaliplatin and 5-FU and irinotecan) or among metformin and targeted drugs were performed. Starting from the IC_{50} value of the drugs previously obtained, I conducted MTT viability assays at 72 hours with combination of multiples and submultiples for each IC_{50}: from 6.25% to 2 times of the IC_{50}.

Effects of the drug interactions were analysed using the CompuSyn software (Compusyn Inc), which determines the dose-effect of each drug. This software is based on Chou and Talalay method (Chou and Talalay, 1984) and can determine synergism and antagonism between drugs through the combination index (CI) theorem: CI =1 is considered additive effect, CI<1 synergism and CI>1 antagonism.

3.18 Viability assays in combinatorial treatments: chemotherapy regimens and metformin

To assess the effect of chemotherapy regimens in combination with metformin, MTT viability assays were performed as previously described. The drugs were tested alone or combined in different sequences as previously described, as reported in Figure 9. The concentrations of regimens used in the experiments were determined using the Compusyn software; metformin was used at the concentration of 5 mM.

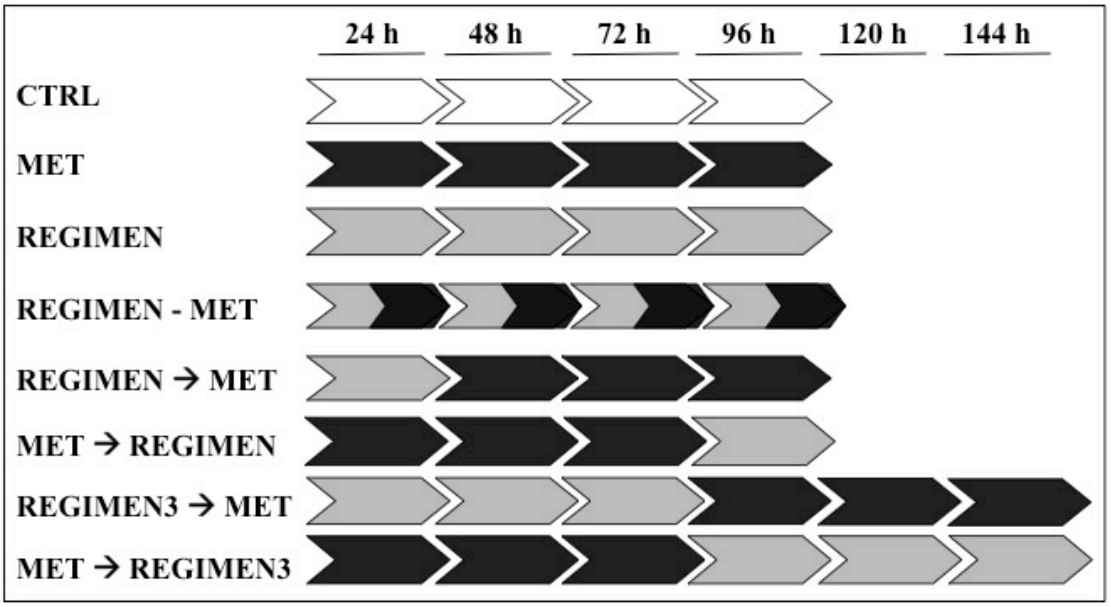

Figure 9. Experimental design of the combined treatments of metformin with the chemotherapy regimens. The cells were left untreated (CTRL, white arrows) or treated with metformin (MET, black arrows) and chemotherapy regimens (REGIMEN, grey arrows) given alone or administered simultanoeulsy (REGIMEN-MET, grey/black arrows) for 96 hours. The cells were also exposed to drugs in different sequences: metformin at first or vice versa; where metformin was always administered for 72 hours (replaced in fresh medium after 48 hours) and the chemotherapy regimen were given for 24 (MET→REGIMEN or REGIMEN→MET) or 72 hours (MET→REGIMEN3 or REGIMEN3→MET). The regimens investigated are: oxaliplatinum-5-FU (OXA-5-FU) and irinotecan-5-FU (IRI-5-FU). For each condition medium was replaced every 48 hours: In CTRL, MET, REGIMEN and REGIMEN -MET treatments fresh (with or without drugs) was replaced every 48 hours. In REGIMEN→MET treatment the medium with chemotherapeutics drugs was added for 24 hours and then replaced for 72 hours with medium containing metformin (fresh medium with metformin was added after 48 hours); in MET→ REGIMEN treatment the cells were treated with metformin for 72 hours (fresh medium with metformin was added after 48 hours) and then for 24 hours with new medium containig chemotherapeutic drugs. In CHEMO3→MET treatment the cells were treated with chemotherapeutic drugs for three days (drugs were added at the beginning of treatment and after 48 hours) then for 72 hours with metformin (replaced after 48 hours); in MET→ REGIMEN3 treatment the cells were treated with metformin for 72 hours (metformin was added at the beginning of treatment and replaced after 48 hours), then for 72 hours with chemotherapeutic drugs (replaced after 48 hours). Because in REGIMEN→MET and MET→REGIMEN treatments the chemotherapeutic drugs were administered once, while in the other treatments they were administered twice, a treatment with chemotherapeutic drugs administered for 24 hours would be added as control.

3.19 Data analyses

Data analyses were done using the GraphPad Prism software. The data are presented as mean values ± standard deviation (SD) and statistically compared between groups using one-way analysis of variance followed by Student's t-test. A P-value of <0.05 was considered statistically significant.

CHAPTER 4
RESULTS

4.1 Effect of metformin on CRC cell lines and organoids

4.1.1 Identification of the concentrations of metformin to use in CRC cell lines and organoids

To determine the best concentrations of metformin to use in the treatments, MTT (3-4,5-Dimethylthiazol-2-yl-2,5-diphenyltetrazolium bromide) viability assays were performed on four CRC cell lines: HT29, HCT116 HCT116*P53*-/- and DLD-1. As shown in Figure 10, the half inhibitory concentration (IC50) after 72 hours of treatment with metformin was about 2.5 mM for HT29, HCT116 and HCT116P53-/- cells and 5 mM for the DLD-1 cell line. However, other experiments conducted on these cell lines in our laboratory and previously published data in CRC (Zakikhani et al., 2008) treated HT29, HCT116 and HCT116P53-/- cells with 5 mM metformin and the most resistant DLD-1 cell line with 10 mM metformin. To be in line with these data, we decided to treat cells as in Zakikhani (Zakikhani et al., 2008).

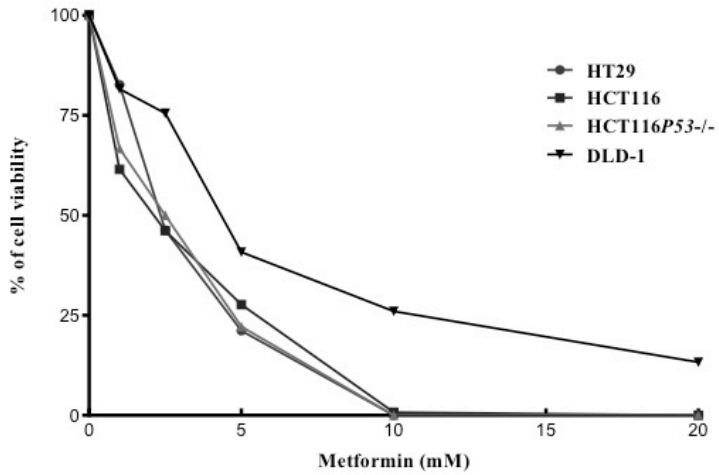

Figure 10. **Determination of the IC_{50} values for metformin in CRC cell lines**. HT29, HCT116, HCT116*P53*-/- and DLD-1 cell lines were seeded in six replicates in a 96-well plate and treated with metformin at different concentrations (from 0.16 to 20 mM). After 72 hours of treatment MTT assay was used to determine the percentage of viable cells. Results are representative of three independent experiments.

In the clinics, metformin is typically administered at doses of 0.5-1g/day, and its median plasma concentration is 330 μM (Foretz et al., 2014). *In vitro* inhibition of cancer cell proliferation, however, has been reported for millimolar concentrations (Lonardo et al., 2013) and the concentration used in our and other CRC *in vitro* studies is therefore higher than the therapeutic one. However, metformin accumulates in tissues at concentrations that are several times those found in blood (Foretz et al., 2014), and drug concentrations in the gut are higher than in the rest of the body (Pernicova et al., 2014). In addition CRC cells express high levels of the main metformin transporter OCT1, which may increase their uptake of metformin (Zhang et al., 2006). These observations may justify testing the use of higher metformin concentrations to treat CRC. MTT viability assay was not applicable to 3D-organoids derived from a CRC mestastasis to the peritoneum (peritoneal carcinomatosis CRC-pc), because the 3D structure of organoids renders difficult to metabolize MTT. As shown in Figure 11 A, the best concentration to use for their treatment (5 mM) was determined by giving to organoids increasing concentrations of metformin (from 1 to 20 mM) and following their growth over time, until they were disaggregated (120 hours). Trypan Blue assay confirmed a reduction in cell viability when organoids were treated with 5mM metformin for 120 hours (Figure 11 B).

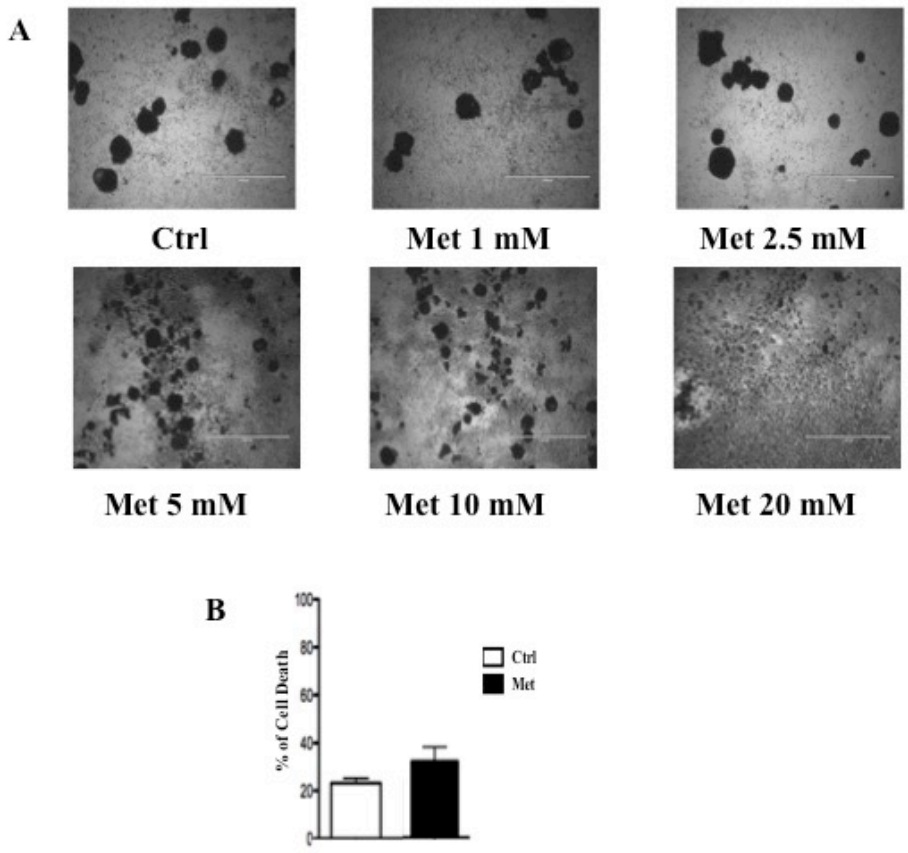

Figure 11. **Microscope images and viability analysis of organoids from CRC-pc**. (A) Micrographs of organoids before and after metformin treatment for 120 hours at different drug concentrations. Metformin treatments induced a marked morphological change in organoids, resulting in a loss of their original spheroid organization. Magnifications: 10X. Scale bars = 50 μm. (B) Organoids were treated with 5 mM metformin for 120 hours. The percentage of cell death was determined by Trypan Blue assay. Data are measured percentage of cell death and expressed as the mean ± SD.

4.1.2 Analysis of cell proliferation in CRC cell lines undergoing metformin treatment

A BrdU incorporation assay confirmed that 5 mM metformin inhibited growth in HT29, HCT116 and HCT116*P53*-/- cells after 24 hours of treatment, but the effect became more significant after 72 hours (from 54% to 23% in HT29, from 78% to 44% in HCT116 and from 50% to 26% in HCT116*P53*-/- cells; Figure 12 A, B, C). In DLD-1 cells a slight reduction in proliferation was observed after 24 hours of treatment (from 61% to 52%), but not after 48 and 72 hours (from 57% to 54% and from 46% to 43% respectively; Figure 12 D).

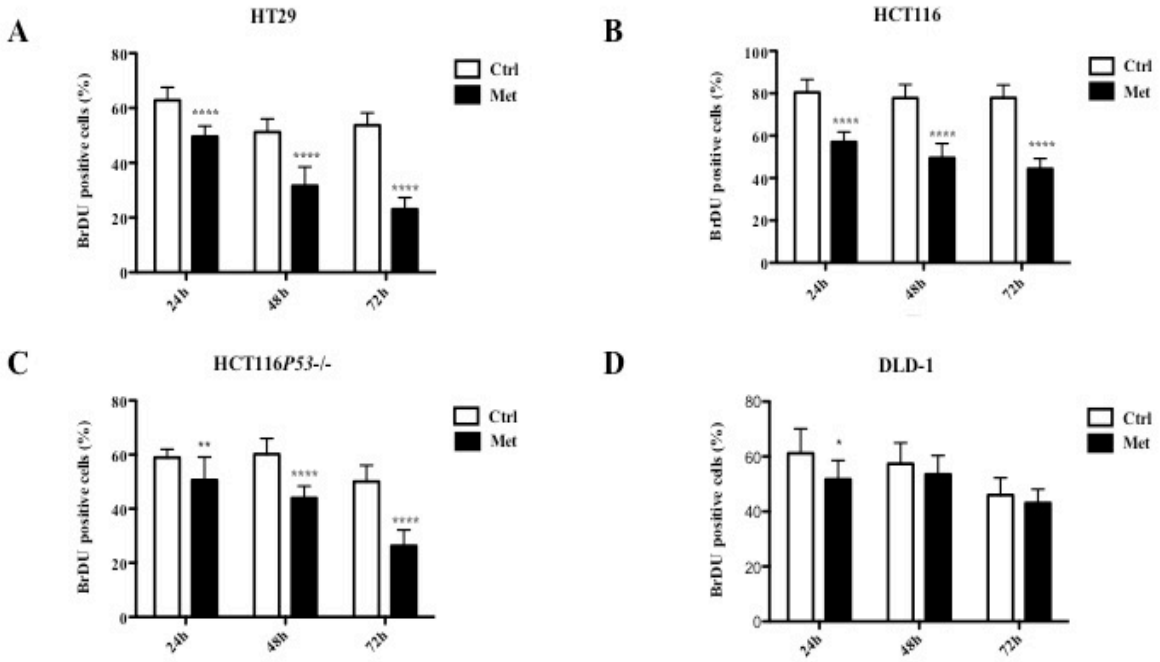

Figure 12. **Evaluation of the proliferation in CRC cell lines**. Cell proliferation in HT29 (A), HCT116 (B), HCT116*P53*-/- (C) and DLD-1 (D) cell lines was evaluated *in vitro* by means of BrdU incorporation in absence (Ctrl) or presence of 5 mM for HT29, HCT116 and HCT116*P53*-/- or 10 mM metformin for DLD-1 after 24, 48 and 72 hours of treatment. Metformin inhibits proliferation in HT29, HCT116 and HCT116*P53*-/- cell lines at all time points. In DLD-1 cells the reduction is observed only after 24 hours of treatment. Results, derived from three independent experiments, are represented as the mean ± SD compared with the untreated control group (*P < 0.05, **P < 0.01, ****P < 0.0001).

4.1.3 Evaluation of stem cell markers in CRC cell lines and organoids

The expression of the CRC stem cell markers CD44, CD133 and of Lgr5 was evaluated on the four CRC cell lines and on the organoids. As shown in Figure 13, treatment with metformin significantly decreased the expression of CD133 (not expressed in HCT116*P53 -/-* cells), CD44 and Lgr55 (which was expressed only in HT29 cells (Chen et al., 2014) and in the organoids).

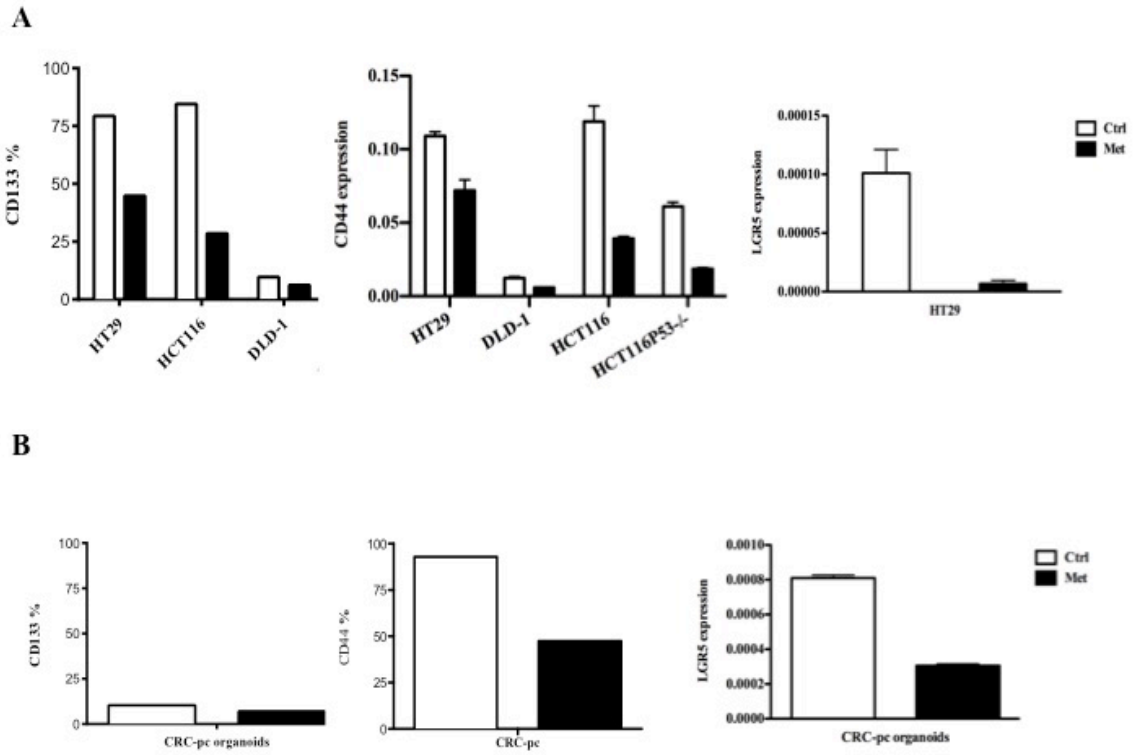

Figure 13. Effects of metformin on the expression of the CRC stemness markers CD44, CD133 and Lgr5. FACS and qRT-PCR analyses on (A) Cell lines and (B) organoids. A representative FACS analysis showing changes in the proportion of $CD133^+$ cells and organoids and $CD44^+$ organoids induced by metformin. qRT-PCR results of the expression of $CD44^+$ in cell lines and Lgr5 in cell lines and in the organoids. Data are indicated as $2^{-\Delta Ct}$ (delta cycle threshold), which is directly related to the gene expression levels in each sample, and represent mean ±SD from three different replicates.

4.1.4 Metformin increases G0/G1 phase in HT29, HCT116, HCT116*P53*-/- and organoids but not in DLD-1 cells

To study the cellular mechanisms that reduce proliferation regulated by metformin, I evaluated changes in the cell cycle progression. After 72 hours, for cell lines, or 120 hours, for organoids, of treatment, the distribution of cells in the cell-cycle phases was determined by analyzing their DNA content by FACS. The DNA profiles of HT29, HCT116 WT and *TP53*-null cells and of CRC-pc organoids treated with metformin

compared to that of untreated cells (or organoids) showed a slight accumulation of cells in G0/G1 phase (from 50% to 63% in HT29, from 49% to 64% in HCT116, from 36% to 46% in HCT116*P53*-/- cells and from 56% to 70% in the organoids; Figure 14 A). A corresponding decrease in the percentage of the G2/M phase fraction (from 7% to 5.5% in HT29, from 16% to 13% in HCT116 and from 29% to 22% in HCT116*P53*-/- cells) respect to the untreated cells was observed. Organoids treated with metformin showed a decrease of cells in S phase (from 31% to 17%), while DLD-1 cells had no changes in the cell cycle.

To confirm that metformin treatment induced an increase of cells in the G0/G1 phase I evaluated the expression of two cyclins, cyclin D1 and cyclin E, which are involved in the progression through G1 phase (cyclin D1) and the transition from G1 to S phase (cyclin E). Decrease in their levels could be associated with cell cycle arrest. Western blot analysis showed that cyclin D1 (expressed at low levels in HT29 cells) was downregulated in all the cell lines tested, included DLD-1 cells, and even in CRC-pc organoids, which support the cell cycle arrest in the G0/G1 phase observed (Figure 14 B). In line with the inactivation of cyclin D1, metformin decreased the phosphorylation of its downstream target retinoblastoma protein (pRb; Ser780) in all the cell lines; the organoids did not express this protein. Cyclin E (not expressed in the organoids) had no change of expression in HT29, HCT116 and HCT116*P53*-/- but decreased in DLD-1 cells (Figure 14 B). The strong reduction of the expression of c-Myc confirmed the decrease of cells in S phase.

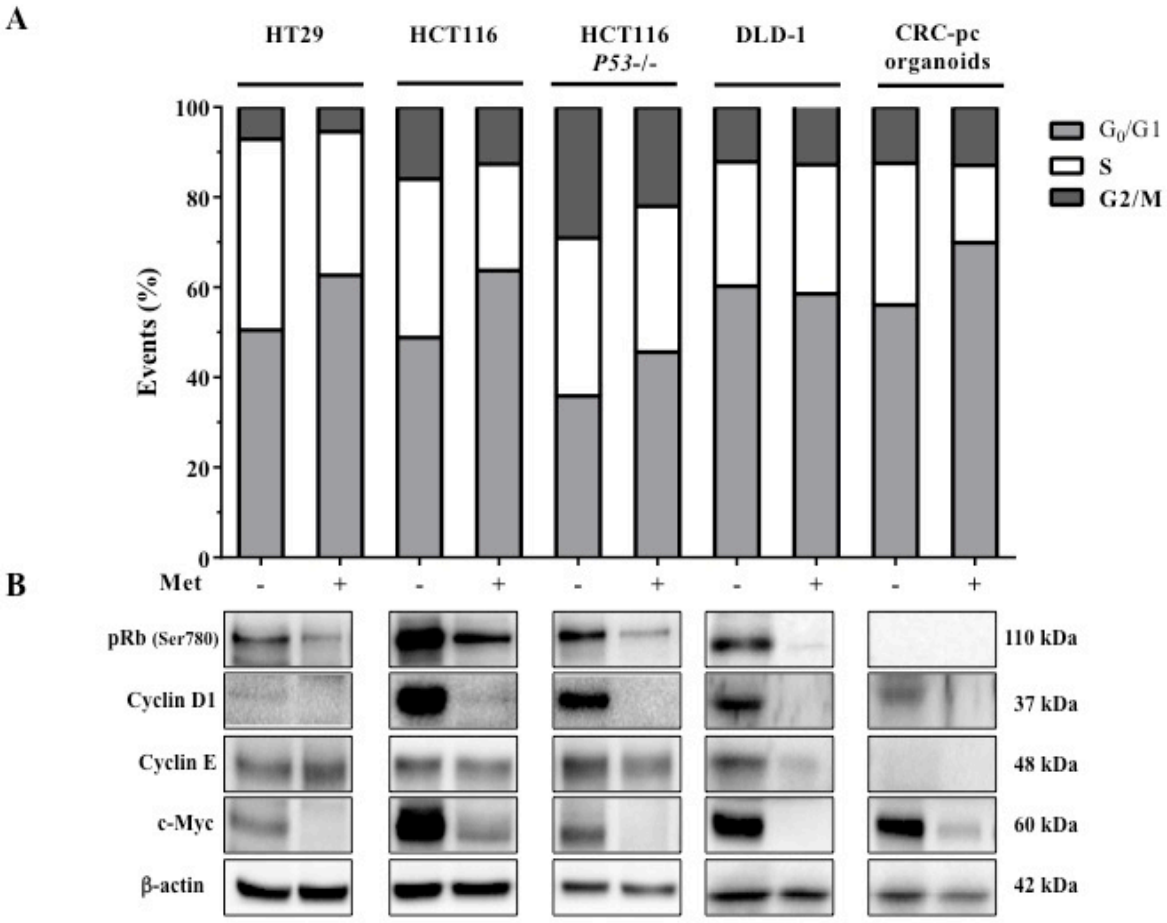

Figure 14. Cell cycle analysis and expression of related protein in CRC cell lines and in organoids. (A) Proliferating colorectal cancer cell lines and CRC-pc were treated with metformin, Met, (+) or left untreated (-) for 72 hours (cell lines) or 120 hours (organoids). The cell cycle profiles were analysed by flow cytometry; an increase in G0/G1 fraction was observed in HT29, HCT116 WT and *TP53*-null cells and in the organoids. (B) Immunoblotting of pRb, cyclin D1, cyclin E and c-Myc in the CRC cell lines and in organoids treated with metformin (+) or left untreated (-) at the same times reported above. Cyclin D1, pRb and c-Myc, when expressed, are downregulated in all the cell lines, cyclin E decreased only in DLD-1 cell line. β-actin was used as loading control. The presented data derive from one of the three independent experiments performed.

4.1.5 Treatment with metformin does not induce senescence, apoptosis or autophagy

To investigate the biological mechanisms by which metformin appears to inhibit cell cycle progression, I assessed its ability to induce a permanent cell cycle arrest (senescence) or trigger cell death programs (apoptosis or autophagy) in the four cell lines. As regards the organoids, which grow as 3D structures, I could only evaluate protein changes by western blotting since most the assays I used are designed for disaggregated

cells that grow as monolayer. Cellular senescence is an irreversible form of cell cycle arrest in which cells change their morphology, become flat and display a pH-dependent β-galactosidase activity. Using a commercial system that detects the β-galactosidase activity of senescent cells, I observed no changes in morphology and β-galactosidase staining of cells after treatment with metformin in all of the tested cell lines, thus excluding activation of senescence (Figure 15).

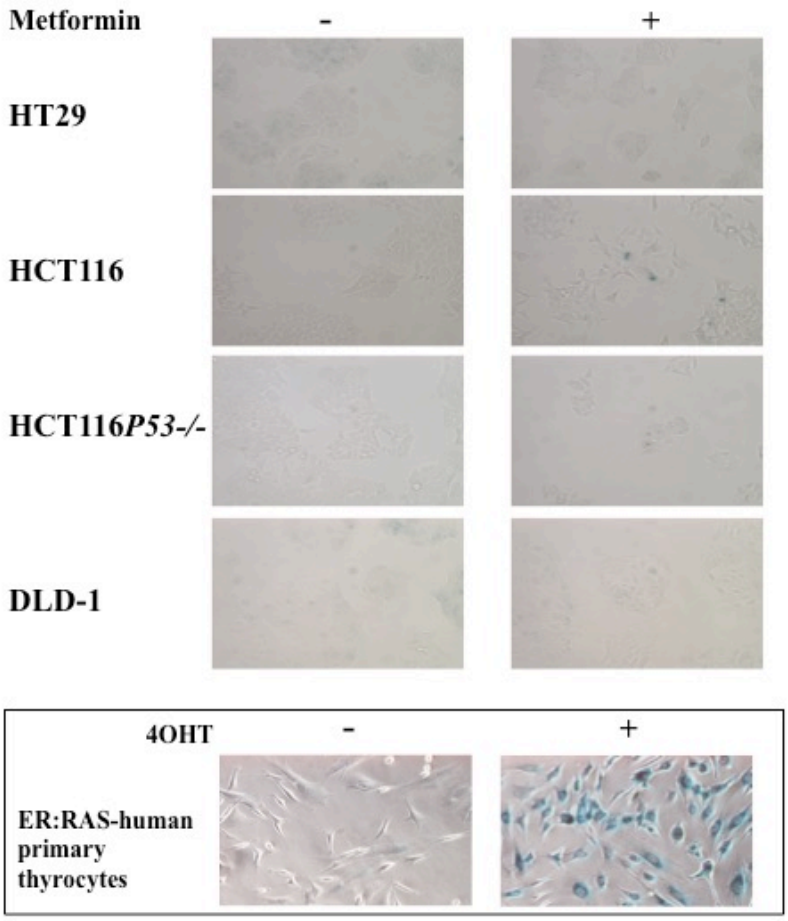

Figure 15. Analysis of senescence in CRC cell lines. Senescence was measured using the senescence-associated β-galactosidase (SA-β-Gal) activity assay. The cells were treated with metformin (+) or left untreated (-) for 72 hours. The images were acquired at 20x magnification. As shown in the images, no induction of senescence was reported in all cell lines. The positive control for the experiment is shown on the bottom panel: human primary thyrocytes carrying *ER:RAS* vector were left untreated (-) or treated (+) with 200 nM 4-hydroxytamoxifen (4-OHT) for 7 days (magnification 40x). Data are from a representative experiment out of the three done independently.

Apoptosis, a programmed mechanism of cellular self-killing, was evaluated by FACS analysis for Caspase-3 and TUNEL (Terminal deoxynucleotidyl transferase dUTP Nick End Labeling) assay, two different methods that detect the early and the late phases of apoptosis, respectively. Both assays showed no induction of apoptosis after 72 hours of treatment for all the tested cell lines (Figure 16 A-B). The absence of apoptosis was also confirmed by the lack of increase in cleavage of Poly (ADP-Ribose) polymerase protein (PARP; Asp214), a marker for late-stage apoptotic events, both in cell lines and in the organoids (Figure 16 C).

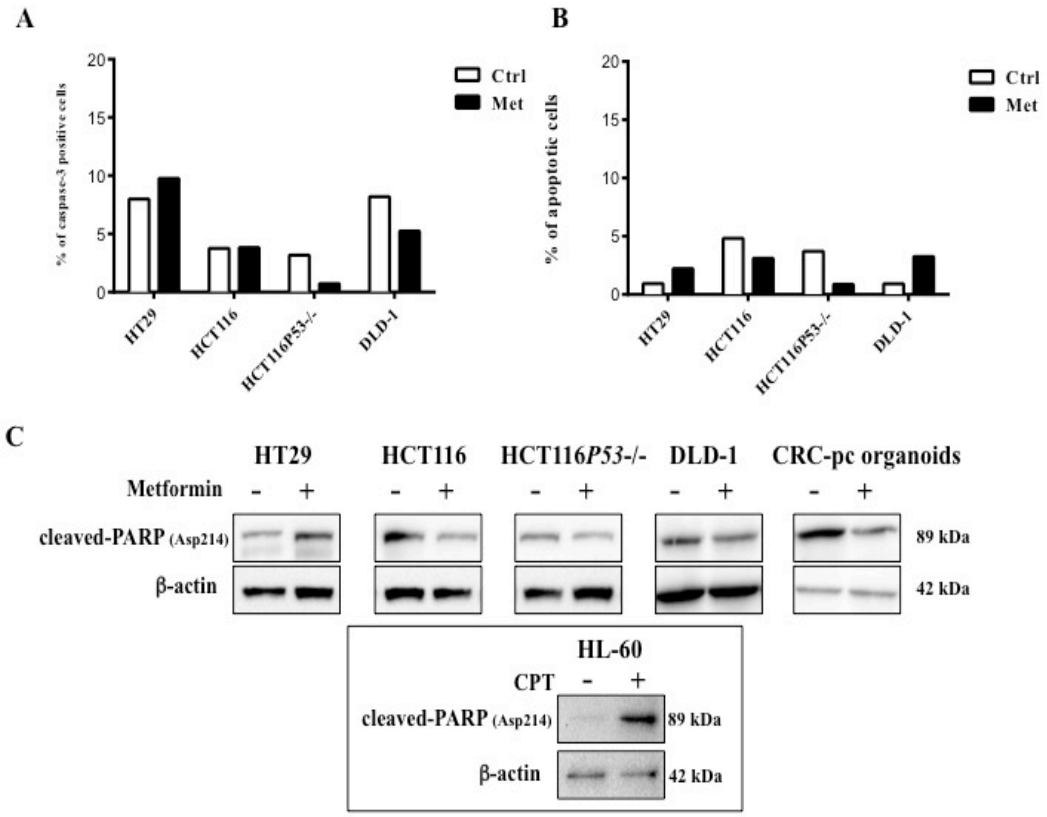

Figure 16. Apoptosis assays in CRC cell lines and in the organoids. (A) Flow cytometric detection of cells containing active caspase-3, (B) TUNEL analysis on the cell lines and (C) protein detection of cleaved-PARP of the cell lines and of organoids treated with metformin (+) or left untreated (-) for 72 hours (cell lines) or 120 hours (organoids). The HL-60 cell line (bottom panel) was used as positive control: cells were treated with camptothecin (CPT +) or left untreated (-) for 8 hours. No apoptosis was reported in all the experiments. β-actin was used as loading controls. Results are representative of three independent experiments.

As regards autophagy, I monitored the conversion of the autophagy marker microtubule-associated protein light chain 3 (LC3) from LC3-I to LC3-II, which is related to the presence of autophagosomes, double-membrane vesicles assembled during autophagy. Western blotting analysis of the ratio between LC3-I and LC3-II, as well as immunofluorescence for LC3B, were not significantly different after treatment with metformin, thus excluding the induction of autophagy in all cell lines and also in CRC-pc organoids (Figure 17).

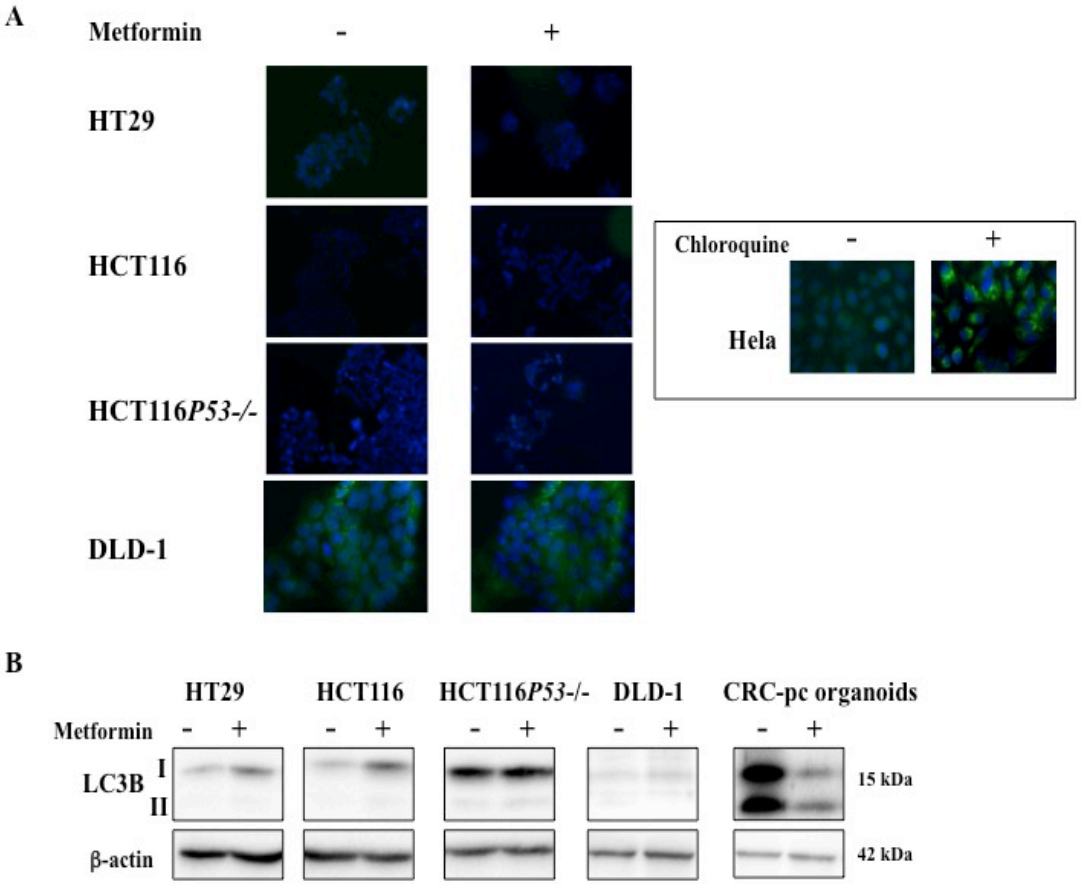

Figure 17. Autophagy detection in CRC cell lines and in the organoids. (A) Immunofluorescence staining of LC3B in the cell lines treated with metformin (+) or left untreated (-) for 72 hours (magnification 20x). The positive control is in the panel on the right: Hela cells treated with 50 mM chloroquine (+) or left untreated (-) for 24 hours (magnification 40x). (B) Immunoblotting determination of LC3B protein in the cell lines and in the organoids treated with metformin (+) or left untreated (-) for 72 or 120 hours. β-actin was used as loading control. No autophagy was detected in both the experiments. The presented data derives from one of the three independent experiments performed.

4.1.6 Metformin-induced inhibition of proliferation is reversible

To clarify the absence of induction of cell death after administration of metformin I examined the clonogenic capacity of the cell lines in the presence of the biguanide. Clonogenic cell survival assay defines the ability of a single cell to proliferate and form a large colony. I evaluated as metformin can stop the proliferation of CRC cells and also if the cells previously treated with metformin and then maintained on growth without the drug (here and after named "rescued cells", R), are able to restore their proliferation capacity in each time of treatment. Treatment for 6 days with metformin significantly reduced both the number and size of colonies compared to the untreated controls in HT29, HCT116 and HCT116*P53*-/- (Figure 18 A). This result was confirmed after 12 days and was maintained up to 18 days of treatment (Figure 18 B-C). At this last time, colonies of untreated and rescued cells were larger and thicker than the other times. The confluence of the cells on these plates caused a massive detachment of the colonies during the treatment with crystal violet.

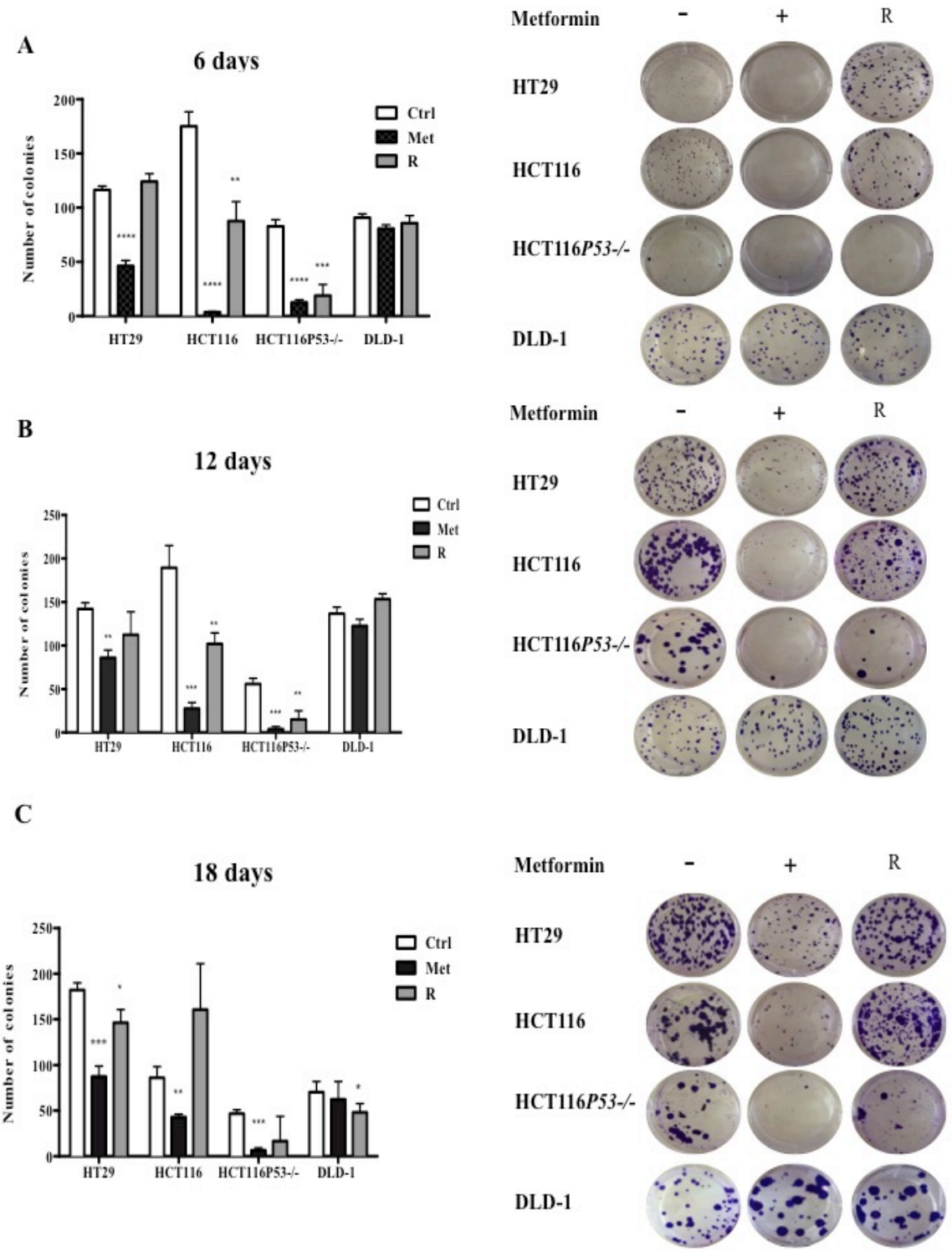

Figure 18. Clonogenic ability of the CRC cell lines. The cells were grown for 6 (A), 12 (B) and 18 (C) days in the presence (Met, or +) or absence (Ctrl, or-) of metformin. The rescued colonies (R) were obtained after growth of cells treated with metformin for 6, 12 or 18 days for further 6, 12 or 18 days respecitively in fresh complete medium without metformin. The graphic representation of the results is shown on the right side of the figure. Metformin reversibly inhibits colony formation of all the cell lines analysed. The bars indicate the mean value ± SD of three independent experiments (*P < 0.05, **P < 0.01, ***P < 0.001, ****P < 0.0001).

At all time points of treatment rescued cells resumed their proliferation capacity, although the recovery was less evident in HCT116 *TP53*-null cells. This effect does not seem to depend on *TTP53* status, which is also mutated in HT29 cells. These results are in agreement with the absence of cell death observed, and highlight that the inhibitory effect of metformin on proliferation of HT29, HCT116 WT and *TP53*-null cells is transient, and may be overcome after the removal of the drug.

In accordance with the absence of cell cycle arrest observed in the DLD-1 cells, differences in the ability of forming colonies did not occur in DLD-1 cells at the three time points analysed.

Although MTT assay demonstrated that the concentration of metformin I used for DLD-1 cells (i.e. 10 mM) was sufficient to stop the growth of 50% of the cells, the results I obtained by testing different mechanisms known as modulated by metformin are controversial and do not fully support an effect of the biguanide on DLD-1 cells, at least at the concentration used. In fact, the DLD-1 cells had a slight decrease in proliferation (BrdU assay) only after 24 hours of treatment with metformin and did not show cell cycle arrest, despite the decrease of c-Myc and cyclins D1 and E.

Most likely the hypermethylation of both alleles of the LKB1 gene, which plays a critical role in activating AMPK, limits the effects of metformin on these cells and makes more difficult understanding the mechanisms modulated by metformin in CRC. This is why I decided to study in details only the other three models of CRC, which all carry a functional LKB1 gene.

4.1.7 Metformin transiently inhibits mTOR proliferation pathway and reduces the activation of IGF1R

To investigate the molecular mechanisms by which metformin may inhibit the proliferation of CRC cells, I assessed by western blotting analysis changes of activation of the Insulin-like growth factor 1 β (IGF1Rβ) protein and of proteins from the

AMPK/mTOR pathway on HT29, HCT116 and HCT116*P53*-/- cells and on the organoids. The inhibition of phosphorylation of mTOR (Serine2448) and of its downstream targets S6 (Ser 240/244) and 4E-BP1 (Thr 37/46) was observed in all cell lines tested after treatment with metformin (Figure 19).

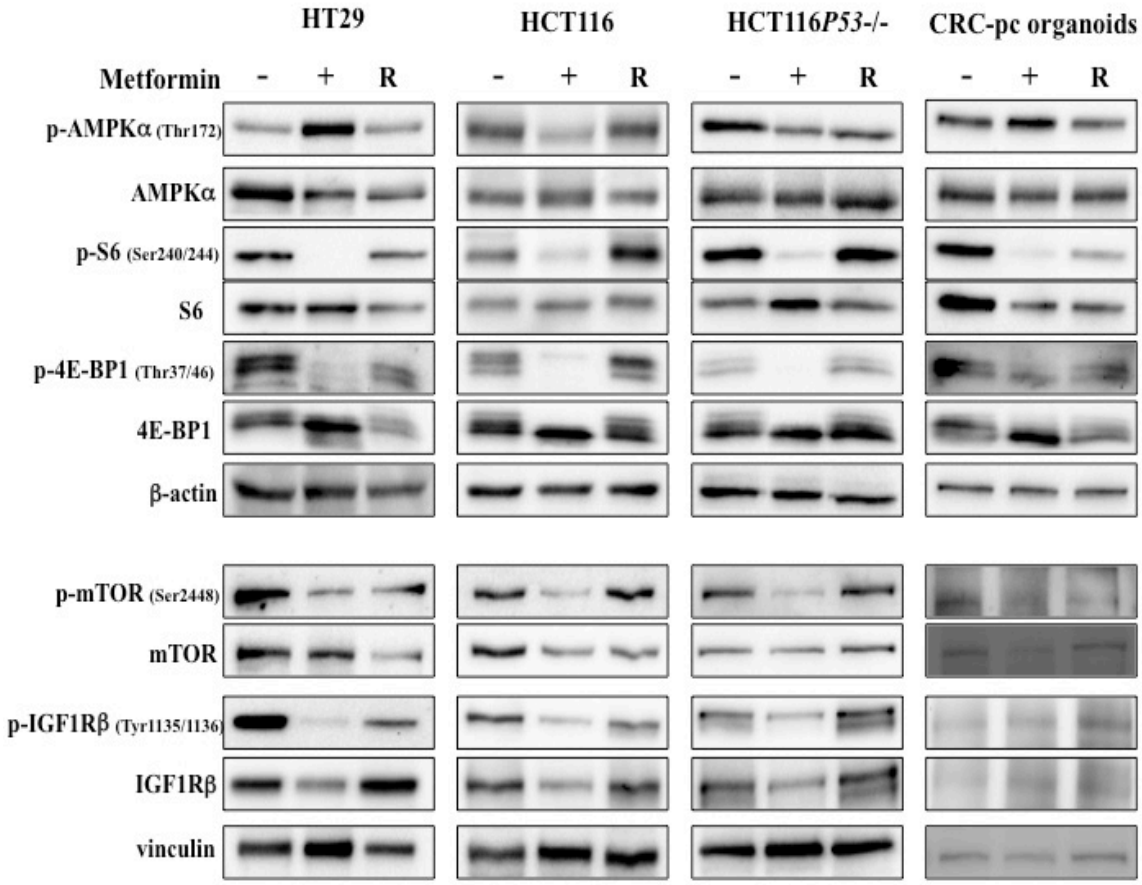

Figure 19. mTOR pathway and IGF1Rβ in CRC cell lines and in the organoids.
Cell lines and CRC-pc organoids were treated with metformin (+) or left untreated (-) for 72 hours (cell lines) or 120 hours (CRC-pc organoids). The "rescued" cells (R) were grown for 72 hours (cell lines) or 120 hours (CRC-pc organoids) with metformin and for a further 72 or 120 hours in fresh complete medium without the drug. Metformin reversibly inhibits the activity of proteins from the mTOR pathway and of IGF1Rβ. β-actin and vinculin were used as loading controls. The results are representative of at least three independent experiments.

However AMPK resulted phosphorylated (Thr172) only in the HT29 cell line and in the organoids, suggesting the presence of alternative mechanisms for the inactivation of this pathway in both HCT116 cell lines. After treatment with metformin, I also observed

reduction of IGF1Rβ protein phosphorylation (Tyr1135/36) in the three cell lines analysed, suggesting a reduced activity of the receptor. Expression of IGF1Rβ was very weak in organoids and its phosphorylation did not change after the addition of metformin.

In all cases the phosphorylation profile of the rescued cells was similar to that of the untreated cells confirming what was observed in the colony formation assays and supporting the hypothesis that the inhibitory effect of the drug on cell proliferation is only transient.

4.1.8 Summary of key findings

Treatment with metformin:

- reduces cell proliferation and induces block in G0/G1 phase
- acts on the cancer stem cell component
- induces a transient and reversible block of cell proliferation
- transiently inhibits the mTOR pathway and IGF1R activation

4.2 Effects of metformin in combination with chemotherapy

The experiments with metformin on the cell lines and on the organoids highlight its cytostatic effect on CRC, and set the bases for testing the biguanide together with other drugs, to identify possible cytotoxic combinations. To this aim I have explored the effects of metformin in combination with the standard chemotherapy drugs used for CRC treatment, (5-FU), oxaliplatin (OXA) and irinotecan (IRI), which interfere with DNA synthesis. The effects of these drugs are different: 5-FU blocks thymidine synthesis and stops DNA replication; OXA forms cross links in DNA, preventing DNA replication and transcription, and IRI inhibits the topoisomerase I, leading to block of both DNA replication and transcription. In our hypothesis their combination with metformin could enhance the effects of chemotherapy and result in increased cell death.

We focused on the CRC cell lines, for which there are data in the literature on the sensitivity or resistance to standard chemotherapy, and also because organoids are difficult to treat with the compounds commonly used for viability assays (for example MTT).

In the literature there are several reports on the IC_{50} for 5-FU, OXA and IRI for the three CRC cell lines that I am using, even though they give different concentrations. This is because different protocols to determine cell viability (e.g. sulphorhodamine B assay, CellTiter 96 Non-Radioactive Cell Proliferation Assay and MTT) as well as various times of exposure to drugs (e.g. 1, 24 or 72 hours) have been used. Several IC_{50}s have been proposed for 5-FU (4.2 μM, 5.2 μM, 8.2 μM, 20 μM and 112 μM), OXA (0.33 μM, 9 μM, 24 μM) and IRI (1 μM, 7.8 μM, 13.8 μM, 550 μM) in HT29 cells. The published IC_{50} concentrations of chemotherapy drugs in HCT116 were 0.7 μM and 4.3 μM for 5-FU, 0.3 μM, 2.2 μM and 38 μM for OXA, 2.2 μM and 3.2 μM for IRI; in HCT116*P53*-/- the identified IC_{50} were 19.7 μM for 5-FU, 1.7 μM for OXA and 3.1 μM for IRI (Barone et al., 2007, Boyer et al., 2004, Flis et al., 2009, Guichard et al., 2001, Guichard et al., 1998, Mans et al., 1999, Mariadason et al., 2003, Nannizzi et al., 2010). Starting from data from the literature, I determined for each cell line the IC_{50} value after 72 hours of treatment with various concentrations of the drugs using an MTT viability assay. I established a range of concentrations for each drug (8 points/treatment) that was applicable to all the cell lines: from 0.3 μM to 64 μM for 5-FU, from 0.064 μM to 8 μM for OXA and from 0.004 μM to 4 μM for IRI. The viability plots and the IC_{50} identified are shown in Figure 20 and Table 7 respectively. The IC_{50} values obtained have been used for the further experiments, also in combination with metformin which was used at the concentration of 5 mM.

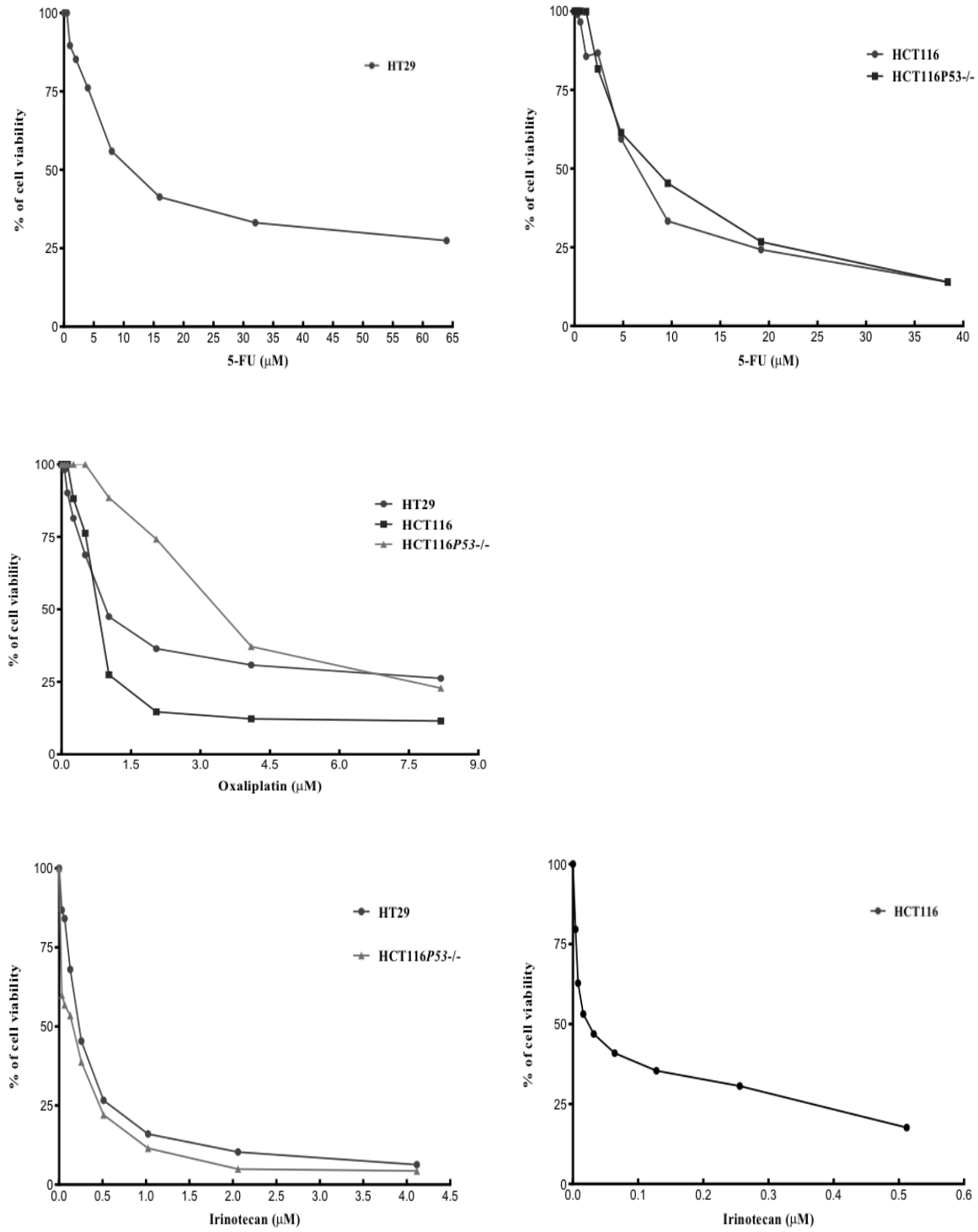

Figure 20. Determination of the IC_{50} values for the chemotherapy drugs in CRC cell lines. HT29, HCT116 and HCT116*P53*-/- cell lines were seeded in six replicates in a 96-well plate and treated with chemotherapy drugs at different concentrations: 0.3 - 64 μM for 5-Fluoro Uracil (5-FU), 0.064 - 8 μM for oxaliplatin (OXA) and 0.004 - 4 μM for irinotecan (IRI). After 72 hours MTT assay was used to determine the cell viability. Table 4 summarizes the IC_{50} values of the drugs obtained for each cell line. Results are representative of two independent experiments.

Table 7. IC_{50} values of chemotherapy drugs in the CRC cell lines analysed

	HT29	HCT116	HCT116*P53*-/-
5-FU	10 μM	6.8 μM	7.2 μM
OXA	0.9 μM	0.77 μM	3.2 μM
IRI	0.2 μM	0.024 μM	0.130 μM

4.2.1 Analysis of combinatorial treatments with metformin and single chemotherapeutic drugs

Because of the various time-serial combinations of metformin with chemotherapeutic drugs we had to analyse, we decided to use a comparison of cell viability (i.e. a cell viability assay) than the analysis with the combination index method. To assess whether combined treatments with metformin and chemotherapy drugs were more effective than individual treatments to induce a decrease in cell viability, the IC_{50} concentrations selected for 5-FU, OXA, IRI and metformin were tested alone or combined in different settings: chemotherapy and metformin administered simultaneously (for 96 hours) or in different sequences, metformin at first or *vice versa* (where metformin and the drugs were given for 72 and 24 hours, respectively). I also exposed the cells to longer treatments with the administration of chemotherapy drugs for 3 days and then the replacement of the medium with metformin for three more days and *vice versa* (at first metformin and then chemotherapy drugs). The experimental design showing the different sequences of administered treatments is summarised in Figure 8 of the Material and Methods chapter.

4.2.1.1 Analysis of combinatorial treatments with metformin and 5-FU

As shown in Figure 21 A, metformin (MET) and 5-FU given alone reduced cell viability in HT29 cells, and the effect was greater for 5-FU (MET vs 5FU, *P* value <

0.0001). The addition of MET to 5-FU (5FU-MET) had almost the same effect of the treatment with 5FU alone, in terms of cell viability. On the contrary, the administration of 5-FU both for short (1 day) or longer (3 days) times before MET (5FU→MET and 5FU3→MET) increased cell viability (5FU vs 5FU→MET, *P* value < 0.0001; 5FU vs 5FU3→MET, *P* value = 0.0005), which is suggestive of an inhibitory effect of MET on 5-FU. The administration of MET before 5-FU, both for short (1 day) or longer (3 days) times (MET→5FU and MET→5FU3), had no effects on the viability of the cells, which was similar to that observed in the untreated control.

In the two HCT116 cell lines (*TP53*-WT and *TP53*-null) MET was more effective than 5-FU in reducing cell viability (MET vs 5FU in HCT116, *P* value = 0.0385; in HCT116*P53*-/- cells, *P* value < 0.0001), both when given alone and in combination with chemotherapy and the effect was stronger for the *TP53*-null cells (5FU vs 5FU-MET, in HCT116 *P* value = 0.0003; in HCT116*P53*-/- cells, *P* value < 0.0001; Figure 21 B and C). Sequential treatment given for a short time (5FU→MET and MET→5FU) had more efficacy than treatments at longer times (5FU→MET vs 5FU3→MET in HCT116, *P* value < 0.0001, in HCT116*P53*-/-, *P* value = 0.0002) and the strongest effect was achieved when MET was administered before 5-FU (5FU→MET vs MET→5FU in HCT116, *P* value < 0.0001; in HCT116*P53*-/- cells, *P* value = 0.0084). In HCT116 cells the longer exposure to 5-FU, both before and after MET (5FU3→MET and MET→5FU3), had the lowest effect on the reduction of cell viability, while in HCT116*P53*-/- cells treatments for longer times had the same effects of 5-FU alone.

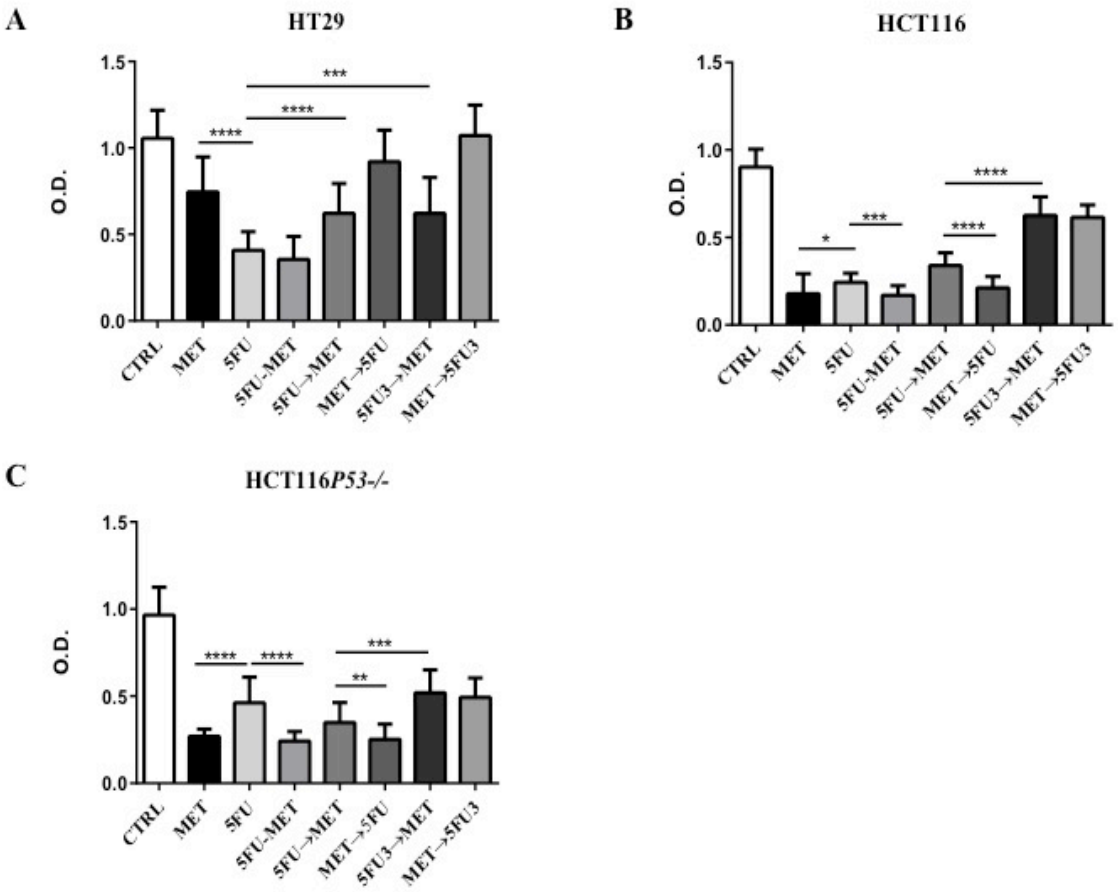

Figure 21. Effects of 5-FU and metformin treatments on CRC cell viability. The cells were seeded in six replicates in a 96-well plate and treated with metformin and/or 5-FU at their respective IC_{50} values. The cell proliferation rate was measured using the MTT assay. The bars indicate the mean value ± SD of three independent experiments (*P < 0.05, **P < 0.01, ***P < 0.001, ****P < 0.0001). O.D.= optical density.

In summary, metformin has little effect on the viability of HT29 cells and, when given before 5-FU, it diminishes the efficacy of the chemotherapy. On the contrary, the biguanide strongly reduces the viability of the two HCT116 cell lines; however, its combination with 5-FU does not enhance the reduction of cell viability.

4.2.1.2 Analysis of combinatorial treatments with metformin and oxaliplatin

Similarly to what was observed for the treatment with 5-FU, MET and OXA given alone reduced viability in HT29 cells, and the effect was stronger for OXA (MET vs OXA, *P* value < 0.0001), while addition of MET to OXA (OXA-MET) gave similar results as treatment with OXA alone (Figure 22 A). Sequential treatments were less effective and

the administration of OXA before MET both for short and longer times (OXA→MET and OXA3→MET) reduced the viability of cells better than the opposite sequences of the drugs (MET→OXA and MET→OXA3; OXA→MET vs MET→OXA and OXA3→MET vs MET→OXA3, *P* value < 0.0001).

In the two HCT116 cell lines the administration of MET and OXA as single drugs markedly reduced the cell viability (Figure 22 B-C) and OXA-MET combination was even more effective (OXA vs OXA-MET in HCT116, *P* value < 0.0001; in HCT116*P53*-/- cells, *P* value = 0.0472). In HCT116 cells the synergistic effect of the two drugs was confirmed when OXA was administered sequentially with MET and for short times (OXA→MET and MET→OXA; OXA vs OXA→MET, *P* value = 0.0078; OXA vs MET→OXA, *P* value = 0.0103; Figure 20 B). Longer exposure to OXA (OXA3→MET and MET→OXA3) was the treatment less effective. These results were not confirmed in the HCT116 *TP53*-null cells where OXA→MET, MET→OXA and OXA3→MET treatments gave similar results to single treatment with MET, and the sequence MET→OXA3 had the lowest reduction of cell viability.

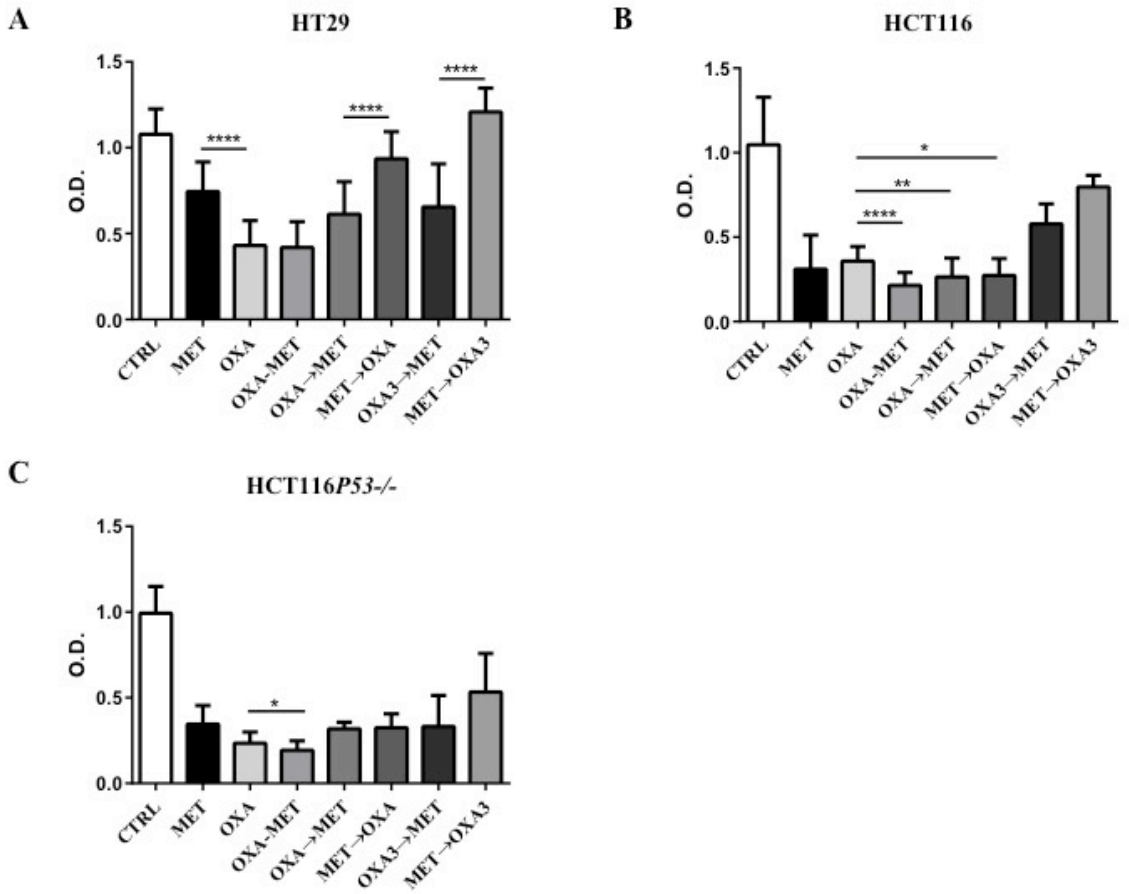

Figure 22. Effects of oxaliplatin and metformin treatments on cell viability. The cells were seeded in six replicates in a 96-well plate and treated with metformin and/or oxaliplatin (OXA) at their respective IC_{50} values. The cell proliferation rate was measured using the MTT assay. The bars indicate the mean value ± SD of three independent experiments (*P < 0.05, **P < 0.01, ****P < 0.0001).

These results confirm the poor efficacy of metformin on HT29 cells and its inhibitory effect on the chemotherapy. Metformin is more effective on the two HCT116 cell lines and shows a synergistic effect when combined with OXA.

4.2.1.3 Analysis of combinatorial treatments with metformin and irinotecan

All cell lines showed the same pattern of response to treatment with IRI and MET (Figure 23 A-B-C). IRI alone strongly reduced cell viability, and addition of MET diminished its effectiveness (IRI vs IRI-MET in HT29 cells, *P* value < 0.0001, in HCT116 cells, *P* value = 0.0267, in HCT116*P53*-/- cells, *P* value < 0.0001). This was particularly

evident for the sequential treatments in which MET was added before IRI (MET→IRI and MET→IRI3), where I observed the highest cell viability, which was almost similar to that obtained for MET in single treatment. On the contrary, treatment with IRI for 3 days, followed by MET was the most effective (IRI vs IRI3→MET in HT29 cells, *P* value = 0.0060, in HCT116 cells, *P* value < 0.0001, in HCT116*P53*-/- cells, *P* value = 0.0154). These data suggest that metformin could act as antagonist for IRI.

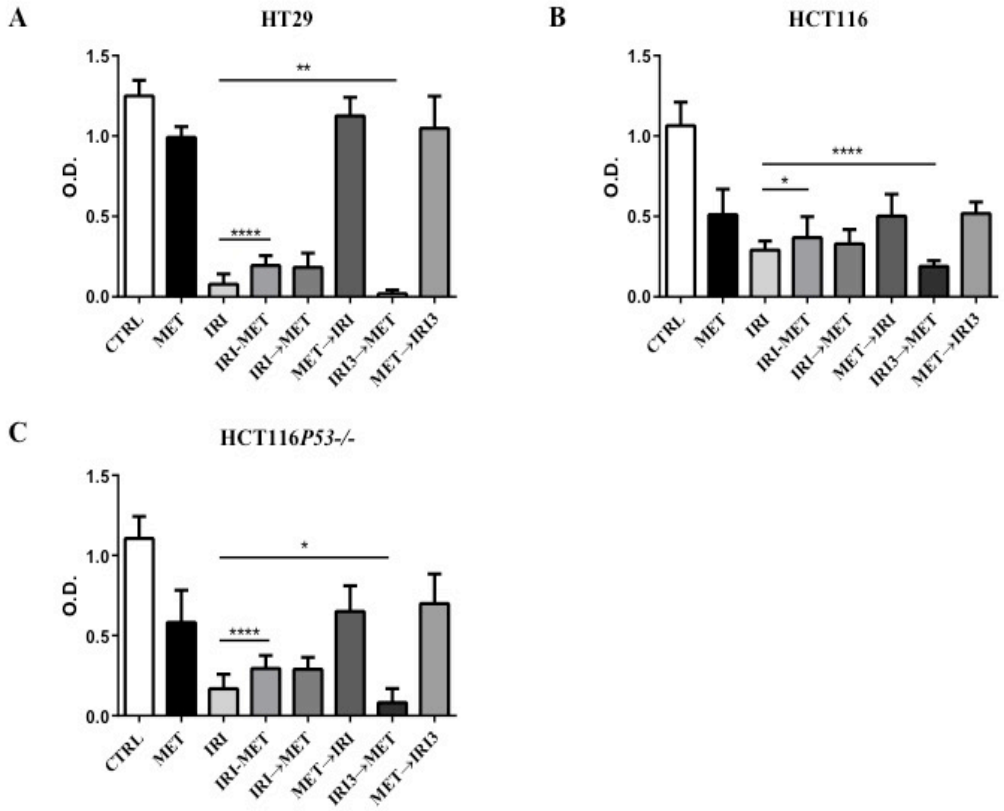

Figure 23. Effect of irinotecan (SN-38) and metformin treatments on cell viability. The cells were seeded in six replicates in a 96-well plate and treated with metformin and/or irinotecan (IRI) at their respective IC_{50} values. The cell proliferation rate was measured using MTT assay. The bars indicate the mean value ± SD of three independent experiments (*P < 0.05, **P < 0.01, ***P < 0.001, ****P < 0.0001).

4.2.2 Analysis of combinatorial treatments with metformin and chemotherapeutic drugs administered as regimens

After having determined the effects of metformin in combination with chemotherapy drugs used for the treatment of CRC, I evaluated the effects of the biguanide in combination with standard chemotherapy regimens used for the first-line treatment of

CRC. These regimes combine 5-FU, folic acid, administered to enhance the effect of chemotherapy drugs, and OXA (FOLFOX) or IRI (FOLFIRI). I combined different concentration of the drugs and I have identified the best dose-effect concentration using the Compusyn software (Chou and Talalay, 1984; Supplementary tables 1-6). The concentrations of 5-FU combined with OXA and IRI I have selected are shown in Table 8.

Table 8. Combined concentration of chemotherapy drugs obtained by Compusyn software

	HT29	**HCT116**	**HCT116*P53*-/-**
OXA + 5-FU	0.1 μM + 2.5 μM	0.385 μM + 0.85 μM	1.6 μM + 0.9 μM
IRI + 5-FU	0.1 μM + 0.625 μM	0.048 μM + 0.425 μM	0.0325 μM + 0.45 μM

Metformin was used at a concentration of 5 mM. Similarly to what was done for the experiments where metformin was combined with single drugs, I have tested different sequences of combined treatments with metformin, whose design is shown in Figure 9 of the Material and Methods chapter.

4.2.2.1 Analysis of combinatorial treatments with metformin and oxaliplatin-5-FU regimen

I observed that in the cell line HT29 the combination OXA-5FU reduced the viability of cells better than metformin administered alone (MET vs OXA-5FU, *P* value = 0.0351) and the simultaneous administration of the regimen and metformin (OXA-5FU-MET) was even more effective (OXA-5FU vs OXA-5FU-MET, *P* value = 0.0425; Figure 24 A). When OXA-5FU regimen was administered prior metformin, for short or longer times (OXA-5FU→MET, (OXA-5FU)3→MET), the reduction of cell growth was comparable to that observed for treatment with only metformin (MET). Similarly to what was observed in the combined treatment of metformin with 5-FU and OXA (Figure 21 A

and 22 A), when metformin was administered before the chemotherapy drug regimens (MET→OXA-5FU and MET→(OXA-5FU)3) reduction of cell viability was less evident. Metformin confirmed to be very effective in the HCT116 cell line. The biguanide was more efficient that chemotherapy in reducing cell viability and its administration alone, along with regimen (OXA-5FU-MET) or before regimen (MET→OXA-5FU) was the most effective treatment in reducing cell viability (MET vs OXA-5FU, *P* value < 0.0001; Figure 24 B). On the contrary, the regimen OXA-5FU administered before metformin, both for short or longer time reduced the effectiveness of the biguanide. Finally, the administration of OXA-5FU for three days after metformin had the same reduction in cell viability as the regimen alone, confirming the greater sensitivity of HCT116 cells to metformin that to the regimen.

In HCT116*P53-/-* cells the OXA-5FU regimen was more effective than metformin administered alone (OXA-5FU vs MET, *P* value = 0.0132) and the combination OXA-5FU-MET (OXA-5FU vs OXA-5FU-MET, *P* value = 0.0011; Figure 24 C). Indeed, administration of the regimen before metformin, at short and longer times (OXA-5FU→MET and (OXA-5FU)3→MET) reduced cell viability more than the opposite treatments (MET→OXA-5FU and MET→(OXA-5FU)3 and OXA-5FU→MET vs MET→OXA-5FU, *P* value = 0.0002; (OXA-5FU)3→MET vs MET→(OXA-5FU)3, *P* value < 0.0001). Exposure to the regimen for 3 days before metformin ((OXA-5FU)3→MET) was the most effective treatment (OXA-5FU vs (OXA-5FU)3→MET, *P* value < 0.0001).

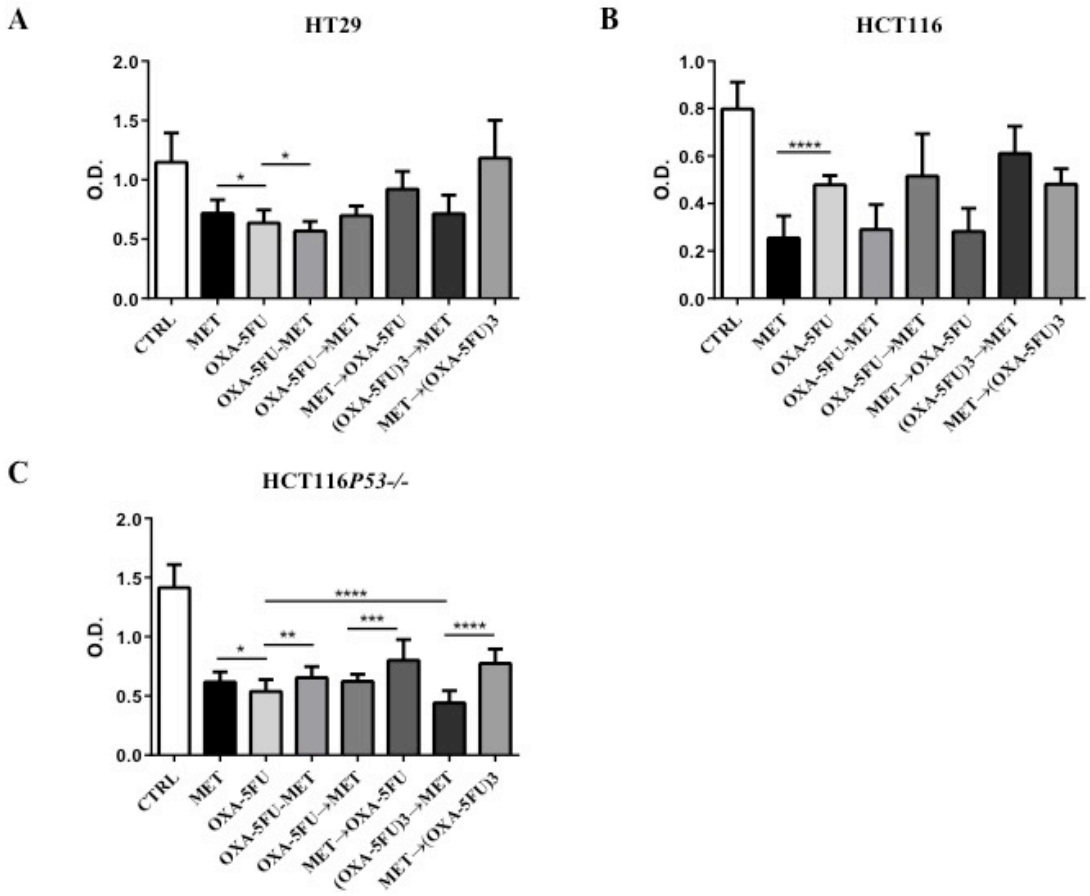

Figure 24. Effect of oxaliplatin-5-FU (OXA-5-FU) regimen and metformin treatments on cell viability. The cells were seeded in six replicates in a 96-well plate and treated with metformin and/or OXA-5FU regimen. Metformin was administered at a 5mM concentration in all the treatments. The regimen concentrations administered have been determined using the Compusyn software: 0.1 μM (OXA) + 2.5 μM (5-FU) for HT29 cells, 0.385 μM (OXA) + 0.85 μM (5-FU) for the HCT116 cell line and 1.6 μM (OXA) + 0.9 μM (5-FU) for HCT116*P53*-/- cells. The cell proliferation rate was measured using the MTT assay. The bars indicate the mean value ± SD of three independent experiments (*P < 0.05, **P < 0.01, ****P < 0.0001).

In conclusion, metformin combined with regimen was the most effective treatment in reducing viability of HT29 cells, indicating a likely synergism. HCT116 cells were highly sensitive to metformin administered alone or in combination with the regimen and its effect was maintained also after one day exposition to the regimen. In HCT116*P53*-/- cells the regimen better reduced cell viability than metformin and the combinatorial treatment with the biguanide.

4.2.2.2 Analysis of combinatorial treatments with metformin and irinotecan-5-FU regimen

I found that the regimen including irinotecan was very efficient in reducing the viability of HT29 cells, and the addition of metformin administered in combination with IRI-5-FU or after 1 day of treatment with the regimen, did not increase the effectiveness of the treatment (Figure 25 A). However, a prolonged exposure to IRI-5-FU followed by treatment with metformin ((IRI-5FU)3→MET) was the most effective treatment (IRI-5FU vs (IRI-5FU)3→MET, *P* value < 0.0001), while administration of metformin before IRI-5FU greatly reduced the effects of the regimen.

The cell line HCT116 was very sensitive both to metformin and IRI-5-FU regimen (Figure 25 B). However, the addition of metformin to the regimen did not further reduce cell viability. The administration of metformin followed by longer exposure to chemotherapy regimen (MET→(IRI-5FU)3) had the lowest reduction of viability. Although in HCT116*P53*-/- cell line the number or viable cells for all the tested treatment was higher than in HCT116 cells, a similar trend of response to the different treatments was observed. Moreover, in the *TP53* null cell line the regimen administered for longer time before metformin (IRI-5FU vs (IRI-5FU)3→MET, *P* value = 0.0002; Figure 25 C) was the most effective treatment.

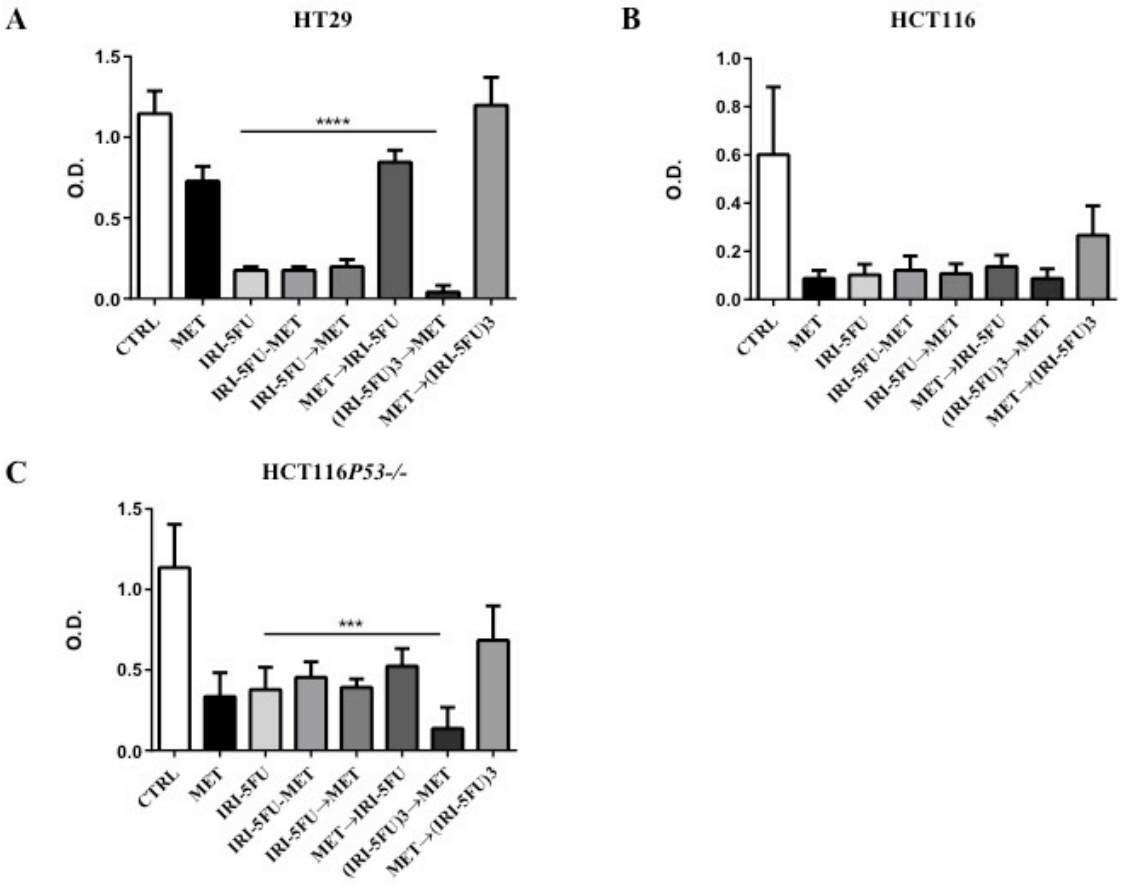

Figure 25. Effect of irinotecan-5-FU (IRI-5-FU) regimen and metformin treatments on cell viability. The cells were seeded in six replicates in a 96-well plate and treated with metformin and/or IRI-5FU regimen. Metformin was administered at a 5mM concentration in all the treatments. The regimen concentrations administered have been determined using the Compusyn software: 0.1 μM (IRI) + 0.625 μM (5-FU) for HT29 cells, 0.048 μM (IRI) + 0.425 μM (5-FU) for the HCT116 cell line and 0.0325 μM (IRI) + 0.45 μM (5-FU) for HCT116*P53*-/- cells. The cell proliferation rate was measured using the MTT assay. The bars indicate the mean value ± SD of three independent experiments (**P < 0.01, ***P < 0.001, ****P < 0.0001).

In the HT29 cell line the addition of metformin increased the effects of the regimen only when it was administered after a long treatment with IRI-5FU. Both metformin and regimen, alone and in all the combinations, strongly affected cell viability of HCT116 cells and the sequential exposure to regimen and metformin for longer times was the most effective treatment. A similar trend was observed in the HCT116*P53*-/- cell line, although with a lower reduction of viability.

4.2.3 Summary of key findings

- metformin is very effective in reducing viability of the HCT116 cell lines
- administration of irinotecan (single or as regimen) for 3 days followed by metformin is the most effective treatment in all the cell lines (probably because they overexpress IRI target), while the opposite treatment is the worst
- in HCT116 cell lines metformin and oxaliplatin administered together act synergistically on reducing viability
- combined treatments of metformin with chemotherapeutic drugs can be more effective than the single biguanide only in some settings and cell lines

4.3 Analysis of combinatorial treatments with metformin and targeted drugs

I also combined metformin with selective inhibitors of specific proteins expressed in CRC. I decided to focus on *in vitro* models of BRAF-mutant CRC because this tumour type has worse prognosis and is poorly sensitive to standard treatments (Kopets et al., 2015). The fact that BRAF-mutant CRCs are highly proliferating supports a possible action of metformin on blocking their growth. I selected three CRC cell lines, differing for their MMR activity, that when is defective can give microsatellite instability, or carrying different BRAF mutations: HT29 (microsatellite stable, MSS) and RKO (with defective MMR activity, microsatellite instable, MSI), both carrying the typical BRAF V600E mutation, and NCI-H508 cells (MSS) that are characterised by the rare BRAF G596R mutation, for which there are no specific treatments reported. I chose to use two CRC cell lines with the same mutation (BRAF V600E) but different in their MMR status because it has been recently demonstrated an association between MMR activity and clinical response: patients with MSI tumours are more responsive to immune checkpoint blockade than patients with MSS tumours (Le et al., 2015). I have treated the three cell lines with

metformin in combination with vemurafenib, a selective inhibitor for BRAF V600E mutation, panitumumab (selective inhibitor for EGFR), dasatinib (Bcr-Abl and Src inhibitor), regorafenib (a multi-kinase inhibitor) and trametinib (MEK inhibitor; Table 9).

Table 9. List of the target of drugs tested in combination with metformin

Type of drug	Target gene
Vemurafenib	BRAF
Panitumumab	EGFR
Dasatinib	Bcr-Abl and Src
Regorafenib	VEGFR-1, -2, -3, TIE-1, KIT, RET, BRAF, PDGFR-β, FGFR
Trametinib	MEK1, MEK2

Similarly to what I have done for testing the effects of the chemotherapy drugs on CRC cells, to identify the best concentration of the targeted drugs to administer in combination with metformin, I conducted MTT viability assays and treated each cell line for 72 hours with different concentrations of the drugs.

For each cell line, I designed a specific concentration range of vemurafenib for the MTT test analysis, based on the data of Yang et al. in which HT29 cells were defined highly-sensitive, RKO intermediate-sensitive and NCI-H508 low-sensitive to the drug (Yang et al., 2012). The concentration ranges that I selected were as follows: 7.75 nM – 0.248 μM for HT29 and 0.156 – 20 μM for RKO and NCI-H508. Similarly, HT29 and RKO cells (carrying the BRAF V600E mutation) are classified as resistant to anti-EGFR treatment, and NCI-H508 (BRAF G596R) as sensitive (Medico et al., 2015) and the concentration ranges I chose for the MTT analysis were: 0.54 nM - 10 μM for HT29 and RKO cells and 0.01 nM – 0.34 nM for NCI-H508 cells. As expected, treatment with panitumumab did not change the viability of HT29 and RKO cells even at the highest concentrations, confirming their resistance to the drug. For dasatinib, regorafenib and trametinib I established the concentrations to test based on those recommended by their leaflet and I drew the following concentration ranges: 30 nM – 100 μM for dasatinib and regorafenib and 0.007

nM – 0.12 μM for trametinib. Finally, I performed MTT assays to evaluate the concentrations of metformin to use for RKO and NCI-H508 cell lines and tested a concentration range of 0.16 – 20 mM. The viability plots and the IC_{50} values identified are shown on Figure 26 and Table 10.

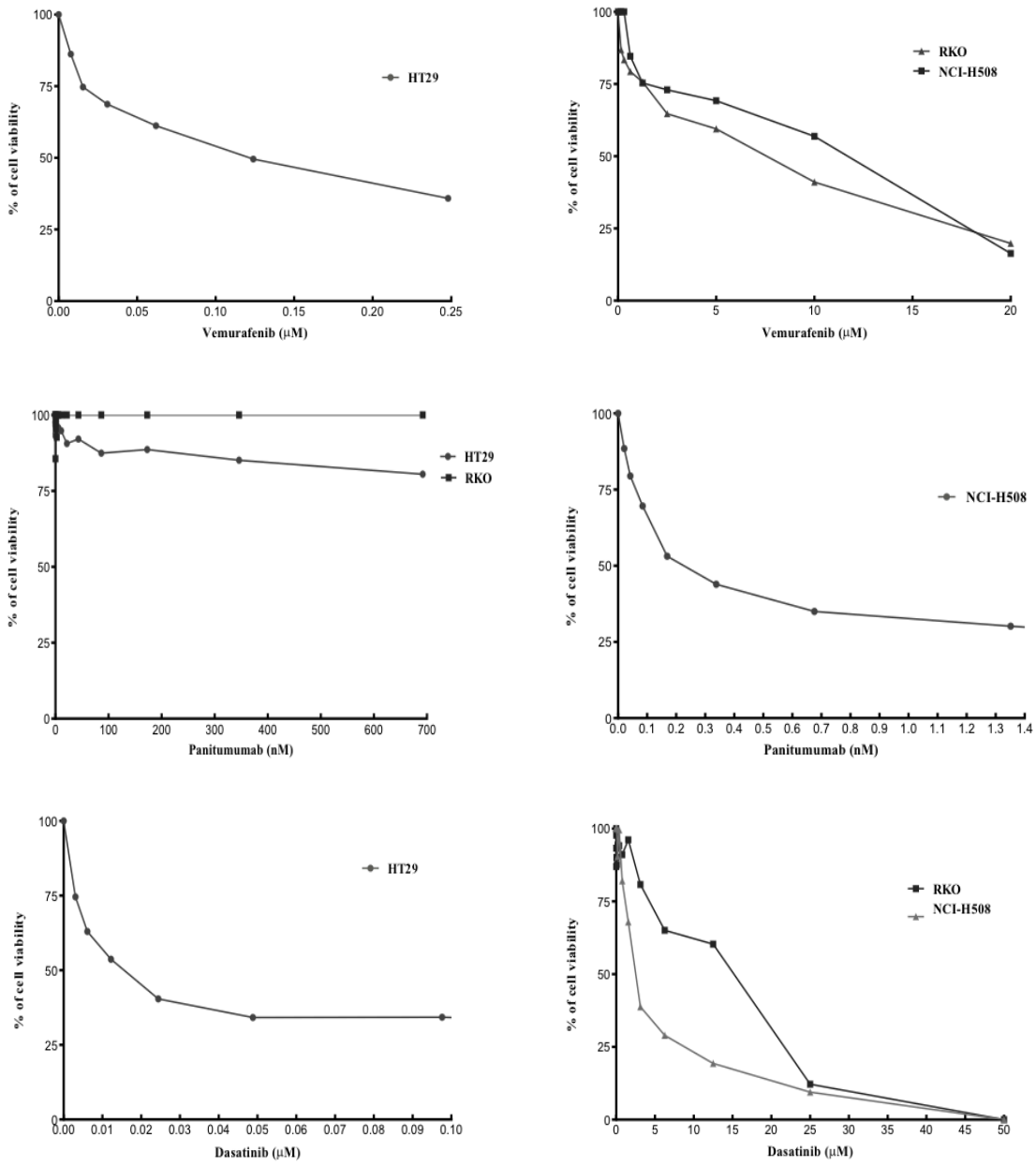

Figure 26. Determination of the IC_{50} values for targeted drugs and metformin in the BRAF-mutant cell lines. HT29, RKO and NCI-H508 cell lines were seeded in six replicates in a 96-well plate and treated with targeted drugs at different concentrations: 7.75 nM - 20 μM for vemurafenib, 0.003 - 10 μM for panitumumab, 30 nM – 100 μM for dasatinib and regorafenib, 0.007 nM – 0.12 μM for trametinib. The concentration range used for determining the IC_{50} values for metformin in RKO and NCI-H508 cells was 0.16 - 20 mM. After 72 hours MTT assay was used to determine the cell viability. Results are representative of two independent experiments.

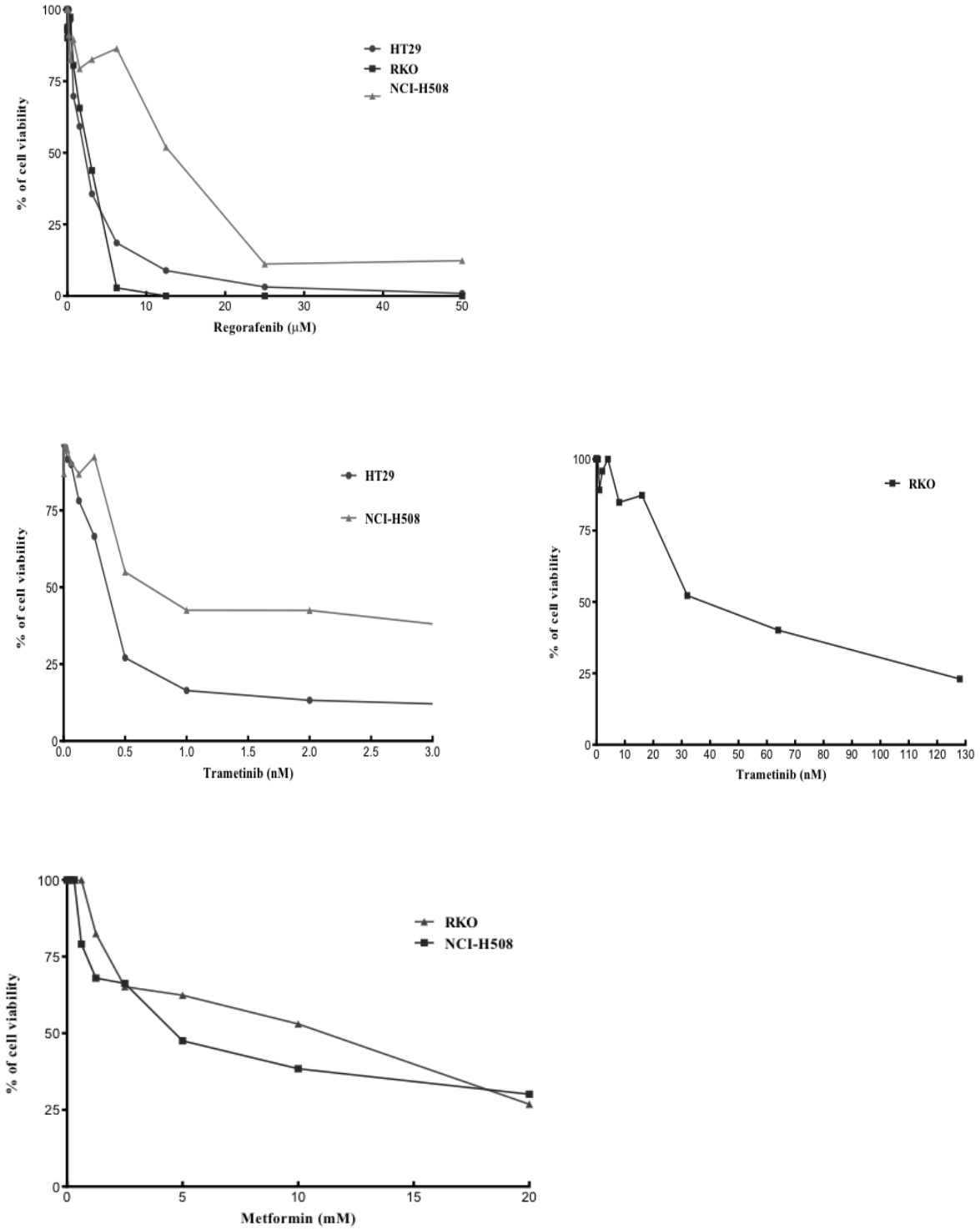

Figure 26. Determination of the IC_{50} values for targeted drugs and metformin in the BRAF-mutant cell lines. HT29, RKO and NCI-H508 cell lines were seeded in six replicates in a 96-well plate and treated with targeted drugs at different concentrations: 7.75 nM - 20 μM for vemurafenib, 0.003 - 10 μM for panitumumab, 30 nM – 100 μM for dasatinib and regorafenib, 0.007 nM – 0.12 μM for trametinib. The concentration range used for determining the IC_{50} values for metformin in RKO and NCI-H508 cells was 0.16 - 20 mM. After 72 hours MTT assay was used to determine the cell viability. Results are representative of two independent experiments.

Table 10. IC_{50} values of targeted drugs in the CRC cell lines analysed.

	HT29	RKO	NCI-H508
vemurafenib	0.12 μM	7.5 μM	10 μM
panitumumab	-	-	0.17 nM
dasatinib	12.2 nM	12.5 μM	2.5 μM
regorafenib	1.5 μM	3.12 μM	12.5 μM
trametinib	0.5 nM	32 nM	0.5 nM
metformin	5 mM	10 mM	5 mM

Using the CompuSyn software, I studied the effects of the interactions of the different combinations of the drugs and metformin and identified the concentrations of each drug to administer to the different cell lines. The combined concentrations of targeted drugs and metformin with CI<1 I selected are shown in Table 11. All the combinations dasatinib-metformin tested on NCI-H508 cells showed only antagonism (CI>1; supplementary table 7).

Table 11. Combined concentrations of targeted drugs and metformin obtained by Compusyn software.

	HT29	RKO	NCI-H508
vemurafenib + metformin	0.062 μM + 2.5 mM	7.5 μM + 5 mM	1.25 μM + 2.5 mM
panitumumab + metformin	-	-	0.02 nM + 2.5 mM
dasatinib + metformin	3.05 nM + 5 mM	6.25 μM + 2.5 mM	-
regorafenib + metformin	0.0976 μM + 1.25 mM	1.56 μM + 2.5 mM	1.56 μM + 1.25 mM
trametinib + metformin	0.5 nM + 10 mM	8 nM + 5 mM	1 nM + 5 mM

To evaluate the contribution of metformin in combinatorial therapies with these drugs I conducted biochemical analyses of the cells treated at the concentrations listed in table 10 and 11, focusing on the specific proteins targeted by the drugs used.

4.3.1 Analysis of changes in proteins from pathways deregulated in CRC

4.3.1.1 Analysis of combinatorial treatments with metformin and vemurafenib

In the HT29 cell line the concentrations of vemurafenib and metformin used in the combined treatment were lower than those used in the single treatments (the IC_{50} value obtained for each drug). In fact, I used 50% and a 25% of the IC_{50} concentrations of vemurafenib and of metformin respectively, obtaining 40% of cell death (Supplementary table 8). For RKO cells, where the mortality observed in the combined treatment was almost 90%, I maintained the IC_{50} concentration of vemurafenib and used 50% of the IC_{50} concentration of metformin (Supplementary table 9). In NCI-H508 I used 12.5% and 50% of the IC_{50} concentrations of vemurafenib and metformin respectively, obtaining more than 70% of cell death (Supplementary table 10).

In the HT29 cell line metformin treatment decreased the phosphorylation of ERK1/2 (Thr202/Tyr204) and blocked that of S6 protein (Ser240/244), while treatment with vemurafenib had a weak effect on the activity of ERK1/2 and S6 protein (Figure 27 A). Combined treatment including metformin and vemurafenib showed a reduction of ERK1/2 and S6 protein activity but an increase of Akt phosphorylation (Ser473). It has been reported that inhibition of the active BRAF-mutant (V600E) causes a feedback activation of EGFR in CRC (Corcoran et al., 2012; Prahallad et al., 2012) and for this reason I also evaluated the effects of vemurafenib on EGFR and found that vemurafenib administered alone reduced EGFR activity, while the concomitant addition of metformin increased EGFR phosphorylation.

Metformin alone markedly reduced the phosphorylation of ERK1/2, Akt and of S6 protein in RKO cells, while vemurafenib administered alone reduced the expression and activity of ERK1/2 and Akt (Figure 27 B). The combined treatment of vemurafenib with metformin reduced the activity of ERK1/2, Akt and of S6 protein; however, single treatment with metformin was more effective on all of them. RKO cells present low constitutive EGFR phosphorylation and for this reason I could not verify possible changes in this protein induced by the treatments.

Metformin administered alone only reduced the activation of S6 protein in the NCI-H508 cell line (Figure 27 C). Treatment with vemurafenib slightly reduced Akt and S6 protein activity and combined treatment of vemurafenib with metformin markedly decreased the phosphorylation of S6 protein, as a result of metformin treatment. As regards EGFR, both treatments reduced its phosphorylation and metformin seemed more effective than vemurafenib.

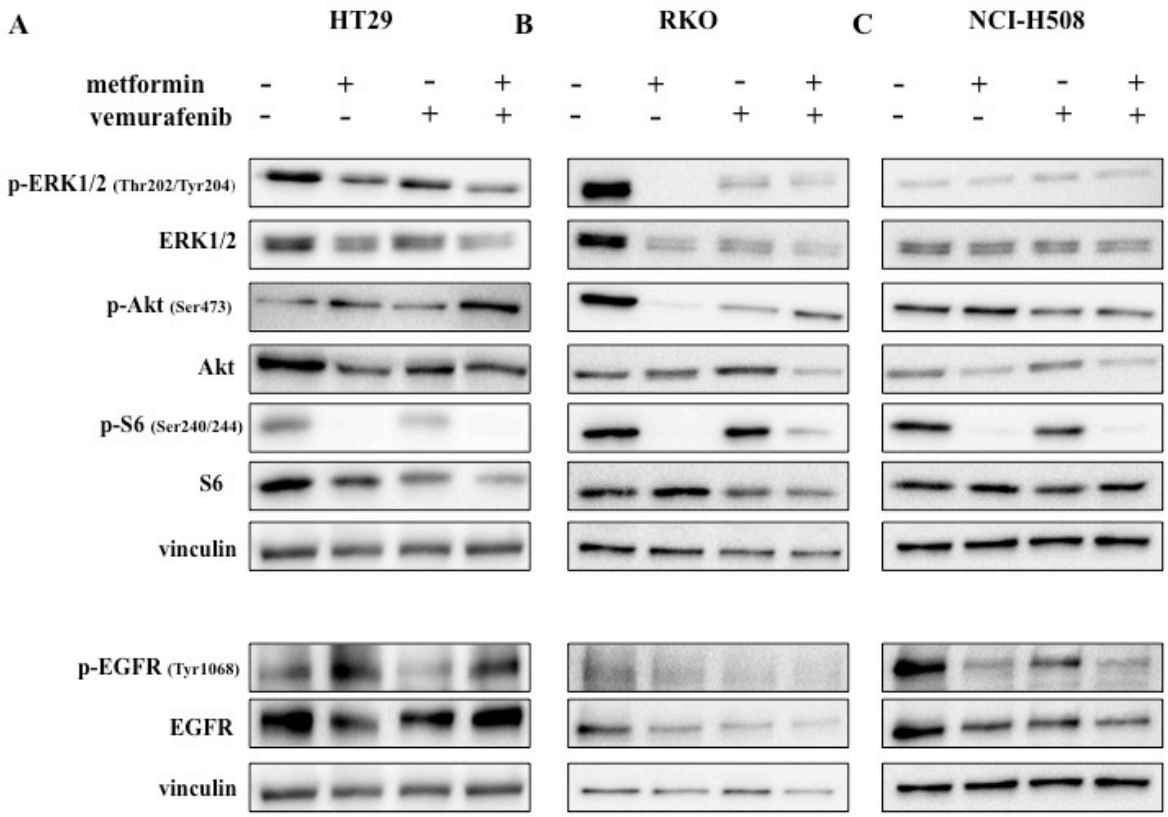

Figure 27. Effects of vemurafenib on cell signalling. HT29, RKO and NCI-H508 cell lines were left untreated or treated with metformin and vemurafenib at their respective IC_{50} values (HT29: 5 mM metformin and 0.062 μM vemurafenib; RKO: 10 mM metformin and 7.5 μM vemurafenib; NCI-H508: 5 mM metformin and 10 μM vemurafenib). The concentrations administered for the combined treatment were those determined using the Compusyn software (HT29: 2.5 mM metformin + 0.062 μM vemurafenib; RKO: 5 mM metformin + 7.5 μM vemurafenib; NCI-H508: 2.5 mM metformin + 1.25 μM vemurafenib). The treatments lasted for 72 hours. The combinatorial treatment of metformin and vemurafenib had no better effect than single treatments alone in all the cell lines analysed. Vinculin was used as the loading control. The results are representative of at least three independent experiments.

In summary, in all cell lines combined treatment of vemurafenib and metformin had no better effect than single treatments.

4.3.1.2 Analysis of combinatorial treatments with metformin and panitumumab

Only the NCI-H508 cell line was sensitive to the drug. The combined treatment of panitumumab and metformin consisted in 12.5% of IC_{50} concentration of panitumumab, plus metformin given at 50% of its IC_{50} and led to almost 40% of cell death (Supplementary table 11). Panitumumab given alone only reduced the activity of its target

EGFR (Figure 28). Interestingly, also metformin reduced EGFR activity. The sumiltaneous administration of panitumumab and metformin blocked the activity of S6 protein (as result of treatment with metformin) and, most of all, of EGFR for which the two drugs seemed to have synergistic effect.

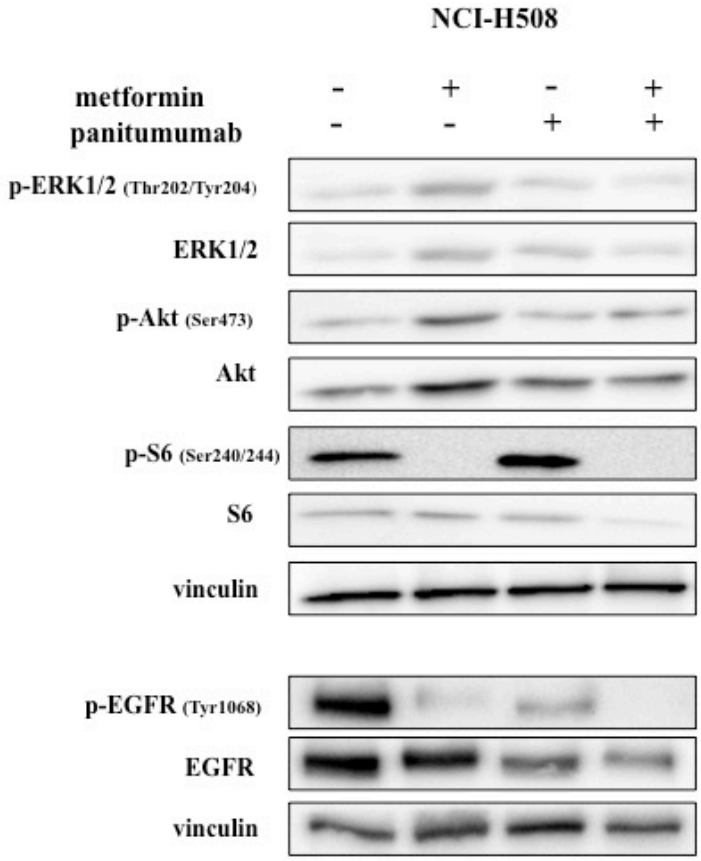

Figure 28. Effects of panitumumab on cell signalling. NCI-H508 cell lines were left untreated or treated with metformin and panitumumab at their respective IC_{50} values (5 mM metformin and 0.17 nM panitumumab). The concentrations administered for the combined treatment were those determined using the Compusyn software (2.5 mM metformin + 0.02 nM panitumumab). The treatments lasted for 72 hours. The combinatorial treatment of metformin and panitumumab reduced EGFR activation. Vinculin was used as the loading control. The results are representative of at least three independent experiments.

4.3.1.3 Analysis of combinatorial treatments with metformin and dasatinib

In combined treatments including dasatinib and metformin HT29 and RKO cells were treated with 25% and 50% of the concentrations of dasatinib and with 50% and 25%

of that of metformin used for the single treatments respectively, and treatment resulted in 50% and 60% of cell death (Supplementary tables 12 and 13).

Metformin reduced the growth of HT29 cells and decreases the expression of all the proteins analysed (Figure 29 A). The biguanide strongly diminished the phosphorylation of ERK1/2 and Src and blocked that of S6 protein. Dasatinib administered alone only resulted in a slight reduction of Akt activation, but not of Src, one of its known targets. Combined treatment of dasatinib and metformin maintained the reduction of ERK1/2 and of S6 protein activity induced by metformin, but did not reduce Src phosphorylation, suggesting that dasatinib antagonises the effect of metformin on Src. Similarly, metformin seemed to antagonise the reduction of Akt phosphorylation induced by dasatinib.

In RKO cells metformin alone markedly reduced the phopshorylation of all the proteins analysed (Figure 29 B). Treatment with dasatinib decreased the activation of ERK1/2 and, even if with weaker intensity, of Akt and S6 protein. Block of Src phosphorylation was stronger than that obtained with metformin. This block was maintained when cells were treated with both the drugs; however, reduction of ERK1/2, Akt and S6 protein activity, seen with metformin alone, were not observed.

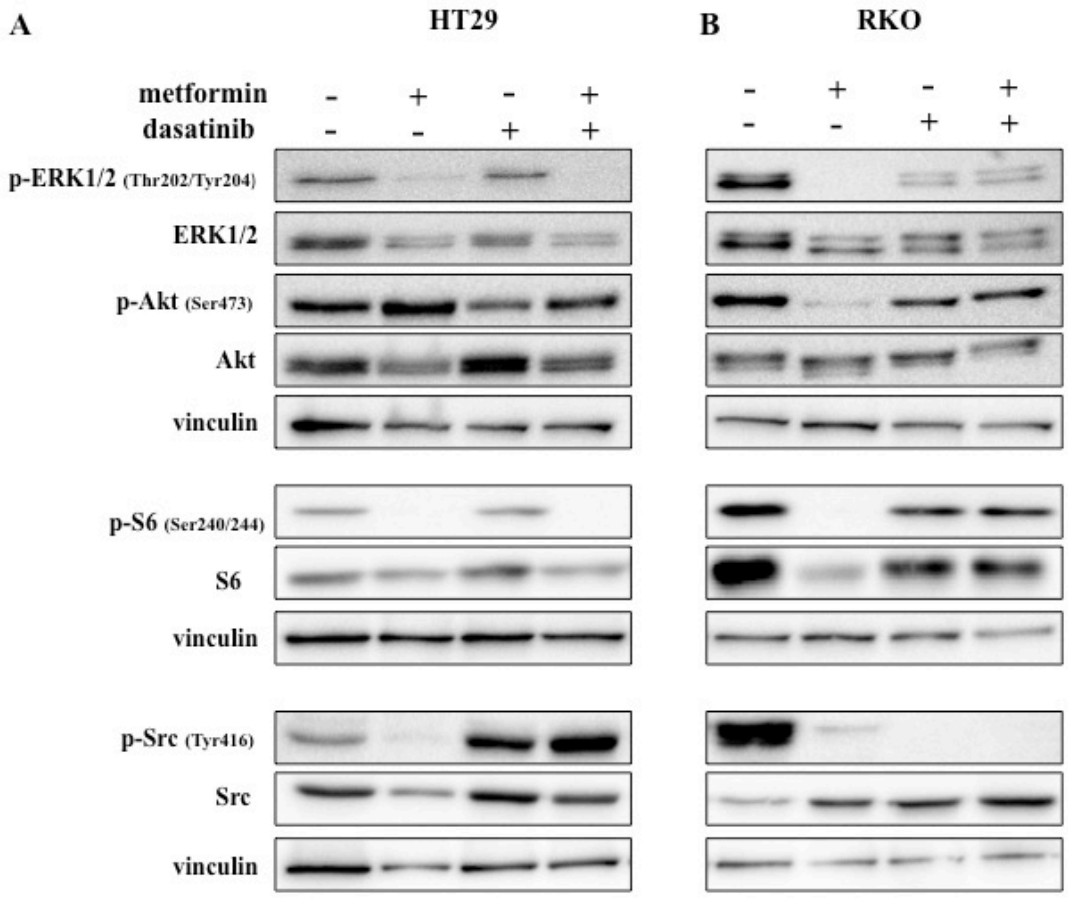

Figure 29. Effects of dasatinib on cell signalling. HT29 and RKO cell lines were left untreated or treated with metformin and dasatinib at their respective IC_{50} values (HT29: 5 mM metformin and 12.2 nM dasatinib; RKO: 10 mM metformin and 12.5 μM dasatinib). The concentrations administered for the combined treatment were those determined using the Compusyn software (HT29: 5 mM metformin + 3.05 nM dasatinib; RKO: 2.5 mM metformin + 6.25 μM dasatinib). The treatments lasted for 72 hours. The combinatorial treatment of metformin and dasatinib reduced ERK activation in HT29. Vinculin was used as the loading control. The results are representative of at least three independent experiments.

In HT29 cells the combination of dasatinib and metformin seemed to have better effect of the single treatments in reducing ERK1/2 phosphorylation, while in RKO cells the combined treatment did not reduce protein activity better than either drugs administered alone.

4.3.1.4 Analysis of combinatorial treatments with metformin and regorafenib

Regorafenib and metformin administered together were given to HT29 cells at 6.25% and 12.5% of the concentration s used in the individual treatments and resulted in 40% cell death (Supplementary table 14). Similarly, RKO cells received 50% and 25% of the concentrations of regorafenib and metformin administered in the single treatments, with almost 70% of cell mortality (Supplementary table 15). As for NCI-H508 cells, they were treated with 12.5% and 25% of the concentrations of regorafenib and metformin given alone and the treatment gave more than 40% of cell death (Supplementary table 16).
I have not been able to evaluate the effects of the combined treatment on the specific proteins targeted by regorafenib. I tested the expression of PDGFR-β and KIT, two target proteins of regorafenib, but the three cell lines I used do not express them. Thus, I assessed the effects of this combinatorial treatment by considering only changes in the activity of ERK1/2, Akt and S6 protein. Regorafenib did not affect the phosphorylation of ERK1/2, Akt and S6 protein in the HT29 cell line (Figure 30 A) and when combined with metformin it only reduced the activity of S6 protein, which was caused by the addiction of the biguanide (indeed, treatment with metformin alone inhibited S6 phosphorylation). Regorafenib did not change the activity of ERK1/2, Akt and S6 protein in RKO cells and when used in combination with metformin antagonised the effects of the biguanide, maintaining the phosphorylation of Akt and S6 protein (Figure 30 B). In NCI-H508 cells regorafenib reduced the phosphorylation of ERK1/2, Akt and also of S6 protein although the decrease of S6 protein activity was less than that observed with metformin (Figure 30 C). Combined treatment with the two drugs significantly increased ERK1/2 activation, while phosphorylation of Akt and of S6 protein was similar to that of treatment with regorafenib.

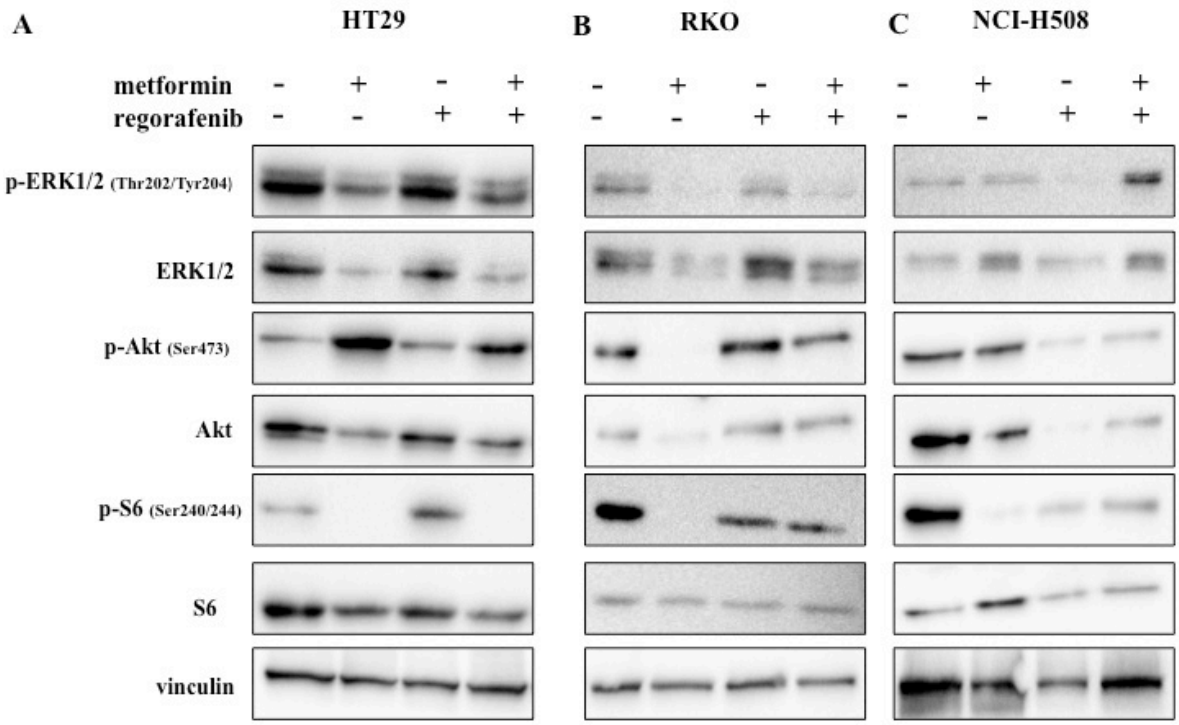

Figure 30. Effects of regorafenib on cell signalling. HT29, RKO and NCI-H508 cell lines were left untreated or treated with metformin and regorafenib at their respective IC_{50} values (HT29: 5 mM metformin and 1.5 μM regorafenib; RKO: 10 mM metformin and 3.12 μM regorafenib; NCI-H508: 5 mM metformin and 12.5 μM regorafenib). The concentrations administered for the combined treatment were those determined using the Compusyn software (HT29: 1.25 mM metformin + 0.0976 μM regorafenib; RKO: 2.5 mM metformin + 1.56 μM regorafenib; NCI-H508: 1.25 mM metformin + 1.56 μM regorafenib). The treatments lasted for 72 hours. The combinatorial treatment of metformin and regorafenib was less effective than single treatments alone in all the cell lines. However treatemtn with regorafenib administered alone reduced the activation of ERK, Akt and S6 in NCI-H508 cells. Vinculin was used as the loading control. The results are representative of at least three independent experiments.

In conclusion, in all cell lines analysed the combined treatment of regorafenib and metformin did not give a better effect than either drug alone.

4.3.1.5 Analysis of combinatorial treatments with metformin and trametinib

Trametinib in combination with metformin was administered to RKO cells using 50% of the concentrations of both the drugs given in single treatments and led to more than 70% cell death (Supplementary table 17). The concentrations used for the other two cell lines were still higher than the values administered in the individual treatments. HT29 cells received the same concentration of trametinib and two times that of metformin used for

individual treatments, while the NCI-H508 cells were treated with double the concentration of trametinib and with the same concentration of metformin given as a single treatment. Cell death was almost 80% for the HT29 cells and more than 50% for the cell line NCI-H508 (Supplementary tables 18 and 19).

Trametinib reduced the activity of its target ERK1/2 and Akt in HT29 cells. Similar results were obtained when metformin was added, and the biguanide reduced the activity of S6 protein (Figure 31 A). I also evaluated changes in the expression of c-Myc, a downstream target of ERK1/2: single treatment with trametinib reduced c-Myc expression, but its reduction was stronger in presence of metformin. Combined treatment gave similar results as the treatment with metformin.

In the RKO cell line trametinib given alone reduced the activity of ERK1/2 and c-Myc expression but increased S6 phosphorylation (Figure 31 B). Combined treatment with trametinib and metformin abolished ERK1/2 activity and decreased c-Myc expression, however I observed a marked increase of Akt activity and no reduction of S6 protein activity.

Trametinib slightly reduced the activity of ERK1/2 but increased S6 protein phosphorylation in NCI-H508 cells (Figure 31 C). The simultaneous administration of trametinib and metformin abolishes ERK1/2 activity, suggesting that it has a synergistic effect on the reduction of ERK1/2 phosphorylation. Block of the activity of S6 protein, caused by metformin, was also observed. Interestingly, no changes in c-Myc expression, even for treatment with metformin, were observed.

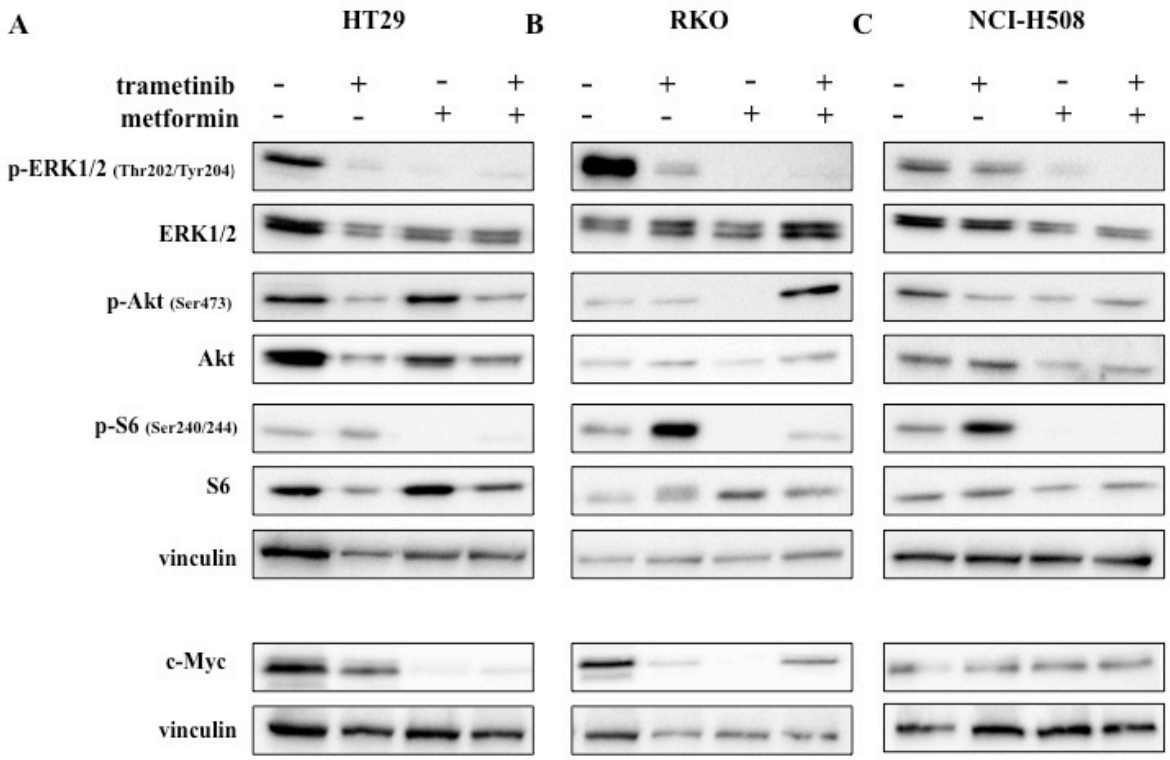

Figure 31. Effects of trametinib on cell signalling. HT29, RKO and NCI-H508 cell lines were left untreated or treated with metformin and trametinib at their respective IC_{50} values (HT29: 5 mM metformin and 0.5 nM trametinib; RKO: 10 mM metformin and 32 nM trametinib; NCI-H508: 5 mM metformin and 0.5 nM trametinib). The concentrations administered for the combined treatment were those determined using the Compusyn software (HT29: 10 mM metformin + 0.5 nM trametinib; RKO: 5 mM metformin 8 nM trametinib; NCI-H508: 5 mM metformin and 1 nM trametinib). The treatments lasted for 72 hours. The combinatorial treatment of metformin and trametinib reduced ERK activation in NCI-H508 cells. Vinculin was used as the loading control. The results are representative of at least three independent experiments.

In conclusion, combined treatment of trametinib and metformin was more effective than single treatments only in NCI-H508 cells, where it provoked the suppression of ERK1/2 activation.

4.3.2 Cell cycle analysis on combinatorial treatments

I observed that the administration of metformin in combination with vemurafenib, dasatinib and trametinib to RKO cells, as well as that of metformin given together with vemurafenib in NCI-H508 cells strongly decreased cell viability. In fact, after 72 hours of treatment, metformin given in combination with vemurafenib, dasatinib and trametinib

reduced viability of more than 80%, about 60% and more than 70% respectively in RKO cells. In the NCI-H508 cell line the combinatorial treatment vemurafenib-metformin caused more than 70% of cell death.

To investigate the cellular mechanisms that reduce viability, I decided to evaluate the changes in cell cycle progression induced by treatments including these drugs. In RKO cells, metformin treatment for 72 hours induced an accumulation of cells in the S phase (on average of 11.5%, specifically from 26.8% to 39.55% in the experiment with vemurafenib; from 29.23% to 43.40% in the experiment with dasatinib and from 20.85% to 28.74% in the experiment with trametinib; Figure 32 A-B-C) and in the G2/M phase (from 9.14% to 19.11% in the experiment with vemurafenib; on average of 10.24%, from 10.36% to 22.28% in the experiment with dasatinib and from 16.85% to 25.32% in the experiment with trametinib; Figure 32 A-B-C) respect to the untreated cells.

Addition of vemurafenib, both alone and in combination with metformin, did not induced substantial variations in the cell cycle profiles (Figure 32 A).

The DNA profiles of RKO cells treated with dasatinib alone or combined with metformin showed an increase in S phase (from 29.23% to 36.14% when dasatinib was administered alone and from 29.23% to 39.56% in the combined treatment; Figure 32 B).

Treatments with trametinib caused a marked accumulation of cells in G0/G1 phase (from 62.3% to 84.25% when trametibin was administered as single drug and from 62.3% to 73.78% in combined treatment trametinib-metformin; Figure 32 C). Moreover when trametinib was administered as single treatment I observed a reduction in the percentage of the G2/M phase fraction (from 16.85% to 6.43%).

In the NCI-H508 cell line treatment with metformin only resulted in a slight accumulation of cells in the S phase (from 24.63% to 30.79%), that I also observed after treatment with vemurafenib (from 24.63% to 33.24%) and which was confirmed in cells that had the combined treatment (from 24.63% to 34.73%; Figure 32 D).

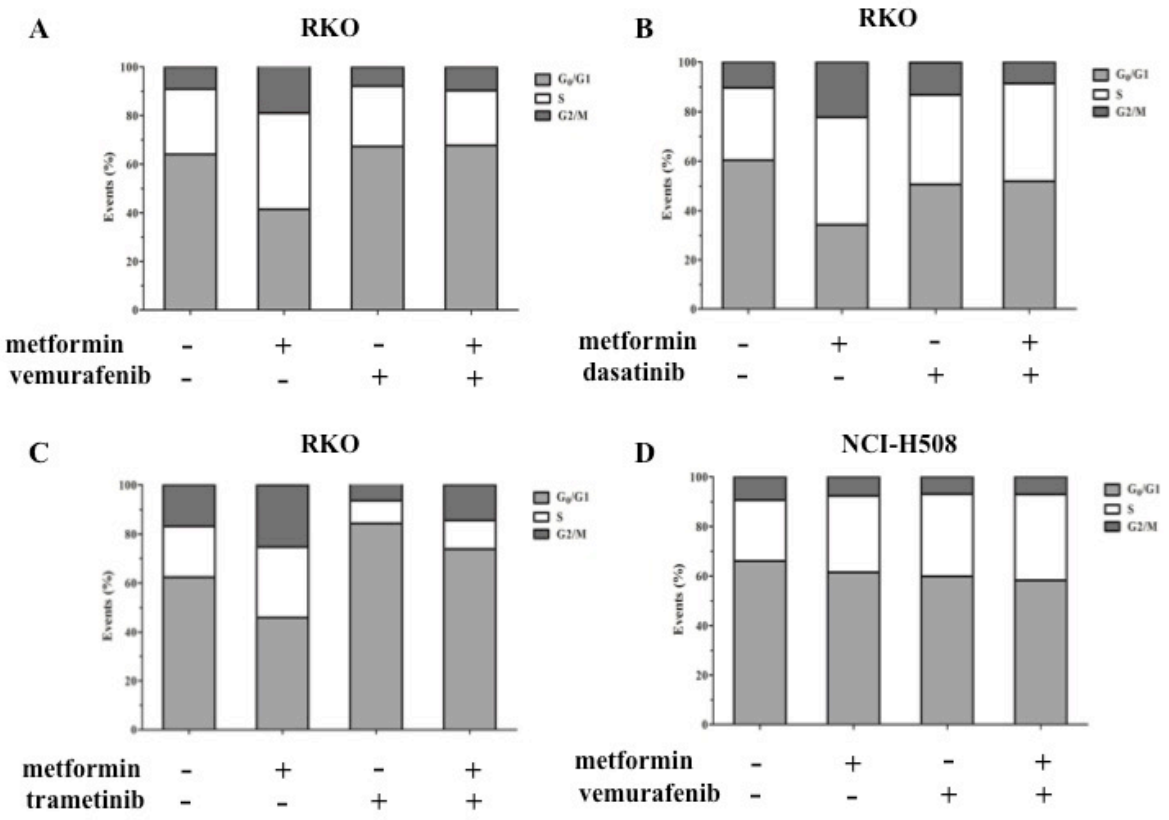

Figure 32. Cell cycle analysis in RKO and NCI-H508 cell lines treated with targeted drugs. The two cell lines were left untreated or treated with metformin and targeted drugs at their respective IC_{50} values (RKO: 10 mM metformin, 7.5 μM vemurafenib, 12.5 μM dasatinib and 32 nM trametinib; NCI-H508: 5 mM metformin and 10 μM vemurafenib). The concentrations administered for the combined treatment were those determined using the Compusyn software (RKO: 5 mM metformin + 7.5 μM vemurafenib; 2.5 mM metformin + 6.25 μM dasatinib; 5 mM metformin + 8 nM trametinib. NCI-H508: 2.5 mM metformin + 1.25 μM vemurafenib). The treatments lasted for 72 hours. In RKO cells metformin induced an accumulation in S and G2/M phases. Vemurafenib, alone or combined with metformin, did not induce changes in cell cycle profile. Treatment with Dasatinib caused an S phase increase, while Trametinib strongly increased G0/G1 phase. In NCI-H508 cells all treatments resulted in a slight accumulation of cells in S phase. Vinculin was used as the loading control. The results are representative of at least three independent experiments.

In conclusion metformin seems to determine a block in S phase of RKO cell lines. The stronger effect of targeted drugs on cell cycle was observed, always in RKO, after trametinib treatments where the drug, alone or in combination with metformin, leads to a cells accumulation in G0/G1 phase.

4.3.3 Summary of key findings

The combination of metformin with targeted drugs does not represent an advantage for treatment of BRAF-mutant CRC cell lines.

In addition, I observed that:

- metformin seems to be more effective in cells with high proliferation rate (RKO and HCT116) than those with slow growth (NCI-H508)
- tumours with BRAF G596R mutation could benefit from treatment with regorafenib

CHAPTER 5
DISCUSSION

We investigated the role of metformin alone or in combination with other drugs as potential anticancer therapy in CRC by analysing its effects on four cell lines (HT29, HCT116, HCT116*P53*-/- and DLD-1) and on 3D-organoids we derived from a peritoneal carcinomatosis. Although previous studies have shown that metformin inhibits the proliferation of CRC cells (Zakikhani et al., 2008), the drug's underlying mechanisms of action on CRC are still unclear. We found that metformin had a cytostatic effect, also on the stem component of the cells, but did not induce cell death. In addition, its effects were reversed after drug removal. In line with the observations in other types of cancer (Pierotti et al., 2013), the cytostatic effect of metformin appears to be determined by a reduction of cell proliferation, an increased accumulation of cells in G0/G1 phase, a decrease in the expression of proteins that regulate cell cycle progression such as cyclin D1 and c-Myc, and inhibited phosphorylation of the downstream target of cyclin D1, pRb.

The results we obtained for the DLD-1 cell line were controversial. In these cells metformin caused reduction of cyclin D1, c-Myc, cyclin E expression and of phosphorylation of pRb; however there was only a very weak decrease of the cell proliferation after 24 hours of treatment and, most of all, changes in the cell cycle were not observed. The fact that both the alleles of *LKB1* gene, the main activator of AMPK, are methylated in DLD-1 cells (Esteller et al., 2000) could, at least in part, explain these results. In fact, it has been demonstrated that LKB1 activity is required for cell cycle arrest in DLD-1 cells (Scott et al., 2007). Most of all, several studies have suggested that metformin can also act via activation of LKB1/AMPK-TSC1/TSC2 pathway and loss of LKB1 functions avoid the suppression of the mTOR-signaling pathway (Carretero et al., 2007). Finally, a recent study, in which the addiction of metformin to DLD-1 cells grown

under glucose-deprived conditions caused inhibition of cell growth (Miyo et al., 2016), suggests that in this cell line metformin requires low glucose conditions to suppress tumour growth.

We investigated whether the blockade of the cell cycle observed in the remaining cell lines and in the organoids could result in a permanent exit from the cell cycle or lead to cell death. Although in other types of cancer metformin promotes senescence, apoptosis or autophagy (Williams et al., 2013, Yi et al., 2013, Malki et al., 2011, Gao et al., 2016, Queiroz et al., 2014, Feng et al., 2014, Tomic et al., 2011), all the cell lines and the organoids analysed showed no permanent cytostatic effects or induction of cell death. Autophagy is a cellular process induced by deprivation of nutrients and growth factors, while we cultured the cells in complete media containing growth factors and nutrients that may have influenced the effects of metformin on our models. We used a standard culture medium containing 17 mM glucose; although several reports show that the biguanide induces apoptosis in this medium, there are data in breast cancer suggesting that metformin increases apoptotic cell death only in glucose deprivation conditions, while the presence of glucose causes cell cycle arrest (Wahdan-Alaswad et al., 2013, Menendez et al., 2012). As for CRC, Buzzai et al. reported that under nutrients deprivation, metformin can promote autophagy in CRC cell lines with wild type *TP53,* while it can induce apoptosis in TP53-deficient cells (Buzzai et al., 2007). The cell lines and the organoids we used were either *TP53* wild-type (HCT116 cells) or mutant (HT29 and DLD-1 cells and also organoids) and HCT116*P53*-/- cells had deletion of both the alleles of the gene, but we did not observe changes in the regulation of cell death related to the TP53 status of the cell lines. Most likely, the presence of nutrients could have exceeded the effects of metformin on these cells.

It has also been suggested that metformin may induce apoptosis when cells are seeded almost at confluence (Silvestri et al., 2015). We worked under low-density conditions (5×10^4 cells/cm^2) because it is required for carrying out drug sensitivity assays. In addition,

the drug induced a high degree of acidosis (a decrease in pH from 8 to 6.5) at a higher density (1.5×10^5 cells/cm^2), which may interfere with its effects. However, we did not observe apoptosis even under acidosis conditions (data not shown).

As for the effects of metformin on cell senescence, they have not yet been clarified and conflicting literature data have reported. In fact it has been demonstrated that metformin can induce TP53-dependent senescence in hepatoma cells (Yi et al., 2013) and in a triple negative breast cancer model (Williams et al., 2013), while Moiseeva et al., reported that metformin reduced the expression of pro-inflammatory cytokines implicated in the senescence process (Moiseeva et al., 2013).

A clonogenic assay showed that in HT29, HCT116 and HCT116*P53-/-* cells the cytostatic effect of metformin was transient and that cells treated with metformin even for 18 days, were still able to form new colonies in fresh complete medium after drug removal. HCT116*P53-/-* cells made more effort to revert this transient effect, thus suggesting that metformin is more effective in the absence of *TTP53*. As for DLD-1 cells, their clonogenic capacity was similar at all the time points analysed, which is in agreement with the absence of cell cycle arrest observed. However, it seems to contradict the immunoblotting data for cyclins D1 and E and for c-Myc, as well as pRB phosphorylation, which are all decreased by the treatment. These results suggest that metformin is only partially effective on these cells and acts only on some routes, which are offset from others and finally result in cell growth. The fact that DLD-1 cells have both the alleles of LKB1 gene inactivated (which is one of the targets of metformin) could contribute to give the observed results. Overall, the results we obtained on DLD-1 cells do not fully support an effect of the biguanide on them, at least at the concentrations used, and for this reason we decided to examine in more detail the effect of metformin only on the other cell lines and on the organoids.

The anti-proliferative action of metformin observed in HT29 and HCT116 and HCT116*P53-/-* cells and organoids seems to be mainly mediated by the inactivation of the mTOR pathway and IGF1R protein (Pierotti et al., 2013), both playing a critical role in cell

growth, and that are often deregulated in patients with various cancers (including CRC). Metformin reduced the phosphorylation of mTOR, of its downstream effectors (ribosome protein S6 and 4E-BP1) and of IGF1R. Interestingly, the inhibition of mTOR was also observed in the HCT116 and HCT116*P53*-/- cells in which AMPK was not activated, thus suggesting that metformin arrests cell growth in CRC cells through mechanisms different than activation of AMPK. There are in fact other pathways, such as RAG GTPase or REDD1 that are known to inhibit mTOR signalling after treatment with metformin (Kalender et al., 2010, Ben Sahra et al., 2011). Metformin may also reversibly inhibit complex I of the mitochondrial respiratory chain and stimulate the production of ROS, which induce cell cycle arrest (Marchi et al., 2012), thus providing an alternative mechanism to AMPK activation (Bridges et al., 2014, Biswas et al., 2006, Mackenzie et al., 2013).

The reversible effect of metformin on cell proliferation observed in the clonogenic assays was confirmed by the finding that mTOR pathway and IGF1R were completely restored after metformin removal and growth in fresh complete medium, without the drug.

The results obtained show that metformin can transiently inhibit the growth and proliferation of CRC, thus suggesting that it is not suitable for the treatment of cancer. Therefore we decided to design strategies that combine metformin with other drugs that can benefit from the inhibition of cell growth functions induced by the biguanide and promote cell death.

The majority of the chemotherapeutic drugs currently used for the treatment of CRC function damaging cells during the S phase of the cell cycle: the antimetabolite 5-FU interferes with DNA synthesis, the alkylating agent oxaliplatin directly damages DNA and the topoisomerase inhibitor irinotecan blocks DNA replication. We designed settings in which metformin and the chemotherapeutic drugs (given alone or in regimen combination) were administered in different combinations and for different times. We also tested longer

exposures to chemotherapy that can mimic the typical environment of patients undergoing prolonged treatment planning.

The addition of metformin to chemotherapy is controversial and in some cases appears to potentiate (Dong et al., 2012, Kim et al., 2014, Illiopulos et al., 2011), in others to antagonise (Janjetovic et al., 2011), the effects of chemotherapeutic drugs.

Irinotecan significantly decreased the viability in all the cell lines and its administration before metformin, especially for longer times, was the most effective treatment. The fact that topoisomerase I, the direct target of the drug, is highly expressed in CRC (Boonsong et al., 2002) may explain the sensitivity of these cells to the drug. Because of its cytostatic effect on CRC, metformin added after irinotecan may prevent the repair of the DNA breaks induced by the drug, driving damaged cells to death. In addition, in CRC the treatment with irinotecan appears to be associated with reduction of the stem cells markers CD44, CD166 and Lgr5 (Dylla et al., 2008, Emmink et al., 2011), which are also targeted by metformin. Since the stem component of tumours is considered the chemo-resistant fraction of cancer, its eradication could explain the high response of these cells to the drug.

On the contrary, metformin given before irinotecan seems to antagonise the chemotherapeutic drug. Most likely, the cytostatic effect of metformin lasts after its removal and prevents irinotecan to function. The same conclusions can be achieved when metformin is added before longer exposure to most of treatments including 5-FU or oxaliplatin.

Other differences observed reflect the individual sensitivity of the cells to the chemotherapeutic drugs. Metformin co-administered with 5-FU or oxaliplatin has a synergistic effect in HCT116 and HCT116*P53-/-* cell lines, while the oxaliplatin-5-FU regimen gives opposite results. In fact, HCT116 cells are more sensitive to metformin than to oxaliplatin-5-FU regimen, suggesting that the biguanide drives reduction of cell viability in the combinatorial treatment. This result is supported by the finding that oxaliplatin-5-FU regimen given before metformin cannot induce growth arrest. On the contrary,

HCT116*P53*-/- cells are more sensitive to oxaliplatin-5-FU regimen than to metformin and a longer administration of the regimen before the biguanide better reduces cell proliferation. Maybe these differences could be related to apoptosis induction.

The different response obtained with chemotherapy can be also attributed to the different status of *TP53*. It was reported that gain of function mutation on TP53, such as R273H present in HT29, or loss of *TP53* gene (in HCT116*P53*-/- cells) can confer resistance to different chemotherapeutic drugs including anti-metabolites, DNA cross-linking agents and topoisomerase inhibitors (Lowe *et al*., 1993, O'Connor et al., 1997, Boyer et al., 2004, Brosh et al., 2009, Fan et al., 1994, Blandino et al., 1999, Chang et al., 2001, Cabelguenne et al., 2000), although other authors showed that mutant TP53 displays sensitivity to chemotherapy (Fan et al., 1995, Bradford et al., 2003, Jackson et al., 2013). Our data highlight that the *TP53* status could be linked to different responses to chemotherapy. As shown in table 7, *TP53*-mutant HT29 cells are less sensitive to 5-FU and irinotecan. In accordance with Boyer et al. in our experiment HCT116*P53*-/- cells were the most resistant to oxaliplatin (Boyer et al., 2004). HCT116 cells (*TP53* WT) were the most sensitive for all the drugs tested and it has been reported that sensitivity to 5-FU and oxaliplatin was a characteristic of *TP53* WT CRC cells (Boyer et al., 2004, Toscano et al., 2007, Bunz et al., 1999). This can be explained considering that most of the chemotherapeutic drugs are anti-apoptotic agents and mutations in the apoptosis pathway, in which TP53 protein is one of the main players, can protect cancer cells from death.

Our data highlight that HCT116 and HCT116*P53*-/- are very sensitive to metformin; both cells have a fast growth and the biguanide may better exert its cytostatic function. In combined treatments metformin added after chemotherapy increases cell death, most likely because its cytostatic effect avoids the repair of DNA damage. The most effective treatment consists of metformin combined with irinotecan. Indeed trials that will establish the clinical relevance of metformin plus irinotecan combination in CRC patients (NCT01930864, on refractory CRC) have been already activated.

Finally we tested metformin in combination with targeted drugs on BRAF-mutant cell lines. Although at first these drugs show a great response rate, resistance develops in a short period of time. Among novel potential therapeutic options, the association of targeted drugs with regulators of the metabolism could be a promising strategy to overcome the inevitable resistance.

The analysis of changes in proteins from pathways deregulated in CRC, and potentially target of the drugs tested, showed that the combination of metformin with vemurafenib (which inhibits V600E-mutant BRAF) increased the phosphorylation of Akt and of EGFR in HT29 and RKO cells, suggesting antagonism between the two drugs. The drug made no protein alterations in NCI-H508 cells (G596R-mutant BRAF) and the reduced activity of EGFR and of S6 protein observed in the combined treatment was driven by metformin. Furthermore, dual treatment induced no modifications of the cell cycle phases in any of the tested cell lines (RKO and NCI-H508). It has been shown that the combination with metformin and vemurafenib inhibits mTOR signalling, induces cell cycle arrest in G1 phase and apoptosis in BRAF V600E-mutant melanoma cell lines, and *in vivo* results in tumour regression (Niehr et al., 2011, Yuan et al., 2013). Similar findings were also obtained in BRAF V600E-mutant thyroid cancer cell lines (Hanly et al., 2015). One possible explanation of our results may be that HT29 and RKO cell lines are mutated in the PIK3CA gene (Ikenoue et al., 2005) and resistance to vemurafenib in BRAF V600E-mutant CRC cells has been associated with the presence of PIK3CA mutations that hyper-activate the PI3K/Akt pathway (Mao et al., 2013). Although metformin strongly inhibited Akt activation in RKO cells, its administration with vemurafenib hampers this effect.

Metformin combined with the EGFR inhibitor panitumumab in NCI-H508 cell line abolished the phosphorylation of EGFR, but maintained active the downstream proteins Akt and ERK1/2.

Combinatorial treatment with the Src inhibitor dasatinib and metformin reduced the activation of ERK1/2 but increased Src phosphorylation in HT29 cells. As for the RKO

cell line, the drug administered with metformin slightly increased the S phase of the cell cycle, but the two drugs given together only showed reduction of EGFR activity. Lin et al. reported that metformin synergizes with dasatinib in head and neck squamous cell carcinoma cells, through AMPK-mediated energy stress (Lin et al., 2014). Further analyses of this pathway on our cells could help in understanding the effects of the dual treatment in CRC.

As for the combinatorial treatment with metformin and the multi-kinase inhibitor regorafenib, it had no advantages compared to the individual drugs in all the cell lines. In a recent paper on non-small cell lung cancer, in which metformin was combined with sorafenib (another multi-kinase inhibitor), the authors report a synergistic growth inhibition induced by AMPK activation and inhibition of mTOR pathway (Groenendijk et al., 2015). This is in agreement with our observation that the combined treatment reduced activation of the S6 protein in HT29 and NCI-H508 cells. Regorafenib administered alone also reduced ERK1/2 and Akt activation in NCI-H508 cells; however, the combinatorial treatment with metformin antagonizes this effect.

The combination of metformin with trametinib, a MAPK inhibitor, had a synergistic effects only in NCI-H508 cells, where it suppressed the activation of ERK1/2 and of S6 protein. Similar results were reported in NRAS-mutant cell lines from melanoma, lung cancer and neuroblastoma, where also phosphorylation of Akt was reduced (Vujic et al., 2015). The reduction of cell viability we observed in RKO cells was similar to that described by these authors and is in line with the increase of G0/G1 phase we observed.

These results suggest that in *BRAF*-mutant CRC cells the combined therapy does not provide advantages over the one with the individual drugs. We found that RKO cells are very sensitive to metformin, most likely because of their fast growth that, as for HCT116 and HCT116*P53*-/- cells, may be targeted the biguanide. On the contrary, the fact that NCI-H508 cells grow very slowly could explain their weak response to metformin. As for NCI-H508 cells, the rare *BRAF* mutation they carry results in CRCs with different

characteristics compared to V600E-mutant tumours and for which there are no specific treatment recommendations (Cremolini et al., 2015). We have confirmed that treatment with anti-EGFR drugs reduced EGFR activity (Misale et al., 2014); however panitumumab did not diminished Akt and ERK1/2 phosphorylation. Instead our data have shown sensitivity of NCI-H508 cells to regorafenib, which decreases the phosphorylation of ERK1/2, Akt and of S6 protein.

Overall, our results show that metformin is cytostatic on CRC cells. They have different responses to treatment with the biguanide, administered either in single or in combined treatments, which are mainly related to their molecular and physiological characteristics. The experiments with the standard chemotherapy drugs highlight that the efficacy of combined treatments strongly hangs on the sequence in which the drugs are given and that, in some settings the biguanide can even antagonise the effects of chemotherapy. Antagonism has been observed also when metformin has been simultaneously administered with target drugs. Although further investigations are still needed to elucidate the results of the treatments including metformin, these data suggest that caution should be used in administering chemotherapy to indviduals taking metformin.

Summary of novel findings

The novel findings emerged from this work can be summarised in three main points:

- the effect of metformin on the block of cell proliferation is only temporary and does not make the drug suitable for the treatment of CRC
- the effectiveness of the combinatorial treatments with metformin and chemotherapeutic drugs depends on the characteristics of the cells and on the sequence in which the drugs are administered. This result suggests that caution should be used in administering chemotherapy in patients taking metformin
- the combination of metformin with targeted drugs do not represent an advantage

for the treatment of BRAF-mutant CRC and the assessment of the mutational status and of the proliferation rate of a tumor could help design effective therapeutic strategies

Summary of future directions

- study of the molecular mechanisms through which metformin induces cell growth arrest
- analysis of variations in the molecular pathways altered by metformin and standard chemotherapy and regimens (i.e. activation/inhibition of apoptosis or DDR?)
- *In vivo* experiments to examine response to the best combinatorial treatments identified *in vitro.*

REFERENCES

Algire C, Amrein L, Zakikhani M, Panasci L, Pollak M. Metformin blocks the stimulative effect of a high-energy diet on colon carcinoma growth in vivo and is associated with reduced expression of fatty acid synthase. Endocr Relat Cancer 2010;17:351–60.

Algire C, Moiseeva O, Deschênes-Simard X, Amrein L, Petruccelli L, Birman E, Viollet B, Ferbeyre G, Pollak MN. Metformin reduces endogenous reactive oxygen species and associated DNA damage, Cancer Prev. Res. 5(April (4)) (2012) 536–543.

Alimova IN, Liu B, Fan Z, Edgerton SM, Dillon T, Lind SE, Thor AD. Metformin inhibits breast cancer cell growth, colony formation and induces cell cycle arrest in vitro. Cell Cycle 2009; 8: 909–915.

Arakawa H "Netrin-1 and its receptors in tumorigenesis". Nat Rev Cancer. 2004 Dec;4(12):978-87.

Bao B, Wang Z, Ali S, Ahmad A, Azmi AS, Sarkar SH, Banerjee S, Kong D, Li Y, Thakur S, Sarkar FH. Metformin inhibits cell proliferation, migration and invasion by attenuating CSC function mediated by deregulating miRNAs in pancreatic cancer cells, Cancer Prev. Res. (Phila.) 5 2012, 355–364.

Barker N, van Es JH, Kuipers J, Kujala P, van den Born M, Cozijnsen M, Haegebarth A, Korving J, Begthel H, Peters PJ, Clevers H. Identification of stem cells in small intestine and colon by marker gene Lgr5. Nature. 2007 Oct 25;449(7165):1003-7.

Barker N. The canonical Wnt/beta-catenin signalling pathway. Methods Mol Biol. 2008;468:5-15.

Barker N, Ridgway RA, van Es JH, van de Wetering M, Begthel H, van den Born M, Danenberg E, Clarke AR, Sansom OJ, Clevers H. Crypt stem cells as the cells-of-origin of intestinal cancer. Nature. 2009 Jan 29;457(7229):608-11.

Barone C, Landriscina M, Quirino M, Basso M, Pozzo C, Schinzari G, Di Leonardo G, D'Argento E, Trigila N, Cassano A. Schedule-dependent activity of 5-fluorouracil and irinotecan combination in the treatment of human colorectal cancer: in vitro evidence and a phase I dose-escalating clinical trial. Br J Cancer. 2007 Jan 15;96(1):21-8.

Ben Sahra I, Laurent K, Loubat A, Giorgetti-Peraldi S, Colosetti P, Auberger P, Tanti JF, Le Marchand-Brustel Y, Bost F. The antidiabetic drug metformin exerts an antitumoral effect in vitro and in vivo through a decrease of cyclin D1 level, Oncogene 2008;27(25):3576-86.

Ben Sahra I, Regazzetti C, Robert G, Laurent K, Le Marchand-Brustel Y, Auberger P Tanti JF, Giorgetti-Peraldi S, Bost F. Metformin, independent of AMPK, induces mTOR inhibition and cell cycle arrest through REDD1. Cancer Res 2011; 71: 4366–4372.

Bennouna, J, Sastre J, Arnold D, Österlund P, Greil R , Van Cutsem E, von Moos R, Viéitez JM, Bouché O, Borg C, Steffens CC, Alonso-Orduña V, Schlichting C, Reyes-Rivera I, Bendahmane B, André T, Kubicka S; ML18147 Study Investigators. Continuation of bevacizumab after first progression in metastatic colorectal cancer

(ML18147): a randomised phase III trial. Lancet Oncol 2013 14: 29–37.

Biswas S, Chida AS, Rahman I. Redox modifications of protein-thiols: emerging roles in cell signaling. Biochem Pharmacol 2006;71(5):551-64.

Blandino G, Levine AJ, Oren M. Mutant TP53 gain of function: differential effects of different TP53 mutants on resistance of cultured cells to chemotherapy. Oncogene (1999) 18:477–485.

Bokemeyer C, Köhne CH, Ciardiello F, Lenz HJ, Heinemann V, Klinkhardt U, Beier F, Duecker K, van Krieken JH, Tejpar S. FOLFOX4 plus cetuximab treatment and RAS mutations in colorectal cancer. Eur J Cancer. 2015 Jul;51(10):1243-52.

Bokemeyer C, Van Cutsem E, Rougier P, Ciardiello F, Heeger S, Schlichting M, Celik I, Köhne CH. Addition of cetuximab to chemotherapy as first-line treatment for KRAS wild-type metastatic colorectal cancer: pooled analysis of the CRYSTAL and OPUS randomised clinical trials. Eur J Cancer. 2012;48(10):1466–1475.

Boonsong A, Curran S, McKay JA, Cassidy J, Murray GI, McLeod HL. Topoisomerase I protein expression in primary colorectal cancer and lymph node metastases. Hum Pathol 2002; 33: 1114–1119.

Boyer J, McLean EG, Aroori S, Wilson P, McCulla A, Carey PD, Longley DB, Johnston PG. Characterization of TP53 wild-type and null isogenic colorectal cancer cell lines resistant to 5-fluorouracil, oxaliplatin, and irinotecan. Clin Cancer Res. 2004 Mar 15;10(6):2158-67.

Bradford CR, Zhu S, Ogawa H, Ogawa T, Ubell M, Narayan A, Johnson G, Wolf GT, Fisher SG, Carey TE. TP53 mutation correlates with cisplatin sensitivity in head and neck squamous cell carcinoma lines. Head Neck (2003) 25:654–661.

Brosh R, Rotter V. When mutants gain new powers: news from the mutant TP53 field. Nat Rev Cancer (2009) 9:701–713.

Bunz F, Hwang PM, Torrance C, Waldman T, Zhang Y, Dillehay L, Williams J, Lengauer C, Kinzler KW, Vogelstein B. Disruption of TP53 in human cancer cells alters the responses to therapeutic agents. *J Clin Invest* 1999; 104: 263-269.

Bridges HR, Jones AJ, Pollak MN, Hirst J. Effects of metformin and other biguanides on oxidative phosphorylation in mitochondria. Biochem J 2014;462(3):475-87.

Buzzai M, Jones RG, Amaravadi RK, Lum JJ, DeBerardinis RJ, Zhao F, Viollet B, Thompson CB. Systemic treatment with the antidiabetic drug metformin selectively impairs TP53-deficient tumor cell growth. Cancer Res 2007; 67: 6745–6752.

Cabelguenne A, Blons H, de Waziers I, Carnot F, Houllier AM, Soussi T, Brasnu D, Beaune P, Laccourreye O, Laurent-Puig P. TP53 alterations predict tumor response to neoadjuvant chemotherapy in head and neck squamous cell carcinoma: a prospective series. J Clin Oncol (2000) 18:1465–1473.

Carretero J, Medina PP, Blanco R, Smit L, Tang M, Roncador G, Maestre L, Conde E, Lopez-Rios F, Clevers HC, Sanchez-Cespedes M. Dysfunctional AMPK activity, signalling through mTOR and survival in response to energetic stress in LKB1-deficient lung cancer. Oncogene 2007; 26: 1616–25.

Chang FL, Lai MD. Various forms of mutant TP53 confer sensitivity to cisplatin and doxorubicin in bladder cancer cells. J Urol (2001) 166:304–310.

Chapman PB, Hauschild A, Robert C, Haanen JB, Ascierto P, Larkin J, Dummer R, Garbe C, Testori A, Maio M, Hogg D, Lorigan P, Lebbe C, Jouary T, Schadendorf D, Ribas A, O'Day SJ, Sosman JA, Kirkwood JM, Eggermont AM, Dreno B, Nolop K, Li J, Nelson B, Hou J, Lee RJ, Flaherty KT, McArthur GA; BRIM-3 Study Group. Improved survival with vemurafenib in melanoma with BRAF V600E mutation. N Engl J Med 2011;364:2507-16.

Chen X, Wei B, Han X, Zheng Z, Huang J, Liu J, Huang Y, Wei H. LGR5 is required for the maintenance of spheroid-derived colon cancer stem cells. Int J Mol Med. 2014 Jul;34(1):35-42.

Chou TC, Talalay P. Quantitative analysis of dose-effect relationships: the combined effects of multiple drugs or enzyme inhibitors. Adv Enzyme Regul. 1984; 22:27-55.

Ciardiello F and Tortora G.“EGFR antagonists in cancer treatment,” The New England Journal of Medicine, vol. 358, no. 11, pp. 1160–1174, 2008.

Corcoran RB, Atreya CE, Falchook GS, Kwak EL, Ryan DP, Bendell JC, Hamid O, Messersmith WA, Daud A, Kurzrock R, Pierobon M, Sun P, Cunningham E, Little S, Orford K, Motwani M, Bai Y, Patel K, Venook AP, Kopetz S. Combined BRAF and MEK Inhibition With Dabrafenib and Trametinib in BRAF V600-Mutant Colorectal Cancer. J Clin Oncol. 2015 Dec 1;33(34):4023-31.

Corcoran RB, Ebi H, Turke AB, Coffee EM, Nishino M, Cogdill AP, Brown RD, Della Pelle P, Dias-Santagata D, Hung KE, Flaherty KT, Piris A, Wargo JA, Settleman J, Mino-Kenudson M, Engelman JA. EGFR-mediated re-activation of MAPK signaling contributes to insensitivity of BRAF mutant colorectal cancers to RAF inhibition with vemurafenib. Cancer Discov. 2012 Mar;2(3):227-35.

Cremolini C, Bartolomeo MD, Amatu A, Antoniotti C, Moretto R, Berenato R, Perrone F, Tamborini E, Aprile G, Lonardi S, Sartore-Bianchi A, Fontanini G, Milione M, Lauricella C, Siena S, Falcone A, de Braud F, Loupakis F, Pietrantonio F.BRAF codons 594 and 596 mutations identify a new molecular subtype of metastatic colorectal cancer at favorable prognosis. Ann Oncol. 2015; 26: 2092-2097.

Dalerba P, Dylla SJ, Park IK, Liu R, Wang X, Cho RW, Hoey T, Gurney A, Huang EH, Simeone DM, Shelton AA, Parmiani G, Castelli C, Clarke MF. Phenotypic characterization of human colorectal cancer stem cells. Proc Natl Acad Sci U S A. 2007 Jun 12;104(24):10158-63.

Daugan M, Dufaÿ Wojcicki A, d'Hayer B, Boudy V. Metformin: An anti-diabetic drug to fight cancer. Pharmacol Res. 2016 Nov;113(Pt A):675-685.

de Lau W, Barker N, Low TY, Koo BK, Li VS, Teunissen H, Kujala P, Haegebarth A, Peters PJ, van de Wetering M, Stange DE, van Es JE, Guardavaccaro D, Schasfoort RB, Mohri Y, Nishimori K, Mohammed S, Heck AJ, Clevers H. Lgr5 homologues associate with Wnt receptors and mediate R-spondin signalling. Nature. 2011 Jul 4;476(7360):293-7.

de Lau W, Peng WC, Gros P, Clevers H. The R-spondin/Lgr5/Rnf43 module: regulator of Wnt signal strength. Genes Dev. 2014 Feb 15;28(4):305-16.

De Roock W, Claes B, Bernasconi D, De Schutter J, Biesmans B, Fountzilas G, Kalogeras KT, Kotoula V, Papamichael D, Laurent- Puig P, Penault-Llorca F, Rougier P, Vincenzi B, Santini D, Tonini G, Cappuzzo F, Frattini M, Molinari F, Saletti P, De Dosso S, Martini M, Bardelli A, Siena S, Sartore-Bianchi A, Tabernero J, Macarulla T, Di Fiore F, Gangloff AO, Ciardiello F, Pfeiffer P, Qvortrup C, Hansen TP, Van Cutsem E, Piessevaux H, Lambrechts D, Delorenzi M, Tejpar S. Effects of KRAS, BRAF, NRAS, and PIK3CA mutations on the efficacy of cetuximab plus chemotherapy in chemotherapy-refractory metastatic colorectal cancer: a retrospective consortium analysis. Lancet Oncol 2010; 11: 753-762.

Denise C, Paoli P, Calvani M, Taddei ML, Giannoni E, Kopetz S, Kazmi SM, Pia MM, Pettazzoni P, Sacco E, Caselli A, Vanoni M, Landriscina M, Cirri P, Chiarugi P. 5-fluorouracil resistant colon cancer cells are addicted to OXPHOS to survive and enhance stem-like traits. Oncotarget. 2015 Dec 8;6(39):41706-21.

Dong L, Zhou Q, Zhang Z, Zhu Y, Duan T, Feng Y. Metformin sensitizes endometrial cancer cells to chemotherapy by repressing glyoxalase I expression. J. Obstet. Gynaecol. Res. 2012 38, 1077–1085.

Douillard JY, Cunningham D, Roth AD, Navarro M, James RD, Karasek P, Jandik P, Iveson T, Carmichael J, Alakl M, Gruia G, Awad L, Rougier P. Irinotecan combined with fluorouracil compared with fluorouracil alone as first-line treatment for metastatic colorectal cancer: a multicentre randomised trial. Lancet 2000; 355: 1041-1047.

Douillard JY, Siena S, Cassidy J, Tabernero J, Burkes R, Barugel M, Humblet Y, Bodoky G, Cunningham D, Jassem J, Rivera F, Kocákova I, Ruff P, Błasińska-Morawiec M, Šmakal M, Canon JL, Rother M, Oliner KS, Wolf M, Gansert J.Randomized, phase III trial of panitumumab with infusional fluorouracil, leucovorin, and oxaliplatin (FOLFOX4) versus FOLFOX4 alone as first-line treatment in patients with previously untreated metastatic colorectal cancer: the PRIME study. J Clin Oncol. 2010;28(31):4697–4705.

Dylla SJ, Beviglia L, Park IK, Chartier C, Raval J, Ngan L, Pickell K, Aguilar J, Lazetic S, Smith-Berdan S, Clarke MF, Hoey T, Lewicki J, Gurney AL. Colorectal cancer stem cells are enriched in xenogeneic tumors following chemotherapy. PLoS ONE 2008;3:e2428.

El-Mir MY, Nogueira V, Fontaine E, Avéret N, Rigoulet M, Leverve X. Dimethylbiguanide inhibits cell respiration via an indirect effect targeted on the respiratory chain complex I. J Biol Chem. 2000; 275(1):223–228.

Elez E, Schellens J, van Geel R, Bendell J, Spreafico A, Schuler M, Yoshino T, Delord J-P, Yamada Y, Lolkema M, Faris JE, Eskens F,Sharma S, Yaeger R, Lenz H-J, Wainberg Z, Avsar E, Chatterjee A,Jaeger S, Demuth T, Tabernero J.Results of a phase 1b study of the selective BRAF V600 inhibitor encorafenib in combination with cetuximab alone or cetuximab + alpelisib for treatment of patients with advanced BRAF-mutant metastatic colorectal cancer. Ann. Oncol. 26 (Suppl. 4), iv120 (2015).

Emmink BL, Van Houdt WJ, Vries RG, Hoogwater FJ, Govaert KM, Verheem A, Nijkamp MW, Steller EJ, Jimenez CR, Clevers H, Borel Rinkes IH, Kranenburg O. Differentiated human colorectal cancer cells protect tumor-initiating cells from irinotecan. Gastroenterology. 2011 Jul;141(1):269-78.

Esteller M, Avizienyte E, Corn PG, Lothe RA, Baylin SB, Aaltonen LA, Herman JG. Epigenetic inactivation of LKB1 in primary tumors associated with the Peutz-Jeghers syndrome. Oncogene. 2000 Jan 6;19(1):164-8.

Evans JM, Donnelly LA, Emslie-Smith AM, Alessi DR, Morris AD. Metformin reduced risk of cancer in diabetic patients. BMJ. 2005;330(7503):1304–1305.

Fan S, el-Deiry WS, Bae I, Freeman J, Jondle D, Bhatia K, Fornace AJ Jr, Magrath I, Kohn KW, O'Connor PM. TP53 gene mutations are associated with decreased sensitivity of human lymphoma cells to DNA damaging agents. Cancer Res (1994) 54:5824–5830.

Fan S, Smith ML, Rivet DJ 2nd, Duba D, Zhan Q, Kohn KW, Fornace AJ Jr, O'Connor PM. Disruption of TP53 function sensitizes breast cancer MCF-7 cells to cisplatin and pentoxifylline. Cancer Res 1995 55:1649–1654.

Fearon ER. Molecular genetics of colorectal cancer. Annu Rev Pathol. 2011;6:479-507.

Fearon ER, Vogelstein B. A genetic model for colorectal tumorigenesis. Cell 1990; 61: 759-767.

Feng Y, Ke C, Tang Q, Dong H, Zheng X, Lin W, Ke J, Huang J, Yeung SC, Zhang H. Metformin promotes autophagy and apoptosis in esophageal squamous cell carcinoma by downregulating Stat3 signaling. Cell Death Dis. 2014 Feb 27;5:e1088.

Ferrara N, Gerber H and LeCouter J. The biology of VEGF and its receptors. Nat Med 2003 9:669–676.

Ferrara N , Hillan K, Gerber H and Novotny W. Discovery and development of bevacizumab, an anti-VEGF antibody for treating cancer. Nat Rev Drug Discov 2004 3: 391–400.

Fischer Y, Thomas J , Rosen P and Kammermeier H. Action of metformin on glucose transport and glucose transporter GLUT1 and GLUT4 in heart muscle cells from healthy and diabetic rats. Endocrinology 136, 412–420 (1995).

Flaherty KT, Puzanov I, Kim KB, Ribas A, McArthur GA, Sosman JA, O'Dwyer PJ, Lee RJ, Grippo JF, Nolop K, Chapman PB. Inhibition of mutated, activated BRAF in metastatic melanoma. N Engl J Med 2010;363:809-19.

Flis S, Spławiński J. Inhibitory effects of 5-fluorouracil and oxaliplatin on human colorectal cancer cell survival are synergistically enhanced by sulindac sulfide. Anticancer Res. 2009 Jan;29(1):435-41.

Foretz M, Guigas B, Bertrand L, Pollak M, Viollet B. Metformin: from mechanisms of action to therapies. Cell Metab 2014;20(6):953-66.

Fujihara S, Kato K, Morishita A, Iwama H, Nishioka T, Chiyo T, Nishiyama N, Miyoshi H, Kobayashi M, Kobara H, Mori H, Okano K, Suzuki Y, Masaki T. Antidiabetic drug metformin inhibits esophageal adenocarcinoma cell proliferation in vitro and in vivo, Int. J. Oncol. 46 (2015) 2172–2180.

Gao ZY, Liu Z, Bi MH, Zhang JJ, Han ZQ, Han X, Wang HY, Sun GP, Liu H. Metformin induces apoptosis via a mitochondria-mediated pathway in human breast cancer cells in vitro. Exp Ther Med. 2016 May;11(5):1700-1706.

Garrett CR, Hassabo HM, Bhadkamkar NA, Wen S, Baladandayuthapani V, Kee BK, Eng C, Hassan MM. Survival advantage observed with the use of metformin in patients with type II diabetes and colorectal cancer. Br J Cancer 2012;106(8):1374-8.

Gong L, Goswami S, Giacomini KM, Altman RB and Klein TE. Metformin pathways: pharmacokinetics and pharmacodynamics. Pharmacogenet. Genomics (2012) 22, 820–827.

Groenendijk FH1, Mellema WW, van der Burg E, Schut E, Hauptmann M, Horlings HM, Willems SM, van den Heuvel MM, Jonkers J, Smit EF, Bernards R. Sorafenib synergizes with metformin in NSCLC through AMPK pathway activation. Int J Cancer. 2015 Mar 15;136(6):1434-44.

Grothey A, Sargent D, Goldberg RM, Schmoll HJ. Survival of patients with advanced colorectal cancer improves with the availability of fluorouracil-leucovorin, irinotecan, and oxaliplatin in the course of treatment. J Clin Oncol 2004; 22: 1209-1214.

Grothey A, Van Cutsem E, Sobrero A, Siena S, Falcone A, Ychou M, Humblet Y, Bouché O, Mineur L, Barone C, Adenis A, Tabernero J, Yoshino T, Lenz HJ, Goldberg RM, Sargent DJ, Cihon F, Cupit L, Wagner A, Laurent D. Regorafenib monotherapy for previously treated metastatic colorectal cancer (CORRECT): an international, multicentre, randomised, placebo-controlled, phase 3 trial. Lancet 2013; 381: 303-312.

Guichard S, Arnould S, Hennebelle I, Bugat R, Canal P. Combination of oxaliplatin and irinotecan on human colon cancer cell lines: activity in vitro and in vivo. Anticancer Drugs. 2001 Oct;12(9):741-51.

Guichard S, Hennebelle I, Bugat R, Canal P. Cellular interactions of 5-fluorouracil and the camptothecin analogue CPT-11 (irinotecan) in a human colorectal carcinoma cell line. Biochem Pharmacol. 1998 Mar 1;55(5):667-76.

Gunderson LL, Jessup JM, Sargent DJ, Greene FL, Stewart AK. Revised TN categorization for colon cancer based on national survival outcomes data. J Clin Oncol. 2010 Jan;28(2):264-71.

Gwinn DM, Shackelford DB, Egan DF, Mihaylova MM, Mery A, Vasquez DS, Turk BE, Shaw RJ. AMPK phosphorylation of raptor mediates a metabolic checkpoint. Mol Cell 2008; 30: 214–226.

Hanly EK, Bednarczyk RB, Tuli NY, Moscatello AL, Halicka HD, Li J, Geliebter J, Darzynkiewicz Z, Tiwari RK. mTOR inhibitors sensitize thyroid cancer cells to cytotoxic effect of vemurafenib. Oncotarget. 2015 Nov 24;6(37):39702-13.

Hirsch HA, Iliopoulos D, Tsichlis PN, Struhl K. Metformin selectively targets cancer stem cells, and acts together with chemotherapy to block tumor growth and prolong remission. Cancer Res 2009; 69: 7507–7511.

Hirsch HA, Iliopoulos D and & Struhl K. Metformin inhibits the inflammatory response associated with cellular transformation and cancer stem cell growth. Proc. Natl Acad. Sci. USA 110, 972–977 (2013).

Hosono K, Endo H, Takahashi H, Sugiyama M, Uchiyama T, Suzuki K Nozaki Y, Yoneda K, Fujita K, Yoneda M, Inamori M, Tomatsu A, Chihara T, Shimpo K, Nakagama H, Nakajima A. Metformin suppresses azoxymethane-induced colorectal aberrant crypt foci by activating AMP-activated protein kinase. Mol Carcing 2010; 49: 662–671.

Hosono K, Endo H, Takahashi H, Sugiyama M , Sakai E, Uchiyama T, Suzuki K, Iida H, Sakamoto Y, Yoneda K, Koide T, Tokoro C, Abe Y, Inamori M, Nakagama H, Nakajima A. Metformin suppresses colorectal aberrant crypt foci in a short-term clinical trial. Cancer Prev. Res. (Phila.) 2010 3, 1077–1083.

Ikenoue T, Kanai F, Hikiba Y, Obata T, Tanaka Y, Imamura J, Ohta M, Jazag A, Guleng B, Tateishi K, Asaoka Y, Matsumura M, Kawabe T, Omata M. Functional analysis of PIK3CA gene mutations in human colorectal cancer. Cancer Res. 2005 Jun 1;65(11):4562-7.

Iliopoulos D, Hirsch HA, Struhl K. Metformin decreases the dose of chemotherapy for prolonging tumor remission in mouse xenografts involving multiple cancer cell types, Cancer Res. (2011) 71:3196–3201.

Jackson JG, Pant V, Li Q, Chang LL, Quintas-Cardama A, Garza D, Tavana O, Yang P, Manshouri T, Li Y, El-Naggar AK, Lozano G. TP53-mediated senescence impairs the apoptotic response to chemotherapy and clinical outcome in breast cancer. Cancer Cell (2013) 21:793–806.

Janjetovic K, Vucicevic L, Misirkic M, Vilimanovich U, Tovilovic G, Zogovic N, Nikolic Z, Jovanovic S, Bumbasirevic V, Trajkovic V, Harhaji-Trajkovic L. Metformin

reduces cisplatin-mediated apoptotic death of cancer cells through AMPK-independent activation of Akt. Eur. J. Pharmacol. 2011 651, 41–50.

Joe SG, Yoon YH, Choi JA, Koh J-Y. Anti-angiogenic effect of metformin in mouse oxygen-induced retinopathy is mediated by reducing levels of the vascular endothelial growth factor receptor Flk-1, PLoS One 10 (3) (2015) e0119708.

Inoki K, Zhu T, Guan KL. TSC2 mediates cellular energy response to control cell growth and survival. Cell 2003; 115: 577–590.

Kalender A, Selvaraj A, Kim SY, Gulati P, Bruˆ le´ S, Viollet B, Kemp BE, Bardeesy N, Dennis P, Schlager JJ, Marette A, Kozma SC, Thomas G. Metformin, independent of AMPK, inhibits mTORC1 in a rag GTPase-dependent manner. Cell Metab 2010; 11: 390–401.

Kawamoto H, Yuasa T, Kubota Y, Seita M, Sasamoto H, Shahid JM, Hayashi T, Nakahara H, Hassan R, Iwamuro M, Kondo E, Nakaji S, Tanaka N, Kobayashi N. Characteristics of CD133(+) human colon cancer SW620 cells. Cell Transplant. 2010;19(6):857-64. 29.

Kelly C, Cassidy J. Chemotherapy in metastatic colorectal cancer. Surg Oncol. 2007 Jul;16(1):65-70.

Kim TH, Suh DH, Kim MK, Song YS. Metformin against cancer stem cells through the modulation of energy metabolism: special considerations on ovarian cancer, Biomed. Res. Int. 2014 (2014).

Kinzler, KW and Vogelstein B. 2002. Colorectal tumors. In Vogelstein, B., and Kinzler, K. W., eds., The Genetic Basis of Human Cancer (2nd edition)., pp. 583–612. McGraw-Hill, New York., ed.

Knudson AG. 1993. Antioncogenes and human cancer. Pro.Natl.Acad.Sci. USA 90:10914-10921.

Koopman M, Antonini NF, Douma J, Wals J, Honkoop AH, Erdkamp FL, de Jong RS, Rodenburg CJ, Vreugdenhil G, Loosveld OJ, van Bochove A, Sinnige HA, Creemers GJ, Tesselaar ME, Slee PH, Werter MJ, Mol L, Dalesio O, Punt CJ. Sequential versus combination chemotherapy with capecitabine, irinotecan, and oxaliplatin in advanced colorectal cancer (CAIRO): a phase III randomised controlled trial. Lancet 370, 135–142 (2007).

Kopetz, S Desai J, Chan E, Hecht JR, O'Dwyer PJ, Maru D, Morris V, Janku F, Dasari A, Chung W, Issa JP, Gibbs P, James B, Powis G, Nolop KB, Bhattacharya S, Saltz L. Phase II pilot study of vemurafenib in patients with metastatic BRAF-mutated colorectal cancer. J. Clin. Oncol. 33, 4032–4038 (2015).

Le DT, Uram JN, Wang H, Bartlett BR, Kemberling H, Eyring AD, Skora AD, Luber BS, Azad NS, Laheru D, Biedrzycki B, Donehower RC, Zaheer A, Fisher GA, Crocenzi TS, Lee JJ, Duffy SM, Goldberg RM, de la Chapelle A, Koshiji M, Bhaijee F, Huebner T, Hruban RH, Wood LD, Cuka N, Pardoll DM, Papadopoulos N, Kinzler KW, Zhou S, Cornish TC, Taube JM, Anders RA, Eshleman JR, Vogelstein B, Diaz LA Jr. PD-1 Blockade in Tumors with Mismatch-Repair Deficiency. N Engl J Med. 2015 Jun 25;372(26):2509-20.

Lee JH, Kim TI, Jeon SM, Hong SP, Cheon JH, Kim WH. The effects of metformin on the survival of colorectal cancer patients with diabetes mellitus. Int J Cancer 2012;131(3):752-9.

Lettieri Barbato D, Vegliante R, Desideri E, Ciriolo MR. Managing lipid metabolism in proliferating cells: new perspective for metformin usage in cancer therapy, Biochim. Biophys. Acta (BBA): Rev. Cancer 1845 (April (2))(2014) 317–324.

Li R, Sutphin PD, Schwartz D, Matas D, Almog N, Wolkowicz R, Goldfinger N, Pei H, Prokocimer M, Rotter V. Mutant TP53 protein expression interferes with TP53-independent apoptotic pathways. Oncogene (1998) 16:3269–3277.

Li W, Wang Q-L, Liu X, Dong S-H, Li H-X, Li C-Y, Guo L-S, Gao J-M, Berger NA, Li L, Ma L, Wu Y-J. Combined use of Vitamin D3 and metformin exhibits synergistic chemopreventive effects on colorectal neoplasia in rats and mice. Cancer Prev Res 2015, 8(2):139–148.

Libby G, Donnelly LA, Donnan PT, Alessi DR, Morris AD, Evans JMM. New users of metformin are at low risk of incident cancer: a cohort study among people with type 2 diabetes. Diabetes Care 2009;32:1620–5.

Lichtenstein P, Holm NV, Verkasalo PK, Iliadou A, Kaprio J, Koskenvuo M, Pukkala E, Skytthe A, Hemminki K. Environmental and heritable factors in the causation of cancer - Analyses of cohorts of twins from Sweden, Denmark, and Finland. New England Journal of Medicine, 2000. 343(2): p. 78-85.

Lievre A, Bachet JB, Le Corre D, Boige V, Landi B, Emile JF, Côté JF, Tomasic

G, Penna C, Ducreux M, Rougier P, Penault-Llorca F, Laurent-Puig P. KRAS mutation status is predictive of response to cetuximab therapy in colorectal cancer. Cancer Res. 2006;66(8):3992–3995.

Lin YC, Wu MH, Wei TT, Lin YC, Huang WC, Huang LY, Lin YT, Chen CC. Metformin sensitizes anticancer effect of dasatinib in head and neck squamous cell carcinoma cells through AMPK-dependent ER stress. Oncotarget. 2014 Jan 15;5(1):298-308.

Lonardo E, Cioffi M, Sancho P, Sanchez-Ripoll Y, Trabulo SM, Dorado J , Balic A, Hidalgo M, and Heeschen C. Metformin targets the metabolic achilles heel of human pancreatic cancer stem cells. PLoS ONE. 2013; 8: e76518.

Lowe SW, Ruley HE, Jacks T, Housman DE. TP53-dependent apoptosis modulates the cytotoxicity of anticancer agents. Cell 1993; 74: 957-967.

Malki A, Youssef A. Antidiabetic drug metformin induces apoptosis in human MCF breast cancer via targeting ERK signaling. Oncol Res. 2011;19(6):275-85.

Mans DR, Grivicich I, Peters GJ, Schwartsmann G. Sequence-dependent growth inhibition and DNA damage formation by the irinotecan-5-fluorouracil combination in human colon carcinoma cell lines. Eur J Cancer. 1999 Dec;35(13):1851-61.

Mao M, Tian F, Mariadason JM, Tsao CC, Lemos R Jr, Dayyani F, Gopal YN, Jiang ZQ, Wistuba II, Tang XM, Bornman WG, Bollag G, Mills GB, Powis G, Desai J, Gallick GE, Davies MA, Kopetz S. Resistance to BRAF inhibition in BRAF-mutant colon cancer can be overcome with PI3K inhibition or demethylating agents. Clin Cancer Res. 2013 Feb 1;19(3):657-67.

Mariadason JM, Arango D, Shi Q, Wilson AJ, Corner GA, Nicholas C, Aranes MJ, Lesser M, Schwartz EL, Augenlicht LH. Gene expression profiling-based prediction of response of colon carcinoma cells to 5-fluorouracil and camptothecin. Cancer Res. 2003 Dec 15;63(24):8791-812.

Markowitz S, Wang J, Myeroff L, Parsons R, Sun L, Lutterbaugh J, Fan RS, Zborowska E, Kinzler KW, Vogelstein B, et al. Inactivation of the type II TGF-beta receptor in colon cancer cells with microsatellite instability. Science. 1995 Jun 2;268(5215):1336-8.

Markowitz SD, Bertagnolli MM. Molecular origins of cancer: Molecular basis of colorectal cancer. N Engl J Med. 2009 Dec 17;361(25):2449-60.

Mackenzie RM, Salt IP, Miller WH, Logan A, Ibrahim HA, Degasperi A Dymott JA, Hamilton CA, Murphy MP, Delles C, Dominiczak AF. Mitochondrial reactive oxygen species enhance AMP-activated protein kinase activation in the endothelium of patients with coronary artery disease and diabetes. Clin Sci (Lond) 2013;124(6):403-11.

Marchi S, Giorgi C, Suski JM, Agnoletto C, Bononi A, Bonora M, De Marchi E, Missiroli S, Patergnani S, Poletti F, Rimessi A, Duszynski J, Wieckowski MR, Pinton P. Mitochondria-ros crosstalk in the control of cell death and aging. J Signal Transduct 2012;2012:329635.

Medico E, Russo M, Picco G, Cancelliere C, Valtorta E, Corti G, Buscarino M, Isella C, Lamba S, Martinoglio B, Veronese S, Siena S, Sartore-Bianchi A, Beccuti M, Mottolese M, Linnebacher M, Cordero F, Di Nicolantonio F, Bardelli A. The molecular landscape of colorectal cancer cell lines unveils clinically actionable kinase targets. Nat

Commun. 2015 Apr 30;6:7002.

Menendez JA, Oliveras-Ferraros C, Cufi S, Corominas-Faja B, Joven J, Martin-Castillo B, Vazquez-Martin A. Metformin is synthetically lethal with glucose withdrawal in cancer cells. Cell Cycle 2012;11(15):2782-92.

Meyerhardt JA and Mayer RJ. Systemic therapy for colorectal cancer. N. Engl. J. Med. 352, 476–487 (2005).

Minassian C, Tarpin S, Mithieux G. Role of glucose-6 phosphatase,glucokinase, and glucose-6 phosphate in liver insulin resistance and its correction by metformin, Biochem. Pharmacol. 55 (April (8)) (1998)1213–1219.

Misale S, Arena S, Lamba S, Siravegna G, Lallo A, Hobor S, Russo M, Buscarino M, Lazzari L, Sartore-Bianchi A, Bencardino K, Amatu A, Lauricella C, Valtorta E,Siena S, Di Nicolantonio F, Bardelli A. Blockade of EGFR and MEK intercepts heterogeneous mechanisms of acquired resistance to anti-EGFR therapies in colorectal cancer. Sci Transl Med. 2014 Feb 19;6(224):224ra26.

Miyo M, Konno M, Nishida N, Sueda T, Noguchi K, Matsui H, Colvin H, Kawamoto K, Koseki J, Haraguchi N, Nishimura J, Hata T, Gotoh N, Matsuda F, Satoh T, Mizushima T, Shimizu H, Doki Y, Mori M, Ishii H. Metabolic Adaptation to Nutritional Stress in Human Colorectal Cancer. Scientific Reports 6, Article number: 38415 (2016).

Moiseeva O, Deschênes-Simard X, St-Germain E, Igelmann S, Huot G, Cadar AE, Bourdeau V, Pollak MN, Ferbeyre G. Metformin inhibits the senescence-associated secretory phenotype by interfering with IKK/NF-κB activation. Aging Cell. 2013 Jun;12(3):489-98.

Montgomery E, Goggins M, Zhou S, Argani P, Wilentz R, Kaushal M, Booker S, Romans K, Bhargava P, Hruban R, Kern S. Nuclear localization of Dpc4 (Madh4, Smad4) in colorectal carcinomas and relation to mismatch repair/transforming growth factor-beta receptor defects. Am J Pathol. 2001 Feb;158(2):537-42.

Nangia-Makker P, Yu Y, Vasudevan A, Farhana L, Rajendra SG, Levi E, Majumdar AP. Metformin: a potential therapeutic agent for recurrent colon cancer. PLoS One. 2014 Jan 20;9(1):e84369.

Nannizzi S, Veal GJ, Giovannetti E, Mey V, Ricciardi S, Ottley CJ, Del Tacca M, Danesi R. Cellular and molecular mechanisms for the synergistic cytotoxicity elicited by oxaliplatin and pemetrexed in colon cancer cell lines. Cancer Chemother Pharmacol. 2010 Aug;66(3):547-58.

NCCN Clinical Practice Guidelines in Oncology (NCCNGuidelines5) Colon Cancer, Version 22016, 2015.

Niehr F, von Euw E, Attar N, Guo D, Matsunaga D, Sazegar H, Ng C, Glaspy JA, Recio JA, Lo RS, Mischel PS, Comin-Anduix B, Ribas A. Combination therapy with vemurafenib (PLX4032/RG7204) and metformin in melanoma cell lines with distinct driver mutations. J Transl Med. 2011 May 24;9:76.

Noto H, Goto A, Tsujimoto T, Noda M. Cancer risk in diabetic patients treated with metformin: a systematic review and meta-analysis. PLoS One. 2012; 7(3):e33411.

O'Brien CA, Pollett A, Gallinger S, Dick JE.A human colon cancer cell capable of initiating tumour growth in immunodeficient mice. Nature. 2007 Jan 4;445(7123):106-10.

O'Connor PM, Jackman J, Bae I, Myers TG, Fan S, Mutoh M, Scudiero DA, Monks A, Sausville EA, Weinstein JN, Friend S, Fornace AJ Jr, Kohn KW. Characterization of the TP53 tumor suppressor pathway in cell lines of the National Cancer Institute anticancer drug screen and correlations with the growth-inhibitory potency of 123 anticancer agents. Cancer Res (1997) 57:4285–4300.

Pernicova I, Korbonits M. Metformin--mode of action and clinical implications for diabetes and cancer. Nat Rev Endocrinol 2014;10(3):143-56.

Pierotti MA, Berrino F, Gariboldi M , Melani C , Mogavero A , Negri T , Pasanisi P , Pilotti S. Targeting metabolism for cancer treatment and prevention: metformin, an old drug with multi-faceted effects. Oncogene 32, 1475–1487 (2013).

Pollak M. The insulin and insulin-like growth factor receptor family in neoplasia: an update. Nat Rev Cancer. 2012;12(3):159–169.

Prahallad A, Sun C, Huang S, Di Nicolantonio F, Salazar R, Zecchin D, Beijersbergen RL, Bardelli A, Bernards R. Unresponsiveness of colon cancer to BRAF(V600E) inhibition through feedback activation of EGFR. Nature. 2012 Jan 26; 483(7387):100-3.

Queiroz EA, Puukila S, Eichler R, Sampaio SC, Forsyth HL, Lees SJ, Barbosa AM, Dekker RF, Fortes ZB, Khaper N. Metformin induces apoptosis and cell cycle arrest mediated by oxidative stress, AMPK and FOXO3a in MCF-7 breast cancer cells. PLoS

One. 2014 May 23;9(5):e98207.

Ricci-Vitiani L, Lombardi DG, Pilozzi E, Biffoni M, Todaro M, Peschle C, De Maria R. Identification and expansion of human colon-cancer-initiating cells. Nature. 2007 Jan 4;445(7123):111-5.

Rodrigues D, Longatto-Filho A, Martins SF. Predictive Biomarkers in Colorectal Cancer: From the Single Therapeutic Target to a Plethora of Options. Biomed Res Int. 2016;2016:6896024.

Saber MM, Galal MA, Ain-Shoka AA, Shouman SA. Combination of metformin and 5-aminosalicylic acid cooperates to decrease proliferation and induce apoptosis in colorectal cancer cell lines. BMC Cancer. 2016 Feb 19;16:126.

Sahlberg SH, Spiegelberg D, Glimelius B, Stenerlow B, Nestor M. Evaluation of cancer stem cell markers CD133, CD44, CD24: association with AKT isoforms and radiation resistance in colon cancer cells. PLoS One 2014;9(4):e94621.

Salani B, Rio AD, Marini C, Sambuceti G, Cordera R, Maggi D. Metformin, cancer and glucose metabolism, Endocr. Relat. Cancer 21 (2014) R461–R471.

Saltz L, Clarke S, Diaz-Rubio E, Scheithauer W, Figer A, Wong R Koski S, Lichinitser M, Yang TS, Rivera F, Couture F, Sirzén F, Cassidy J. Bevacizumab in combination with oxaliplatin-based chemotherapy as first-line therapy in metastatic colorectal cancer: a randomized phase III study. J Clin Oncol. 2008 Apr 20;26(12):2013-9.

Sato T, Vries RG, Snippert HJ, van de Wetering M, Barker N, Stange DE, van Es JH, Abo A, Kujala P, Peters PJ, Clevers H. Single Lgr5 stem cells build crypt-villus structures in vitro without a mesenchymal niche. Nature. 2009 May 14;459(7244):262-5.

Scott KD, Nath-Sain S, Agnew MD, Marignani PA. LKB1 catalytically deficient mutants enhance cyclin D1 expression. Cancer Res. 2007 Jun 15;67(12):5622-7.

Senda T, Iizuka-Kogo A, Onouchi T, Shimomura A.Adenomatous polyposis coli (APC) plays multiple roles in the intestinal and colorectal epithelia. Med Mol Morphol, 2007. 40(2): p. 68-81.

Seow HF, Yip WK, Fifis T. Advances in targeted and immunobased therapies for colorectal cancer in the genomic era. Onco Targets Ther. 2016 Mar 31;9:1899-920.

Seymour MT Maughan TS, Ledermann JA, Topham C, James R, Gwyther SJ, Smith DB, Shepherd S, Maraveyas A, Ferry DR, Meade AM, Thompson L, Griffiths GO, Parmar MK, Stephens RJ; FOCUS Trial Investigators; National Cancer Research Institute Colorectal Clinical Studies Group. Different strategies of sequential and combination chemotherapy for patients with poor prognosis advanced colorectal cancer (MRC FOCUS): a randomised controlled trial. Lancet 370, 143–152 (2007).

Silvestri A, Palumbo F, Rasi I, Posca D, Pavlidou T, Paoluzi S, Castagnoli L, Cesareni G. Metformin Induces Apoptosis and Downregulates Pyruvate Kinase M2 in Breast Cancer Cells Only When Grown in Nutrient-Poor Conditions. PLoS One 2015; 10:e0136250.

Shank JJ, Yang K, Ghannam J, Cabrera L, Johnston CJ, Reynolds RK, Buckanovich RJ. Metformin targets ovarian cancer stem cells in vitro and in vivo, Gynecol. Oncol. 127 (November (2)) (2012) 390–397.

Snippert HJ, van der Flier LG, Sato T, van Es JH, van den Born M, Kroon-Veenboer C, Barker N, Klein AM, van Rheenen J, Simons BD, Clevers H. Intestinal crypt homeostasis results from neutral competition between symmetrically dividing Lgr5 stem cells. Cell. 2010; 143:134-44.

Song CW, Lee H, Dings RPM, Williams B, Powers J, Santos TD, Choi B-H, Park HJ. Metformin kills and radiosensitizes cancer cells and preferentially kills cancer stem cells, Sci. Rep. 2 (2012) 362.

Sosman JA, Kim KB, Schuchter L, Gonzalez R, Pavlick AC, Weber JS, McArthur GA, Hutson TE, Moschos SJ, Flaherty KT, Hersey P, Kefford R, Lawrence D, Puzanov I, Lewis KD, Amaravadi RK, Chmielowski B, Lawrence HJ, Shyr Y, Ye F, Li J, Nolop KB, Lee RJ, Joe AK, Ribas A. Survival in BRAF V600-mutant advanced melanoma treated with vemurafenib. N Engl J Med 2012; 366:707-14.

Spillane S, Bennett K, Sharp L, Barron TI. A cohort study of metformin exposure and survival in patients with stage I-III colorectal cancer. Cancer Epidemiol Biomarkers Prev 2013;22(8):1364-73.

Sui X, Xu Y, Yang J, Fang Y, Lou H, Han W, Zhang M, Chen W, Wang K, Li D, Jin W, Lou F, Zheng Y, Hu H, Gong L, Zhou X, Pan Q, Pan H, Wang X, He C. Use of metformin alone is not associated with survival outcomes of colorectal cancer cell but

AMPK activator AICAR sensitizes anticancer effect of 5-fluorouracil through AMPK activation. PLoS One. 2014 May 21;9(5):e97781.

Tadakawa M, Takeda T, Li B, Tsuiji K, Yaegashi N. The anti-diabetic drug metformin inhibits vascular endothelial growth factor expression via the mammalian target of rapamycin complex 1/hypoxia-inducible factor-1 α signaling pathway in ELT-3 cells, Mol. Cell. Endocrinol. 2015, 399: 1–8.

Takemura Y, Osuga Y, Yoshino O, Hasegawa A, Hirata T, Hirota Y, Nose E, Morimoto C, Harada M, Koga K, Tajima T, Yano T, Taketani Y. Metformin suppresses interleukin (IL)-1beta-induced IL-8 production, aromatase activation, and proliferation of endometriotic stromal cells, J. Clin.Endocrinol. Metab. 92 (August (8)) (2007) 3213–3218.

Taketo MM, Takaku K. Gastro-intestinal tumorigenesis in Smad4 mutant mice. Cytokine Growth Factor Rev. 2000 Mar-Jun;11(1-2):147-57.

Tol J, Nagtegaal ID, Punt CJ. BRAF mutation in metastatic colorectal cancer. N Engl J Med. 2009;361(1):98–99.

Tomic T, Botton T, Cerezo M, Robert G, Luciano F, Puissant A, Gounon P, Allegra M, Bertolotto C, Bereder JM, Tartare-Deckert S, Bahadoran P, Auberger P, Ballotti R, Rocchi S. Metformin inhibits melanoma development through autophagy and apoptosis mechanisms. Cell Death Dis. 2011 Sep 1;2:e199.

Tomimoto A, Endo H, Sugiyama M, Fujisawa T, Hosono K, Takahashi H, Nakajima N, Nagashima Y, Wada K, Nakagama H, Nakajima A. Metformin suppresses intestinal polyp growth in ApcMin/. mice. Cancer Sci 2008; 99: 2136–2141.

Torre LA, Siegel RL, Ward EM, Jemal A. Global Cancer Incidence and Mortality Rates and Trends--An Update. Cancer Epidemiol Biomarkers Prev. 2016 Jan; 25(1):16-27.

Toscano F, Parmentier B, Fajoui ZE, Estornes Y, Chayvialle JA, Saurin JC, Abello J. TP53 dependent and independent sensitivity to oxaliplatin of colon cancer cells. Biochem Pharmacol. 2007;74(3):392-406.

Van Cutsem, E Lenz HJ, Köhne CH, Heinemann V, Tejpar S, Melezínek I, Beier F, Stroh C, Rougier P, van Krieken JH, Ciardiello F. Fluorouracil, leucovorin, and irinotecan plus cetuximab treatment and RAS mutations in colorectal cancer. J. Clin. Oncol. 33, 692–700 (2015).

Van Cutsem E, Atreya CE, Bendell JC, Andre T, Schellens JHM, Gordon MS, McRee AJ, O'Dwyer PJ, Muro K, Tabernero J, van Geel R, Sidhu R, Greger JG, Rangwala FA, Motwani M, Wu Y, Orford KW, Corcoran RB. Updated results of the MEK inhibitor trametinib (T), BRAF inhibitor dabrafenib (D), and anti-EGFR antibody panitumumab (P) in patients (pts) with BRAF V600E mutated (BRAFm) metastatic colorectal cancer (mCRC). Ann. Oncol. 26 (Suppl. 4), iv119 (2015).

van de Wetering M, Sancho E, Verweij C, de Lau W, Oving I, Hurlstone A, van der Horn K, Batlle E, Coudreuse D, Haramis AP, Tjon-Pon-Fong M, Moerer P, van den Born M, Soete G, Pals S, Eilers M, Medema R, Clevers H. The beta-catenin/TCF-4 complex imposes a crypt progenitor phenotype on colorectal cancer cells. Cell. 2002 Oct 18;111(2):241-50.

Van der Flier LG, Sabates-Bellver J, Oving I, Haegebarth A, De Palo M, Anti M, Van Gijn ME, Suijkerbuijk S, Van de Wetering M, Marra G, Clevers H. The Intestinal Wnt/TCF Signature. Gastroenterology. 2007 Feb;132(2):628-32.

Vazquez-Martin A, Oliveras-Ferraros C, Cufí S, Del Barco S, Martin-Castillo B, Menendez JA. Metformin regulates breast cancer stem cell ontogeny by transcriptional regulation of the epithelial-mesenchymal transition (EMT) status. Cell Cycle (2010) 9(18):3831–3838.

Vazquez-Martin A, Oliveras-Ferraros C, Cufı´ S, Martin-Castillo B, Menendez JA. Metformin activates an Ataxia Telangiectasia Mutated (ATM)/Chk2-regulated DNA damage-like response. Cell Cycle 2011; 10: 1499–1501.

Venook A, Niedzwiecki D, Hollis D, Sutherland S, Goldberg R, Alberts S, Benson A, Wade J, Schilsky R, Mayer R. Phase III study of irinotecan/5FU/LV (FOLFIRI) or oxaliplatin/5FU/LV (FOLFOX){+/-} cetuximab for patients (pts) with untreated metastatic adenocarcinoma of the colon or rectum (MCRC):CALGB 80203 preliminary results. J Clin Oncol. 2006;24(18 Suppl):3509.

Vizioli MG, Santos J, Pilotti S, Mazzoni M, Anania MC, Miranda C, Pagliardini S, Pierotti MA, Gil J, Greco A. Oncogenic RAS-induced senescence in human primary thyrocytes: molecular effectors and inflammatory secretome involved. Oncotarget. 2014 Sep 30;5(18):8270-83.

Vujic I, Sanlorenzo M, Posch C, Esteve-Puig R, Yen AJ, Kwong A, Tsumura A, Murphy R, Rappersberger K, Ortiz-Urda S. Metformin and trametinib have synergistic

effects on cell viability and tumor growth in NRAS mutant cancer. Oncotarget. 2015 Jan 20;6(2):969-78.

Wahdan-Alaswad R, Fan Z, Edgerton SM, Liu B, Deng XS, Arnadottir SS, Richer JK, Anderson SM, Thor AD. Glucose promotes breast cancer aggression and reduces metformin efficacy. Cell Cycle 2013;12(24):3759-69.

Weinberg RA. The biology of cancer. 2007, New York, NY: Garland Science. 1 v. (various pages).

Wielenga VJ, Smits R, Korinek V, Smit L, Kielman M, Fodde R, Clevers H, Pals ST. Expression of CD44 in Apc and Tcf mutant mice implies regulation by the WNT pathway. Am J Pathol. 1999 Feb;154(2):515-23.

Wilhelm SM, Dumas J, Adnane L, Lynch M, Carter CA, Schütz G, Thierauch KH, Zopf D. Regorafenib (BAY 73-4506): a new oral multikinase inhibitor of angiogenic, stromal and oncogenic receptor tyrosine kinases with potent preclinical antitumor activity. Int J Cancer 2011; 129: 245-255.

Williams CC, Singleton BA, Llopis SD, Skripnikova EV. Metformin induces a senescence-associated gene signature in breast cancer cells. J Health Care Poor Underserved. 2013 Feb;24(1 Suppl):93-103.

Winawer SJ, Zauber AG, Ho MN, O'Brien MJ, Gottlieb LS, Sternberg SS, Waye JD, Schapiro M, Bond JH, Panish JF, Ackroyd F, Shike M, Kurtz RC, Hornsby-Lewis L, Gerdes H, Stewart ET, the National Polyp Study Workgroup. Prevention of colorectal cancer by colonoscopic polypectomy. The National Polyp Study Workgroup. N Engl J

Med. 1993 Dec;329(27):1977-81.

Winton D.J., Blount M.A., Ponder B.A. A clonal marker induced by mutation in mouse intestinal epithelium. Nature, 333 (1988), pp. 463–466

Woods A, Johnstone SR, Dickerson K, Leiper FC, Fryer LG, Neumann D, Schlattner U, Wallimann T, Carlson M, Carling D. LKB1 is the upstream kinase in the AMP-activated protein kinase cascade. Curr Biol. 2003;13(22):2004-8.

Yaeger, R. Cercek A, O'Reilly EM, Reidy DL, Kemeny N, Wolinsky T, Capanu M, Gollub MJ, Rosen N, Berger MF, Lacouture ME, Vakiani E, Saltz LB. Pilot trial of combined BRAF and EGFR inhibition in BRAF-mutant metastatic colorectal cancer patients. Clin. Cancer Res. 21, 1313–1320 (2015).

Yang H, Higgins B, Kolinsky K, Packman K, Bradley WD, Lee RJ, Schostack K, Simcox ME, Kopetz S, Heimbrook D, Lestini B, Bollag G, Su F. Antitumor activity of BRAF inhibitor vemurafenib in preclinical models of BRAF-mutant colorectal cancer. Cancer Res. 2012 Feb 1;72(3):779-89.

Yi G, He Z, Zhou X, Xian L, Yuan T, Jia X, Hong J, He L, Liu J. Low concentration of metformin induces a TP53-dependent senescence in hepatoma cells via activation of the AMPK pathway. Int J Oncol. 2013 Nov;43(5):1503-10.

Yuan P, Ito K, Perez-Lorenzo R, Del Guzzo C, Lee JH, Shen CH, Bosenberg MW, McMahon M, Cantley LC, Zheng B. Phenformin enhances the therapeutic benefit of BRAF(V600E) inhibition in melanoma. Proc Natl Acad Sci U S A. 2013 Nov 5;110(45):18226-31.

Zakikhani M, Dowling RJ, Sonenberg N, Pollak MN. The effects of adiponectin and metformin on prostate and colon neoplasia involve activation of AMP activated protein kinase. Cancer Prev Res (Phila) 2008; 1: 369–375.

Zhang HH, Guo XL. Combinational strategies of metformin and chemotherapy in cancers. Cancer Chemother Pharmacol. 2016 Jul;78(1):13-26.

Zhang P, Li H, Tan X, Chen L, Wang S. Association of metformin use with cancer incidence and mortality: A meta-analysis. Cancer Epidemiol. 2013; 37(3):207–218.

Zhang S, Lovejoy KS, Shima JE, Lagpacan LL, Shu Y, Lapuk A, Chen Y, Komori T, Gray JW, Chen X, Lippard SJ, Giacomini KM. Organic cation transporters are determinants of oxaliplatin cytotoxicity. Cancer Res. 2006 Sep 1;66(17):8847-57.

Zhang ZJ, Zheng Z, Kan H, Song Y, Cui W, Zhao G, Kip KE. Reduced Risk of Colorectal Cancer With Metformin Therapy in Patients With T2DM. A meta-analysis. Diabetes Care 2011;34:2323-8.

Zhou G, Myers R, Li Y, Chen Y, Shen X, Fenyk-Melody J, Wu M, Ventre J, Doebber T, Fujii N, Musi N, Hirshman MF, Goodyear LJ, Moller DE. Role of AMP-activated protein kinase in mechanism of metformin action. J. Clin. Invest. 108, 1167–1174 (2001).

Zhuang Y, Miskimins WK. Cell cycle arrest in Metformin treated breast cancer cells involves activation of AMPK, downregulation of cyclin D1, and requires p27Kip1 or p21Cip1. J Mol Signal 2008; 3: 1

SUPPLEMENTARY TABLES

Supplementary table 1. CI of oxaliplatin (OXA) and 5-FU in HT29

OXA (µM)	5FU (µM)	Effect	CI
0.05625	0.625	0.09564	1.96317
0.1125	0.625	0.16982	1.03385
0.225	0.625	0.22237	0.99194
0.45	0.625	0.39984	0.88434
0.9	0.625	0.54912	1.20393
1.8	0.625	0.66040	1.90164
0.05625	1.25	0.23311	0.99213
0.1125	1.25	0.28289	0.83941
0.225	1.25	0.32710	0.88088
0.45	1.25	0.46769	0.86205
0.9	1.25	0.56914	1.21982
1.8	1.25	0.66752	1.91018
0.05625	2.5	0.39873	0.70364
0.1125	**2.5**	**0.40192**	**0.78356**
0.225	2.5	0.41970	0.89883
0.45	2.5	0.51196	0.93700
0.9	2.5	0.62016	1.18816
1.8	2.5	0.79140	1.46732
0.05625	5	0.46309	0.94442
0.1125	5	0.45345	1.07502
0.225	5	0.51032	0.97346
0.45	5	0.55096	1.10541
0.9	5	0.60396	1.43681
1.8	5	0.66711	0.89847
0.05625	10	0.54966	1.15697
0.1125	10	0.57032	1.10821
0.225	10	0.59374	1.11731
0.45	10	0.59651	1.36476
0.9	10	0.64948	1.57457
1.8	10	0.68355	2.29212
0.05625	20	0.64491	1.33933
0.1125	20	0.63015	1.5162
0.225	20	0.64917	1.48603
0.45	20	0.66258	1.61732
0.9	20	0.66765	2.03844
1.8	20	0.70982	2.5537

Supplementary table 2. CI of oxaliplatin (OXA) and 5-FU in HCT116

OXA (µM)	5FU (µM)	Effect	CI
0.04813	0.425	0.13023	1.71477
0.09625	0.425	0.12901	1.95370
0.1925	0.425	0.19850	1.38384
0.385	0.425	0.36670	0.94079
0.77	0.425	0.45496	0.85006
1.54	0.425	0.74689	0.94602
0.04813	0.85	0.28469	0.93977
0.09625	0.85	0.35163	0.73143
0.1925	0.85	0.35959	0.87814
0.385	**0.85**	**0.42651**	**0.80087**
0.77	0.85	0.47975	1.14181
1.54	0.85	0.73619	1.01544
0.04813	1.7	0.50129	1.19280
0.09625	1.7	0.42165	0.89477
0.1925	1.7	0.46137	0.86871
0.385	1.7	0.40472	1.43658
0.77	1.7	0.53039	1.29635
1.54	1.7	0.75114	1.01771
0.04813	3.4	0.44143	1.41429
0.09625	3.4	0.40778	1.76489
0.1925	3.4	0.44354	1.60674
0.385	3.4	0.52458	1.31171
0.77	3.4	0.59761	1.31450
1.54	3.4	0.74859	1.14545
0.04813	6.8	0.59737	1.21952
0.09625	6.8	0.58927	1.32015
0.1925	6.8	0.57553	1.51528
0.385	6.8	0.60801	1.46091
0.77	6.8	0.68104	1.29712
1.54	6.8	0.80451	1.03865
0.04813	13.6	0.71813	1.18423
0.09625	13.6	0.70558	1.31512
0.1925	13.6	0.70254	1.40653
0.385	13.6	0.72687	1.33398
0.77	13.6	0.77568	1.18271
1.54	13.6	0.80725	1.32269

Supplementary table 3. CI of oxaliplatin (OXA) and 5-FU in HCT116*P53-/-*

OXA (μM)	5FU (μM)	Effect	CI
0.2	0.45	0.12132	0.94304
0.4	0.45	0.14612	1.16563
0.8	0.45	0.26093	1.0702
1.6	0.45	0.48535	0.90065
3.2	0.45	0.75327	0.69611
6.4	0.45	0.78022	1.22498
0.2	0.9	0.15712	1.05066
0.4	0.9	0.27193	0.74527
0.8	0.9	0.34036	0.89162
1.6	**0.9**	**0.57905**	**0.70383**
3.2	0.9	0.70937	0.84828
6.4	0.9	0.80048	1.12485
0.2	1.8	0.15742	1.72681
0.4	1.8	0.21458	1.43821
0.8	1.8	0.32843	1.16485
1.6	1.8	0.50682	0.99238
3.2	1.8	0.65657	1.07909
6.4	1.8	0.80001	1.14943
0.2	3.6	0.28606	1.36099
0.4	3.6	0.38728	0.98223
0.8	3.6	0.40973	1.16085
1.6	3.6	0.54791	1.03123
3.2	3.6	0.66030	1.16355
6.4	3.6	0.74436	1.53901
0.2	7.2	0.50150	0.92604
0.4	7.2	0.52230	0.94060
0.8	7.2	0.54544	1.02854
1.6	7.2	0.64052	0.95218
3.2	7.2	0.67003	1.31016
6.4	7.2	0.75270	1.60488
0.2	14.4	0.63110	0.97826
0.4	14.4	0.66501	0.89064
0.8	14.4	0.64558	1.10379
1.6	14.4	0.71850	0.97392
3.2	14.4	0.73184	1.2836
6.4	14.4	0.77277	1.67595

Supplementary table 4. CI of irinotecan (IRI) and 5-FU in HT29

IRI (µM)	5FU (µM)	Effect	CI
0.0125	0.625	0.20188	1.19559
0.025	0.625	0.28624	0.87777
0.05	0.625	0.38511	0.76966
0.1	**0.625**	**0.52384**	**0.67709**
0.2	0.625	0.57480	0.98324
0.4	0.625	0.69722	1.0373
0.0125	1.25	0.32059	0.89699
0.025	1.25	0.33358	0.99866
0.05	1.25	0.43342	0.79309
0.1	1.25	0.47239	1.00814
0.2	1.25	0.44486	1.94979
0.4	1.25	0.56899	2.0199
0.0125	2.5	0.36885	1.21428
0.025	2.5	0.43050	0.96919
0.05	2.5	0.45364	1.05001
0.1	2.5	0.43364	1.58445
0.2	2.5	0.41019	2.71896
0.4	2.5	0.61622	1.75518
0.0125	5.0	0.53050	0.94344
0.025	5.0	0.53238	1.00175
0.05	5.0	0.54587	1.05994
0.1	5.0	0.49741	1.68143
0.2	5.0	0.48411	2.4706
0.4	5.0	0.57960	2.42407
0.0125	10.0	0.45335	2.76143
0.025	10.0	0.42683	3.30226
0.05	10.0	0.40344	4.00003
0.1	10.0	0.36839	5.43853
0.2	10.0	0.38619	5.97202
0.4	10.0	0.34178	10.2121
0.0125	20.0	0.64975	1.82307
0.025	20.0	0.64208	1.9488
0.05	20.0	0.62245	2.27395
0.1	20.0	0.62426	2.4292
0.2	20.0	0.63367	2.64479
0.4	20.0	0.63833	3.24495

Supplementary table 5. CI of irinotecan (IRI) and 5-FU in HCT116

IRI (μM)	5FU (μM)	Effect	CI
0.0015	0.425	0.18575	1.40433
0.0030	0.425	0.21204	1.36419
0.0060	0.425	0.28993	1.05359
0.012	0.425	0.43334	0.71247
0.024	0.425	0.55286	0.66790
0.048	**0.425**	**0.73619**	**0.45101**
0.0015	0.85	0.28469	1.03905
0.0030	0.85	0.35163	0.75232
0.0060	0.85	0.35959	0.92276
0.012	0.85	0.45496	0.76590
0.024	0.85	0.50129	0.98058
0.048	0.85	0.75114	0.44058
0.0015	1.7	0.42651	0.71657
0.0030	1.7	0.42165	0.81362
0.0060	1.7	0.46137	0.75473
0.012	1.7	0.40472	1.39465
0.024	1.7	0.53039	1.00151
0.048	1.7	0.74859	0.51883
0.0015	3.4	0.44143	1.23593
0.0030	3.4	0.40778	1.61735
0.0060	3.4	0.44354	1.41777
0.012	3.4	0.52458	1.03164
0.024	3.4	0.59761	0.89586
0.048	3.4	0.80451	0.41527
0.0015	6.8	0.59737	0.88341
0.0030	6.8	0.58927	0.96249
0.0060	6.8	0.57553	1.11849
0.024	6.8	0.77568	0.59720
0.048	6.8	0.62574	0.84855
0.012	6.8	0.60801	1.01727
0.024	13.6	0.68104	0.76945
0.0015	13.6	0.71813	0.73401
0.0030	13.6	0.70558	0.82485
0.0060	13.6	0.70254	0.87619
0.012	13.6	0.72687	0.78068
0.048	13.6		0.56754

Supplementary table 6. CI of irinotecan (IRI) and 5-FU in HCT116*P53-/-*

IRI (μM)	5FU (μM)	Effect	CI
0.008125	0.45	0.17644	1.48995
0.01625	0.45	0.30111	0.88533
0.0325	**0.45**	**0.43565**	**0.64213**
0.065	0.45	0.46080	1.01865
0.13	0.45	0.49643	1.55827
0.26	0.45	0.54184	2.27398
0.008125	0.9	0.25272	0.97661
0.01625	0.9	0.29725	1.08331
0.0325	0.9	0.41959	0.80505
0.065	0.9	0.51143	0.79968
0.13	0.9	0.48701	1.72407
0.26	0.9	0.51213	2.81766
0.008125	1.8	0.31988	0.92245
0.01625	1.8	0.37022	0.90663
0.0325	1.8	0.43893	0.88565
0.065	1.8	0.52520	0.84941
0.13	1.8	0.50276	1.68777
0.26	1.8	0.55133	2.29115
0.008125	3.6	0.43879	0.82109
0.01625	3.6	0.46062	0.85509
0.0325	3.6	0.50465	0.86022
0.065	3.6	0.54128	0.98549
0.13	3.6	0.53956	1.55871
0.26	3.6	0.55448	2.44694
0.008125	7.2	0.45113	1.41969
0.01625	7.2	0.51210	1.14761
0.0325	7.2	0.47562	1.58389
0.065	7.2	0.48736	1.88778
0.13	7.2	0.51106	2.34088
0.26	7.2	0.55698	2.80721
0.008125	14.4	0.60565	1.3135
0.01625	14.4	0.62484	1.23561
0.0325	14.4	0.58862	1.57857
0.065	14.4	0.57567	1.90519
0.13	14.4	0.57027	2.41896
0.26	14.4	0.59789	2.84657

Supplementary table 7. CI of dasatinib (DAS) and metformin (MET) in NCI-H508

DAS (μM)	MET	Effect	CI
0.1565	0.3125	0.16166	0.39302
0.3125	0.3125	0.13435	0.87186
0.625	0.3125	0.02366	13.2395
1.25	0.3125	0.14549	3
2.5	0.3125	0.33563	1.66
5.0	0.3125	0.57831	1.06
0.1565	0.625	0.03837	2.16
0.3125	0.625	0.24120	0.49199
0.625	0.625	0.08332	3.1
1.25	0.625	0.31138	1.04
2.5	0.625	0.40310	1.26
5.0	0.625	0.58898	1.05
0.1565	1.25	1.0E-5	25208.4
0.3125	1.25	0.01335	13.69
0.625	1.25	1.0E-5	100635
1.25	1.25	0.08731	5.86
2.5	1.25	0.33488	1.86
5.0	1.25	0.47889	1.81
0.1565	2.5	0.09680	1.49
0.3125	2.5	0.13610	1.54
0.625	2.5	0.13067	2.40
1.25	2.5	0.26000	1.8
2.5	2.5	0.29602	2.52
5.0	2.5	0.47414	2.06
0.1565	5.0	0.21914	1.47
0.3125	5.0	0.32408	1.26
0.625	5.0	0.32716	1.46
1.25	5.0	0.39520	1.53
2.5	5.0	0.40354	2.07
5.0	5.0	0.48768	2.36
0.1565	10.0	0.61281	1.40
0.3125	10.0	0.62666	1.39
0.625	10.0	0.59069	1.54
1.25	10.0	0.63911	1.50
2.5	10.0	0.62626	1.75
5.0	10.0	0.69454	1.77

Supplementary table 8. CI of vemurafenib (VEM) and metformin (MET) in HT29

VEM (μM)	MET	Effect	CI
0.00775	0.625	0.08410	0.22357
0.0155	0.625	0.11584	0.29471
0.031	0.625	0.18937	0.41582
0.062	0.625	0.34926	0.60948
0.124	0.625	0.39064	1.09996
0.248	0.625	0.51469	1.90565
0.00775	1.25	0.05157	0.40257
0.0155	1.25	0.20119	0.34405
0.031	1.25	0.18864	0.51169
0.062	1.25	0.30976	0.71340
0.124	1.25	0.42971	1.12861
0.248	1.25	0.54107	1.92094
0.00775	2.5	0.12484	0.52979
0.0155	2.5	0.23666	0.50135
0.031	2.5	0.32204	0.58397
0.062	**2.5**	**0.40377**	**0.78716**
0.124	2.5	0.48307	1.20158
0.248	2.5	0.59613	1.93811
0.00775	5.0	0.24987	0.76086
0.0155	5.0	0.30921	0.76865
0.031	5.0	0.38270	0.83123
0.062	5.0	0.48409	0.98005
0.124	5.0	0.52456	1.39727
0.248	5.0	0.65038	2.04627
0.00775	10.0	0.40462	1.17715
0.0155	10.0	0.45752	1.16633
0.031	10.0	0.49979	1.22793
0.062	10.0	0.56300	1.36476
0.124	10.0	0.63354	1.67552
0.248	10.0	0.71699	2.28235
0.00775	20.0	0.69129	1.61766
0.0155	20.0	0.70492	1.63571
0.031	20.0	0.73308	1.6647
0.062	20.0	0.74518	1.82002
0.124	20.0	0.79068	2.04457
0.248	20.0	0.84160	2.51547

Supplementary table 9. CI of vemurafenib (VEM) and metformin (MET) in RKO

VEM (μM)	MET	Effect	CI
0.46875	0.625	0.41893	0.57519
0.9375	0.625	0.48005	0.59736
1.875	0.625	0.43184	1.26809
3.75	0.625	0.51202	1.41167
7.5	0.625	0.61877	1.39345
15.0	0.625	0.95259	0.06829
0.46875	1.25	0.34719	1.31258
0.9375	1.25	0.41480	1.17664
1.875	1.25	0.37563	2.15231
3.75	1.25	0.45555	2.21457
7.5	1.25	0.61605	1.53534
15.0	1.25	0.94402	0.09498
0.46875	2.5	0.63387	0.50475
0.9375	2.5	0.66130	0.49529
1.875	2.5	0.71810	0.43529
3.75	2.5	0.75384	0.46746
7.5	2.5	0.82736	0.38528
15.0	2.5	0.99999	9.85E-7
0.46875	5.0	0.68793	0.69633
0.9375	5.0	0.68875	0.74359
1.875	5.0	0.71502	0.72004
3.75	5.0	0.83131	0.36846
7.5	**5.0**	**0.87812**	**0.29635**
15.0	5.0	0.91392	0.25703
0.46875	10.0	0.83887	0.47127
0.9375	10.0	0.84904	0.44179
1.875	10.0	0.88255	0.32664
3.75	10.0	0.90723	0.25857
7.5	10.0	0.95114	0.12566
15.0	10.0	0.99891	0.00110
0.46875	20.0	0.90615	0.43901
0.9375	20.0	0.91736	0.37542
1.875	20.0	0.91584	0.39424
3.75	20.0	0.95765	0.16806
7.5	20.0	0.94714	0.24234
15.0	20.0	0.97748	0.09058

Supplementary table 10. CI of vemurafenib (VEM) and metformin (MET) in NCI-H508

VEM (μM)	MET	Effect	CI
0.625	0.3125	0.22475	2.62875
1.25	0.3125	0.13503	8.32378
2.5	0.3125	0.25716	2.07034
5.0	0.3125	0.21873	3.24244
10.0	0.3125	0.59140	0.59297
20.0	0.3125	0.86567	0.47039
0.625	0.625	0.25416	3.85292
1.25	0.625	0.23645	4.65866
2.5	0.625	0.01504	1256.53
5.0	0.625	0.17763	9.46419
10.0	0.625	0.36691	2.12244
20.0	0.625	0.73167	0.77016
0.625	1.25	0.41558	1.96152
1.25	1.25	0.59316	0.56032
2.5	1.25	0.49434	1.19979
5.0	1.25	0.51622	1.16856
10.0	1.25	0.49802	1.58693
20.0	1.25	0.77412	0.72361
0.625	2.5	0.76688	0.23948
1.25	**2.5**	**0.73987**	**0.33069**
2.5	2.5	0.71295	0.46175
5.0	2.5	0.61772	1.05014
10.0	2.5	0.59657	1.43945
20.0	2.5	0.79149	0.76092
0.625	5.0	0.68764	0.95440
1.25	5.0	0.71096	0.80168
2.5	5.0	0.65018	1.38014
5.0	5.0	0.56273	2.78266
10.0	5.0	0.60023	2.35962
20.0	5.0	0.73742	1.2731
0.625	10.0	0.61642	3.37811
1.25	10.0	0.59286	4.08566
2.5	10.0	0.53161	6.54596
5.0	10.0	0.59472	4.20161
10.0	10.0	0.58914	4.61295
20.0	10.0	0.78729	1.30486

Supplementary table 11. CI of panitumumab (PAN) and metformin (MET) in NCI-H508

PAN (nM)	MET	Effect	CI
0.01071	0.3125	0.03958	3.29196
0.02143	0.3125	0.06185	3.51799
0.04285	0.3125	0.21925	1.10097
0.08571	0.3125	0.36566	0.85992
0.17141	0.3125	0.52316	0.73658
0.34283	0.3125	0.61458	0.88023
0.01071	0.625	0.18798	0.52511
0.02143	0.625	0.25892	0.55687
0.04285	0.625	0.27747	0.84143
0.08571	0.625	0.37114	0.91328
0.17141	0.625	0.44314	1.1665
0.34283	0.625	0.56037	1.22781
0.01071	1.25	0.25277	0.55913
0.02143	1.25	0.25857	0.7375
0.04285	1.25	0.31366	0.86377
0.08571	1.25	0.28728	1.59603
0.17141	1.25	0.40372	1.5647
0.34283	1.25	0.52849	1.56551
0.01071	2.5	0.29897	0.82498
0.02143	**2.5**	**0.38253**	**0.79118**
0.04285	2.5	0.27351	1.38762
0.08571	2.5	0.37862	1.34297
0.17141	2.5	0.43877	1.62288
0.34283	2.5	0.56816	1.55569
0.01071	5.0	0.32081	1.44885
0.02143	5.0	0.34892	1.49183
0.04285	5.0	0.36905	1.62982
0.08571	5.0	0.46410	1.57662
0.17141	5.0	0.54067	1.63998
0.34283	5.0	0.60301	1.83376
0.01071	10.0	0.59040	1.97411
0.02143	10.0	0.62138	1.92595
0.04285	10.0	0.64644	1.90733
0.08571	10.0	0.71220	1.7912
0.17141	10.0	0.68805	1.99798
0.34283	10.0	0.81715	1.63635

Supplementary table 12. CI of dasatinib (DAS) and metformin (MET) in HT29

DAS (nM)	MET (mM)	Effect	CI
0.76	0.625	0.17735	1.04
1.52	0.625	0.18933	1
3.05	0.625	0.24009	0.81628
6.1	0.625	0.16803	1.76
12.2	0.625	0.21675	1.89
24.4	0.625	0.33370	2.23
0.76	1.25	0.36713	0.45598
1.52	1.25	0.37823	0.48317
3.05	1.25	0.38080	0.59066
6.1	1.25	0.34141	0.96293
12.2	1.25	0.41218	1.16
24.4	1.25	0.49408	1.69
0.76	2.5	0.37250	0.82488
1.52	2.5	0.39520	0.77024
3.05	2.5	0.42527	0.75353
6.1	2.5	0.22607	2.96
12.2	2.5	0.45283	1.26
24.4	2.5	0.50521	1.82
0.76	5.0	0.47017	0.86248
1.52	5.0	0.49743	0.77860
3.05	**5.0**	**0.50379**	**0.84429**
6.1	5.0	0.46872	1.22
12.2	5.0	0.55005	1.18
24.4	5.0	0.66557	1.37
0.76	10.0	0.48286	1.55
1.52	10.0	0.52052	1.27
3.05	10.0	0.53566	1.25
6.1	10.0	0.52281	1.53
12.2	10.0	0.57962	1.47
24.4	10.0	0.67279	1.56
0.76	20.0	0.66235	0.96566
1.52	20.0	0.68987	0.83052
3.05	20.0	0.68963	0.90046
6.1	20.0	0.70961	0.92048
12.2	20.0	0.72169	1.11
24.4	20.0	0.79719	1.18

Supplementary table 13. CI of dasatinib (DAS) and metformin (MET) in RKO

DAS (μM)	MET	Effect	CI
0.78	0.625	0.36741	0.66116
1.56	0.625	0.36873	1.14
3.12	0.625	0.37623	1.97
6.25	0.625	0.59943	0.43827
12.5	0.625	0.67605	0.37057
25.0	0.625	0.99999	3.90E-6
0.78	1.25	0.25265	2.47
1.56	1.25	0.30780	2.37
3.12	1.25	0.34580	2.88
6.25	1.25	0.43518	2.21
12.5	1.25	0.73648	0.23316
25.0	1.25	0.9999	5.94E-5
0.78	2.5	0.38235	1.03
1.56	2.5	0.38841	1.39
3.12	2.5	0.51404	0.82131
6.25	2.5	0.59735	0.65865
12.5	2.5	0.76000	0.25588
25.0	2.5	0.999	9.05E-4
0.78	5.0	0.45957	1.11
1.56	5.0	0.51047	0.99901
3.12	5.0	0.58314	0.81252
6.25	**5.0**	**0.65576**	**0.65323**
12.5	5.0	0.82186	0.25068
25.0	5.0	0.98748	0.01705
0.78	10.0	0.51629	1.61
1.56	10.0	0.64366	1
3.12	10.0	0.56934	1.5
6.25	10.0	0.70615	0.84953
12.5	10.0	0.78520	0.58729
25.0	10.0	0.90419	0.23508
0.78	20.0	0.63820	1.97
1.56	20.0	0.68249	1.66
3.12	20.0	0.69429	1.61
6.25	20.0	0.81692	0.87869
12.5	20.0	0.86543	0.63823
25.0	20.0	0.9999	9.50E-4

Supplementary table 14. CI of regorafenib (REG) and metformin (MET) in HT29

REG (μM)	MET	Effect	CI
0.0976	0.625	0.19536	2.08
0.195	0.625	0.20173	2.01
0.39	0.625	0.24625	1.43
0.78	0.625	0.24933	1.62
1.56	0.625	0.42127	0.96768
3.12	0.625	0.56860	1.17
0.0976	**1.25**	**0.37682**	**0.86633**
0.195	1.25	0.32079	1.36
0.39	1.25	0.31438	1.53
0.78	1.25	0.32493	1.61
1.56	1.25	0.37799	1.53
3.12	1.25	0.59242	1.20
0.0976	2.5	0.37196	1.74
0.195	2.5	0.35990	1.95
0.39	2.5	0.28355	3.65
0.78	2.5	0.35251	2.34
1.56	2.5	0.36945	2.46
3.12	2.5	0.55516	1.55
0.0976	5.0	0.45474	1.91
0.195	5.0	0.46038	1.87
0.39	5.0	0.44966	2.10
0.78	5.0	0.47495	1.93
1.56	5.0	0.46730	2.33
3.12	5.0	0.60431	1.66
0.0976	10.0	0.55684	1.86
0.195	10.0	0.56316	1.81
0.39	10.0	0.56316	1.88
0.78	10.0	0.57351	1.89
1.56	10.0	0.63125	1.55
3.12	10.0	0.69462	1.52
0.0976	20.0	0.73660	0.92910
0.195	20.0	0.73188	0.99371
0.39	20.0	0.76577	0.78269
0.78	20.0	0.75290	0.97277
1.56	20.0	0.79241	0.88217
3.12	20.0	0.83850	0.94254

Supplementary table 15. CI of regorafenib (REG) and metformin (MET) in RKO

REG (μM)	MET	Effect	CI
0.195	0.625	0.19052	0.59543
0.39	0.625	0.15836	0.99607
0.78	0.625	0.41852	0.49227
1.56	0.625	0.49489	0.65820
3.12	0.625	0.73191	0.52018
6.25	0.625	0.9999	0.00116
0.195	1.25	0.30707	0.54803
0.39	1.25	0.31679	0.65531
0.78	1.25	0.31266	0.92855
1.56	1.25	0.56003	0.60744
3.12	1.25	0.51253	1.24
6.25	1.25	0.74911	0.96741
0.195	2.5	0.37286	0.73753
0.39	2.5	0.42951	0.68235
0.78	2.5	0.53679	0.58577
1.56	**2.5**	**0.66108**	**0.52950**
3.12	2.5	0.54246	1.29
6.25	2.5	0.91709	0.34859
0.195	5.0	0.51356	0.81198
0.39	5.0	0.45137	1.1
0.78	5.0	0.37193	1.69
1.56	5.0	0.61995	0.86780
3.12	5.0	0.74396	0.75174
6.25	5.0	0.87308	0.58466
0.195	10.0	0.57473	1.24
0.39	10.0	0.64475	0.99170
0.78	10.0	0.70957	0.82252
1.56	10.0	0.75928	0.75999
3.12	10.0	0.82909	0.66801
6.25	10.0	0.86342	0.77210
0.195	20.0	0.78763	0.96501
0.39	20.0	0.74501	1.22
0.78	20.0	0.76885	1.14
1.56	20.0	0.76905	1.24
3.12	20.0	0.79085	1.29
6.25	20.0	0.89738	0.79878

Supplementary table 16. CI of regorafenib (REG) and metformin (MET) in NCI-H508

REG (μM)	MET	Effect	CI
0.78	0.3125	0.16102	0.83768
1.56	0.3125	0.18448	1.39
3.12	0.3125	0.28676	1.56
6.25	0.3125	0.36335	2.20
12.5	0.3125	0.56444	1.93
25.0	0.3125	0.98210	0.09484
0.78	0.625	0.28842	0.42759
1.56	0.625	0.19152	1.36
3.12	0.625	0.23296	2.09
6.25	0.625	0.31177	2.78
12.5	0.625	0.50957	2.42
25.0	0.625	0.86981	0.76305
0.78	1.25	0.26515	0.52318
1.56	**1.25**	**0.42261**	**0.49617**
3.12	1.25	0.31699	1.42
6.25	1.25	0.35417	2.34
12.5	1.25	0.66917	1.28
25.0	1.25	0.97280	0.15695
0.78	2.5	0.22856	0.72369
1.56	2.5	0.35938	0.71172
3.12	2.5	0.41425	1.02
6.25	2.5	0.44233	1.70
12.5	2.5	0.51806	2.44
25.0	2.5	0.99265	0.05809
0.78	5.0	0.34739	0.61387
1.56	5.0	0.42932	0.69668
3.12	5.0	0.52666	0.80438
6.25	5.0	0.59208	1.08
12.5	5.0	0.62803	1.68
25.0	5.0	0.91884	0.54579
0.78	10.0	0.58685	0.55841
1.56	10.0	0.62694	0.60709
3.12	10.0	0.60537	0.84187
6.25	10.0	0.70180	0.90249
12.5	10.0	0.78027	1.02
25.0	10.0	0.9999	0.01775

Supplementary table 17. CI of metformin (MET) and trametinib (TRA) in RKO

MET (mM)	TRA (nM)	Effect	CI
0.625	2.0	0.24210	2.72152406
1.25	2.0	0.34713	1.03152596
2.5	2.0	0.47174	0.59930
5.0	2.0	0.55458	0.63599
10.0	2.0	0.71681	0.43285
20.0	2.0	0.64300	1.39152916
0.625	4.0	0.33743	1.49152145
1.25	4.0	0.46960	0.50611
2.5	4.0	0.51410	0.53260
5.0	4.0	0.60225	0.50321
10.0	4.0	0.91032	0.05936
20.0	4.0	100152000	3.5E-10
0.625	8.0	0.42636	1.02152311
1.25	8.0	0.48238	0.68799
2.5	8.0	0.60236	0.34373
5.0	**8.0**	**0.76069**	**0.16988**
10.0	8.0	0.86936	0.10970
20.0	8.0	0.97170	0.02089
0.625	16.0	0.53030	0.63604
1.25	16.0	0.61106	0.32742
2.5	16.0	0.68025	0.23292
5.0	16.0	0.88048	0.04974
10.0	16.0	0.91001	0.06068
20.0	16.0	0.96988	0.02292
0.625	32.0	0.60790	0.51529
1.25	32.0	0.69671	0.21775
2.5	32.0	0.68529	0.31326
5.0	32.0	0.73851	0.27082
10.0	32.0	0.77601	0.32286
20.0	32.0	0.84216	0.31008
0.625	64.0	0.49855	3.23152353
1.25	64.0	0.62810	0.82466
2.5	64.0	0.51672	2.92152760
5.0	64.0	0.86104	0.08004
10.0	64.0	0.91223	0.06202
20.0	64.0	0.95836	0.03741

Supplementary table 18. CI of metformin (MET) and trametinib (TRA) in HT29

MET (mM)	TRA (nM)	Effect	CI
0.625	0.03125	0.41507	0.80448
1.25	0.03125	0.52401	0.53584
2.5	0.03125	0.57145	0.64205
5.0	0.03125	0.57090	1.24153662
10.0	0.03125	0.61752	1.51153799
20.0	0.03125	0.71779	0.97323
0.625	0.0625	0.44215	0.69274
1.25	0.0625	0.49612	0.75593
2.5	0.0625	0.55138	0.82868
5.0	0.0625	0.55843	1.45153817
10.0	0.0625	0.63689	1.27153227
20.0	0.0625	0.76038	0.58516
0.625	0.125	0.43324	0.89727
1.25	0.125	0.49221	0.90188
2.5	0.125	0.49490	1.52153862
5.0	0.125	0.51207	2.39153871
10.0	0.125	0.59746	1.98153893
20.0	0.125	0.71808	1.04153345
0.625	0.25	0.47761	0.88563
1.25	0.25	0.49999	1.07153622
2.5	0.25	0.53262	1.29153554
5.0	0.25	0.57217	1.54153051
10.0	0.25	0.62977	1.58153328
20.0	0.25	0.75232	0.77529
0.625	0.5	0.61798	0.68677
1.25	0.5	0.64310	0.67941
2.5	0.5	0.67272	0.67984
5.0	0.5	0.72337	0.60454
10.0	**0.5**	**0.77905**	**0.50090**
20.0	0.5	0.84648	0.33030
0.625	1.0	0.63518	1.18153862
1.25	1.0	0.61774	1.37153510
2.5	1.0	0.65044	1.30153581
5.0	1.0	0.69646	1.17153092
10.0	1.0	0.76280	0.89800
20.0	1.0	0.89004	0.32497

Supplementary table 19. CI of metformin (MET) and trametinib (TRA) in NCI-H508

MET (mM)	TRA (nM)	Effect	CI
0.3125	0.0625	0.04260	9.35154192
0.625	0.0625	0.22093	0.30234
1.25	0.0625	0.14097	1.12154756
2.5	0.0625	0.40646	0.37297
5.0	0.0625	0.30580	1.19154793
10.0	0.0625	0.58227	0.68411
0.3125	0.125	0.02378	8.39154222
0.625	0.125	0.04440	1.68154014
1.25	0.125	0.12378	1.82154050
2.5	0.125	0.18880	1.39154003
5.0	0.125	0.53749	0.41850
10.0	0.125	0.79147	0.23306
0.3125	0.25	0.21125	0.43317
0.625	0.25	0.27354	0.30013
1.25	0.25	0.28934	0.42289
2.5	0.25	0.37957	0.44887
5.0	0.25	0.48944	0.52146
10.0	0.25	0.75697	0.28849
0.3125	0.5	0.26436	0.37632
0.625	0.5	0.27588	0.41633
1.25	0.5	0.31201	0.44000
2.5	0.5	0.37876	0.48638
5.0	0.5	0.46674	0.59062
10.0	0.5	0.69549	0.40413
0.3125	1.0	0.37835	0.19518
0.625	1.0	0.30553	0.48253
1.25	1.0	0.40109	0.29910
2.5	1.0	0.44844	0.37175
5.0	**1.0**	**0.55915**	**0.39889**
10.0	1.0	0.72695	0.34388
0.3125	2.0	0.15152	7.31154300
0.625	2.0	0.20735	2.87154569
1.25	2.0	0.15761	7.03154876
2.5	2.0	0.27059	1.75154582
5.0	2.0	0.55628	0.42584
10.0	2.0	0.72134	0.35777

CI	Sinergy
< 0.1	very strong synergy
0.1-0.3	strong synergy
0.3-0.7	moderate synergy
0.7-0.85	slight synergy
0.85-1	additivity
> 1	antagonism